SUPERCONVERGENCE ANALYSIS OF THE DISCONTINUOUS GALERKIN METHOD FOR SINGULARLY PERTURBED DIFFERENTIAL EQUATIONS

by

Gautam Singh

DEPARTMENT OF MATHEMATICS
INDIAN INSTITUTE OF TECHNOLOGY GUWAHATI
GUWAHATI-781039, INDIA

July, 2020

SUPERCONVERGENCE ANALYSIS OF THE DISCONTINUOUS GALERKIN METHOD FOR SINGULARLY PERTURBED DIFFERENTIAL EQUATIONS

A thesis submitted
in partial fulfillment of the requirements
for the degree of

DOCTOR OF PHILOSOPHY

by

Gautam Singh

(Roll Number: 156123007)

to the

DEPARTMENT OF MATHEMATICS
INDIAN INSTITUTE OF TECHNOLOGY GUWAHATI
July, 2020

DECLARATION

It is certified that the work contained in this thesis entitled **"Superconvergence Analysis of the Discontinuous Galerkin Method for Singularly Perturbed Differential Equations"** has done by me, under the supervision of **Dr. Natesan Srinivasan**, Professor, Department of Mathematics, Indian Institute of Technology Guwahati for the award of the degree of Doctor of Philosophy and this work has not been submitted elsewhere for a degree.

July, 2020

Gautam Singh
Roll No. 156123007
Department of Mathematics
Indian Institute of Technology Guwahati

CERTIFICATE

It is certified that the work contained in this thesis entitled **"Superconvergence Analysis of the Discontinuous Galerkin Method for Singularly Perturbed Differential Equations"** by **Gautam Singh,** a student of Department of Mathematics, Indian Institute of Technology Guwahati, for the award of the degree of Doctor of Philosophy has been carried out under my supervision and this work has not been submitted elsewhere for a degree.

July, 2020

Dr. Natesan Srinivasan
Professor
Department of Mathematics
Indian Institute of Technology Guwahati

Dedicated

to

my Parents

Acknowledgement

It is indeed a moment of great pleasure and honour to express my gratitude for everyone who have been a part of my journey. Foremost, I would express my thankfulness for my thesis supervisor Prof. Natesan Srinivasan. His encouragement, advice and patience during my research work have been a guiding light for me throughout my tenure. He was always there for me, and never left my hand. There were times when I faced difficulty, but he was always that inspiration, whose positive vibes got imbibed in me. His tireless working ability, patience, motivation and enthusiasm have strongly motivated me. Without his guidance and persistent help this dissertation would not have been possible. Really, he has been friend, mentor and critic, who always ensured to shell out the best of me.

I want to convey my gratitude to my HOD and Professors of Doctoral Committee members: Prof. D. C. Dalal, Prof. R. K. Sinha and Prof. S. N. Bora for their cooperation and useful comments during the progress of my research work. My thankfulness for all the faculties of Department of Mathematics, who have been with me since 2013, when I came to IITG for my masters degree. This journey of 7 years will be an inseparable part of my life, because, I have been groomed here.

I sincerely acknowledge Indian Institute of Technology Guwahati for providing facilities to me during my research work. I am most grateful to Ministry of Human Resource Development, Government of India, for providing me financial assistance for the completion of my thesis work.

I thank our technical superintendent Mr. Santanu Majumdar, Mr. Pranpratim Borgohain and Mr. Pranab Jyoti Boro and office staff members Mr. Sridhar Samal, Mr. Phatik Kumar, Mr. Saurav Choudhury and Mr. Jayanta Kumar Kalita of the department, for their assistance in various ways during my research period.

I express my regards to Prof. A. K. Mishra, Prof. A. K. Singh, Prof. Shyam Lal and Prof. S. K. Mishra of Department of Mathematics, Banaras Hindu University for motivating me for higher studies in Mathematics during my undergraduate.

I would like to thank my seniors, Dr. Abhishek Das, Dr. Anirban Majumdar and Dr. Maneesh Kumar Singh, who have been constantly with me, and taught me many basics about this topic. Their research papers were too helpful for me to understand various insights of our domain.

During my stay, all these years, the best thing was the beautiful campus. Its melting beauty and positive ambience, infuses freshness. In my daily work I have been blessed with a friendly and cheerful group of fellow students. I thank my fellow students and for all the fun we have had in these years. I would particularly like to thank Mohit, Deb, Sumit, Rakesh, Somnath, Sunil, Abhijit, Ram Manohar, Ayan and all my friends, for their friendly and wonderful company in throughout my research life.

I am also thankful to my friends and seniors Ranjan, Ramesh, Ashish, Ankur, Swapnendu, Sougata, Balasubramani, Devanand, Biswajit, Debasish, Jibrail, Jogen and my junior Mrityunjoy, Avijit, Aniruddha, Sandip and many others for sharing all the unforgettable moments.

I would always be grateful, to my mother Smt. Kaushilya Singh, my father Shri Vijay Bahadur Singh and my brother Mr. Gaurav Singh. They have been my strength and always trusted me in every odds. My brother has been my best friend and he used to motivate me everytime we interacted. I am also grateful to my grandfather Shri Badri Narayana Singh for being my first teacher. I likewise pass on my appreciation to my uncle Shri Shyam Bahadur Singh. I would thank God for being so benevolent. This journey will always be cherished.

July, 2020

Gautam Singh

Abstract

This thesis provides efficient numerical methods for solving singular perturbation problems (SPPs) of convection-diffusion and reaction-diffusion types with boundary layers. A differential equation is called singularly perturbed when a small parameter is multiplied with the highest-order derivative and this small parameter is called the perturbation parameter. Because of the presence of the parameter in the solution of the differential equation, steep, thin layers occur at the boundaries or/and interior of the domain. Solution of singularly perturbed problems normally has smooth and singular components and its singular component is called the boundary layer function which varies very rapidly in the boundary layer region and behaves smoothly in the outer region. Due to this layer phenomena, it is a very difficult and challenging task to provide parameter-uniform numerical methods for solving SPPs. Parameter-uniform numerical methods means those numerical methods in which the approximate solution converges to the corresponding exact solution of SPPs independently with respect to the perturbation parameter(s).

It is well-known that uniform meshes with classical schemes fail to converge uniformly with respect to the singular perturbation parameter. It is desirable to develop methods which converges uniformly. In this thesis we develop and analyze superconvergence properties of the non-symmetric interior penalty Galerkin (NIPG) method for solving SPPs in one- and two-dimensions on layer-adapted meshes.

We begin the thesis with an introduction followed by a section describing the objectives and the motivation for solving SPPs. Then, we discuss preliminaries which are used throughout the thesis. Next, we move forward to the main work of the thesis. First, we have studied the superconvergence properties of the NIPG for singularly perturbed two-point boundary-value problems (BVPs) of reaction-diffusion and convection-diffusion types. Then, we have considered two-parameter singularly perturbed convection-diffusion-reaction BVPs. Here, in order to discretize the domain, we used the layer-adapted piecewise-uniform Shishkin mesh, the Bakhvalov mesh and the exponentially-graded mesh. Also, here, we have established the superconvergence result of the NIPG method. Further, singularly perturbed coupled system of two-point BVPs of reaction-diffusion type is considered. The solutions of these problems exhibit twin overlapping exponential boundary layers. We applied the NIPG method on layer-adapted piecewise uniform Shishkin mesh. Numerical results are presented to support the theoretical results.

Then we discuss the numerical solution of singularly perturbed 1D parabolic PDEs. For the discretization of the parabolic PDEs, one often uses the space semidiscretization, also called the method of lines. In this approach, discontinuous Galerkin (DG) discretization is applied only to the spatial variable, whereas the temporal variable remains continuous. These method have lower-order of accuracy in time. In order to improve the order of convergence in time also, here, we have used DG discretization for both the variables and showed the superconvergence properties of the DG method. Finally, we dealt with the numerical solution of singularly perturbed 2D elliptic BVPs. Here, we applied the NIPG method on the layer-adapted piecewise-uniform Shishkin mesh and superconvergence results of the NIPG method are established. Numerical results are produced to validate the theoretical error estimates.

At the end of the thesis, conclusion and possible future works are discussed.

Contents

NOMENCLATURE

BVP	boundary-value problem
IBVP	initial-boundary-value problem
ODE	ordinary differential equation
PDE	partial differential equation
SPPs	singular perturbation problems
SPDEs	singularly perturbed differential equations
FEMs	finite element methods
DG	discontinuous Galerkin
NIPG	non-symmetric interior penalty Galerkin
SIPG	symmetric interior penalty Galerkin
IIPG	incomplete interior penalty Galerkin
ε, ε_d, ε_c, ε_1, ε_2	singular perturbation parameters
$\mathcal{O}(\cdot)$, $o(\cdot)$	Landau order symbol
N	number of mesh-intervals in the spatial direction
M	number of mesh-intervals in the time direction
T	final time
x, x_i, y, y_j	continuous and discrete spatial variables
t, t_m	continuous and discrete temporal variables
$h_i, h_{x,i}, h_{y,j}, H$	mesh-sizes in spatial direction
Δt	mesh-size in time direction
C	generic positive constant independent of perturbation and the mesh parameters.
$\|\|\|\cdot\|\|\|_{\varepsilon}$	energy norm
$\|\|\|\cdot\|\|\|$	discrete energy norm
$\|\cdot\|_{dG}$	discrete energy norm for parabolic problem
$\|\cdot\|_{\infty}$	standard supremum norm
Ω	continuous spatial domain in 1D
$\mathcal{D}$	continuous spatial domain in 2D

List of Figures

List of Tables

CHAPTER 1

Introduction

1.1 Singular Perturbation Problem

Singular perturbation problems (SPPs) arise in several branches of applied mathematics which include fluid dynamics, quantum mechanics, elasticity, chemical reactor theory, gas porous electrodes theory, etc. The presence of small parameter(s) in these problems prevents us from obtaining satisfactory numerical solutions. It is a well-known fact that the solutions of SPPs have a multi-scale character. That is, there are thin layer(s) where the solution varies very rapidly, while away from the layer(s) the solution behaves regularly and varies slowly. This class of problem is an attractive area for researchers due to its application nature. For example, consider the time dependent Navier-Stokes equations appearing in fluid dynamics in two space variables x and y:

$$\begin{cases} \dfrac{\partial u}{\partial t} - \dfrac{1}{Re}\Delta u + u(\nabla \cdot u) + \nabla p = f, \\ \text{div } u = 0, \\ \\ u = 0 \quad \text{on the boundary} \quad y = 0 \end{cases} \tag{1.1.1}$$

where $u = (u_1, u_2)$ is the velocity component along the x, y directions and p is pressure and f represents body accelerations acting on the continuum. The parameter 'Re' is called Reynolds number, proportional to length, velocity and inversely proportional to kinetic viscosity. The singularly perturbed nature of these equations becomes apparent when the magnitude of the convective term is much larger than that of the diffusion term *i.e.*, when the magnitude of the terms involving first-order derivatives is much larger than that of the second-order derivatives. The Equation (1.1.1) becomes singularly perturbed when velocity flow is large, such that $Re \geq 10^3$.

In 1904, Prandtl used the word boundary layer for the first time in his seven page report, which was published in the proceedings [49]. He discussed about how a quantity as small as the viscosity of common fluid such as water and air could play a crucial role in determining their flow. In his paper, Prandtl had shown that the flow about a body can be divided into two regions: a very thin layer (boundary layer) where the frictional effect are prominent and remaining as the outside regions. Whereas the term "singular perturbation" was first introduced by Friedrichs and Wasow in their paper [20] on nonlinear vibrations.

In general, a differential equation becomes singularly perturbed when the magnitude of the highest order derivative is dominated by the lower order terms and is often attributed to a small parameter multiplied with the highest order derivative. The small parameter is called the singular perturbation parameter. So it is natural to impose question about the role of the "small" parameter (say ε) where $0 < \varepsilon \ll 1$. Because of the presence of the singular perturbation parameter in the differential equation, the solution of the differential equation exhibits boundary layer(s), *i.e.,* steep, thin layers occur at the boundaries and interior of the domain, where the solution varies rapidly and away from the layer(s) the solution varies slowly and behaves smoothly. Solution of SPPs normally has smooth and singular components and its singular component is called the boundary layer function which varies very rapidly in the boundary layer region and behaves smoothly in the outer region. Finite difference methods (FDMs) and standard finite element methods (FEMs) give oscillatory and inaccurate solution for such type of problems on uniform meshes. One can find more details about the numerical solution of SPPs in the book of Roos et al. [56].

Therefore, it is desirable to develop parameter-uniform numerical methods *i.e.,* independent of the small parameter ε and the space variables x and y in the limiting case; that solve the singularly perturbed differential equations (SPDEs) effectively. This is indeed the reason why the methods of singular perturbation are of practical interest. More precisely, the purpose of SPP theory is to study and capture the boundary and interior layers in the 'limiting case' as $\varepsilon \to 0$.

The numerical methods for SPPs are widely classified into two categories, namely, the fitted operator methods (FOMs) and the fitted mesh methods (FMMs). In FOMs, exponential fitting factors (artificial viscosity) will be used to control the rapid growth or the decay of the numerical solution in the boundary layers. In [13], Allen et al. introduced FOMs for solving the problem of a viscous fluid flow past a cylinder. Many work on FOMs can be seen in the books of Doolan et al. [15] and Miller et al. [42].

The extensions of FOMs to higher-dimensional problems are too difficult and in some cases it may not be even possible. Whereas, FMMs use nonuniform grids, which will be

fine (dense) in the boundary layer regions and coarse outside the layer regions. The well-known layer resolving fitted meshes are the Shishkin meshes [42], which are piecewise uniform and easy to obtain, the Bakhvalov meshes [33], which are graded and obtained from some nonlinear mesh generating function. These two meshes will require *apriori* information about the location and width of the boundary layers. For more details on FMMs, one can refer the books by Farrell et al. [16], Miller et al. [42] and Roos et al. [56] and survey articles of Kadalbajoo et al. [24, 25, 26].

1.2 Objective and Motivation

The main aim of this thesis is to develop and analyze superconvergence properties of the non-symmetric interior penalty Galerkin (NIPG) method for solving SPPs in one- and two-dimensions on the piecewise uniform Shishkin mesh. A brief survey of the literature illustrating the motivation behind the present work, carried out in the thesis, is presented below:

There are several numerical methods available in the literature to solve SPDEs, for more details, one can refer the books [16, 33, 42, 56], articles [4, 11, 19, 21, 32, 40, 43, 45, 52, 58] and references therein. The solution of SPDEs has a multi-scale character, it varies rapidly inside the boundary layer, and varies slowly away from the boundary layers, therefore, classical numerical schemes fail to yield satisfactory numerical approximate solution on uniform meshes. Special care has to be taken to devise parameter-uniform numerical methods to these problems.

FEMs will fail to provide parameter-uniform numerical solutions to SPDEs on uniform meshes. Therefore, one has to use exponential basis functions as the trial functions [47], or one has to use layer-adapted nonuniform meshes for classical FEM [56]. There are several research articles deal with the numerical solution of SPDEs by FEM, we cite a few of them [55, 59, 60, 67], and the references therein. It is desirable to develop methods which converges uniformly. In this thesis, we develop and analyze superconvergence properties of the non-symmetric interior penalty Galerkin (NIPG) for solving SPPs.

Some of the numerical methods for two-parameter SPPs can be found in [37, 61] using simple upwind finite difference scheme on the Shishkin mesh and fitted finite difference scheme on uniform mesh, respectively. FEMs are more effective numerical methods over finite difference schemes to obtain the numerical solutions of SPPs. Kadalbajoo and Yadaw [27] applied the FEM on the Shishkin mesh for two-parameter singularly perturbed convection-diffusion-reaction problem and proved almost second-order convergence in the maximum norm. Brdar and Zarin [7] applied the FEM for the same problem on the Bakhvalov mesh and proved uniform convergence in the discrete energy

norm. Instead of the Bakhvalov mesh, Zarin used the exponentially graded mesh in [65]. Recent work on two-parameter SPPs can be seen in [6].

There are several research articles available in the literature deal with the numerical solution of singularly perturbed scalar boundary-value problems (BVPs), whereas only a few articles exist for singularly perturbed system of BVPs. To cite a few, Madden and Stynes [39] presented a uniformly convergent numerical method for system of reaction-diffusion BVPs. Natesan and Deb studied the system of reaction-diffusion problems, and obtained the numerical solution on Shishkin mesh in [46]. One can see some more work on the numerical solution of system of reaction-diffusion problems in [12, 29, 34, 35, 36, 41], and the references therein. Some articles on system of convection-diffusion equations can be seen in [5, 9, 48, 53, 54].

Discontinuous Galerkin (DG) methods [2, 10] have been widely used for solving a wide range of problems from computational fluid dynamics. These methods are preferred over FEMs because of their flexibility in approximating globally rough solutions, their local mass conservation, their possible definition on unstructured meshes, their potential for error control and mesh adaptation, etc. DG methods are effective numerical methods for solving differential equations. Early work on DG methods can be found in Reed and Hill [50] and Arnold [2], etc.

Most popular DG method is the NIPG method. The NIPG method uses penalty parameters to enforce weakly both the continuity of the solution and the boundary conditions. Some of the general attractive features of the NIPG method are the flexibility due to local mesh refinement and ability to handle unstructured meshes and discontinuous coefficients. More specific properties include the coercivity property of the bilinear form, stability and convergent for any nonnegative penalty parameters, whereas in other variants of the DG methods, for example, the symmetric interior penalty Galerkin (SIPG) method and the incomplete interior penalty Galerkin (IIPG) method, we have to choose the penalty parameters so that the method should be stable and convergent and also the proof of the coercivity property is also too complicated. Some work on DG methods can be seen in [23, 64, 66, 69].

Superconvergence is a property in numerical analysis that shows faster convergence for the approximate solution arising from the numerical method. Many works have been done by different researchers in this field. Some of them are: In [68], Zhang shows the superconvergence properties by improving the order of convergence in the interpolation error. Chen shows superconvergence properties using piecewise Lagrange interpolation on Gauss points [10]. Superconvergence in FEMs for SPPs have been studied by Zhang [67] and references therein. Also, there are some superconvergence results obtained for the local DG method [63]. But, no superconvergence results are available in the literature

about the DG method in its primal formulation for SPPs (the local DG method is in mixed formulation). For an overview of these methods, one can refer the book [51], the research articles [3, 8, 57, 70], and the references therein.

For the discretization of the parabolic PDEs, one often uses the space semidiscretization, also called the method of lines [18]. In this approach, the DG discretization is applied only with respect to the spatial variable, whereas the temporal variable remains continuous. These method have low order of accuracy in time. In order to improve the order of convergence in time also we have used DG discretization with respect to both the variables. Some recent work in this direction can be seen in [1, 17, 28].

Finally, we have extended the idea of the superconvergence proof for 1D convection-diffusion BVPs given in Chapter 2 to 2D elliptic BVPs of convection-diffusion type on a square domain. Here, we apply the NIPG method on the layer-adapted piecewise uniform Shishkin mesh. In order to improve the order of convergence of the interpolation error, the piecewise Lagrange interpolation is used at Gauss points. We used this improved order of convergence to prove the discretization error.

Some of the most recent articles can be seen in [14, 30]. In [14], authors propose an efficient high order semi-Lagrangian (SL) discontinous Galerkin (DG) method for solving linear convection-diffusion equations. Proposed method have many attractive features of the DG and SL methods. These include the uniformly high order accuracy in space and in time, compact, mass conservative, and stability under large time stepping size. In [30], authors applied discontinuous Galerkin finite element method for convection-diffusion-reaction problems with singular perturbation and established a priori error estimate in a suitable energy norm.

1.3 Preliminaries

In this section, we provide some definitions, notations which will be used throughout the thesis.

Definition 1.3.1. *(**Uniformly convergent**) Let u be the solution of a singular perturbation problem, and let u_h be a numerical approximation of u obtained by a numerical method with N degrees of freedom. The numerical method is said to be uniformly convergent or robust with respect to the perturbation parameter ε in the norm $\|\cdot\|$ if*

$$\|u - u_h\| \leq \nu(N) \quad \text{for} \quad N \geq N_0$$

with a function ν and a threshold value $N_0 > 0$ that are both independent of ε and

$$\lim_{N\to\infty} \nu(N) = 0.$$

The next definition is of ***Landau's order symbols*** $\mathcal{O}$ (big-oh) and o (little-oh), which are used throughout the thesis. Let $f(\varepsilon)$ and $g(\varepsilon)$ be two real valued functions, where $0 < \varepsilon \leq \varepsilon_0 \ll 1$.

Definition 1.3.2. *The expression $f(\varepsilon) = \mathcal{O}(g(\varepsilon))$ as $\varepsilon \to 0$, defines that there exist some positive constants C and ε_0 satisfying $\varepsilon \in (0, \varepsilon_0]$ such that*

$$|f(\varepsilon)| \leq C\,|g(\varepsilon)|\,, \quad \varepsilon \to 0.$$

Definition 1.3.3. *The expression $f(\varepsilon) = o(g(\varepsilon))$ as $\varepsilon \to 0$, defines that*

$$\lim_{\varepsilon \to 0} \frac{f(\varepsilon)}{g(\varepsilon)} = 0.$$

Definition 1.3.4. *A matrix $\boldsymbol{A} = (a_{lm}) \in \mathbb{R}^{n,n}$ is an L_0–matrix if $a_{ll} > 0$ and $a_{lm} \leq 0$, for all $l \neq m$, $1 \leq l, m \leq n$.*

Definition 1.3.5. *A matrix $\boldsymbol{A} = (a_{lm}) \in \mathbb{R}^{n,n}$ is an M–matrix if $\boldsymbol{A}$ is nonsingular, $\boldsymbol{A}^{-1} \geq 0$ and $a_{lm} \leq 0$, for all $l \neq m$, $1 \leq l, m \leq n$.*

1.3.1 Basic notations for 1D problems

The space of square integrable functions on an interval $\Omega \subset \mathbb{R}$ will be denoted by $L^2(\Omega)$, with the associated inner product

$$(u,\, v)_\Omega = \int_\Omega u(x)v(x)dx.$$

Let $\mathcal{T}_N = \{K_j = (x_{j-1}, x_j) : j = 1, \ldots, N\}$ be a partition of the domain Ω. For each element $K_j \in \mathcal{T}_N$, define the broken Sobolev space of order s as

$$H^s(\Omega,\, \mathcal{T}_N) = \{u \in L^2(\Omega) : u|_{K_j} \in H^s(K_j), \forall K_j \in \mathcal{T}_N\}.$$

The corresponding broken Sobolev norm and seminorm are given by

$$\|u\|^2_{s,\mathcal{T}_N} = \sum_{j=1}^{N} \|u\|^2_{s,K_j}, \quad |u|^2_{s,\mathcal{T}_N} = \sum_{j=1}^{N} |u|^2_{s,K_j},$$

where, $\|.\|_{0,K_j}$ and $|.|_{1,K_j}$ are the usual Sobolev norm and seminorm defined over the domain K_j, respectively.

Let us define the finite element space $V_N^k(\Omega)$ associated with the family $\mathcal{T}_N$ as follows

$$V_N^k(\Omega) = \{u \in L^2(\Omega) : u|_{K_j} \in P^k(K_j), \forall K_j \in \mathcal{T}_N\},$$

where $P^k(K_j)$ denotes the space of polynomials of degree at most k on K_j. The functions in $V_N^k(\Omega)$ are completely discontinuous across inter element boundaries.

In case of the coupled system of singularly perturbed reaction-diffusion equations, we get solution as vector-valued function $\vec{u} = (u_1(x),\, u_2(x))$. Inner product and Sobolev space for vector-valued function are defined as follows:

The space of square integrable functions on an interval $K_j \subset R$ will be denoted by $L^2(K_j)$, with the associated inner product

$$(\vec{u},\, \vec{v})_{K_j} = \int_{K_j} u_1(x)v_1(x)dx + \int_{K_j} u_2(x)v_2(x)dx.$$

We use the usual Sobolev space $H^k(K_j)$ to denote the space of functions on K_j whose generalized derivatives are in $L^2(K_j)$ and it is equipped with the norm and seminorm $\|.\|_{k,K_j}$ and $|.|_{k,K_j}$, respectively. For any vector-valued function $\vec{u} = (u_1(x),\, u_2(x))^T$, we will define the norm as

$$\|\vec{u}\|^2_{k,K_j} = \|u_1\|^2_{k,K_j} + \|u_2\|^2_{k,K_j}.$$

The corresponding broken Sobolev norm and seminorm are given by

$$\|\vec{u}\|^2_{s,\mathcal{T}_N} = \sum_{j=1}^{N} \|u_1\|^2_{s,K_j} + \sum_{j=1}^{N} \|u_2\|^2_{s,K_j}, \quad |\vec{u}|^2_{s,\mathcal{T}_N} = \sum_{j=1}^{N} |u_1|^2_{s,K_j} + \sum_{j=1}^{N} |u_2|^2_{s,K_j},$$

where, $\|.\|_{0,D}$ and $|.|_{1,D}$ are the usual Sobolev norm and seminorm defined over the domain D, respectively.

In DG method, we allow discontinuity across inter element boundaries. Hence, we need to introduce jump and average of the trace of v at the interior node x_j, by

$$[v(x_j)] = v^+(x_j) - v^-(x_j), \quad \{v(x_j)\} = \frac{1}{2}(v^+(x_j) + v^-(x_j)),\ j = 1, \cdots, N-1,$$

and at the boundary points

$$[v(x_0)] = v(x_0), \quad \{v(x_0)\} = v(x_0), \quad [v(x_N)] = -v(x_N), \quad \{v(x_N)\} = v(x_N),$$

where

$$v^+(x_j) = \lim_{x \to x_j +} v(x), \quad v^-(x_j) = \lim_{x \to x_j -} v(x).$$

1.3.2 Basic notations for parabolic problem

Here, we define the finite element space where we have approximated the numerical solution for parabolic problems. Let us define the finite element space $V_N^k(\Omega)$ associated with the family $\mathcal{T}_N$ as follows

$$V_N^k(\Omega) = \{u \in L^2(\Omega) : u|_{K_j} \in P^k(K_j), \forall K_j \in \mathcal{T}_N\},$$

where $P^k(K_j)$ denotes the space of polynomials of degree at most k on K_j. The functions in $V_N^k(\Omega)$ are completely discontinuous across inter element boundaries. Finite element space to approximate the solution of parabolic problem is given by

$$V_{N,M}^{k,l}(\mathcal{G}) = \{u \in L^2(\mathcal{G}) : u|_{I_m} = \sum_{i=0}^{l} t^i u_i \quad \text{with} \quad u_i \in V_N^k(\Omega)\}.$$

And for the discontinuous functions in time we introduce the jump at t_m by

$$[[v]]_m = v_m^+ - v_m^-,$$

where

$$v_m^+ = v^+(t_m) = \lim_{t \to t_m +} v(t), \quad v_m^- = v^-(t_m) = \lim_{t \to t_m -} v(t).$$

1.3.3 Basic notations for 2D elliptic BVP

Let $\mathcal{T}_N$ denote partition of $\mathcal{D} = (0,\, 1)^2$ which contains rectangles K such that

$$\overline{\mathcal{D}} = \bigcup_{K \in \mathcal{T}_N} K.$$

Sobolev space on rectangles K is defined as

$$H^s(\mathcal{D},\, \mathcal{T}_N) = \{u \in L^2(\mathcal{D}) : u|_K \in H^s(K), \forall K \in \mathcal{T}_N\}.$$

Corresponding to the above defined space, we can define Sobolev norm and seminorm as

$$\|u\|_{s,\mathcal{T}_N}^2 = \sum_{K \in \mathcal{T}_N} \|u\|_{H^s(K)}^2, \quad |u|_{s,\mathcal{T}_N}^2 = \sum_{K \in \mathcal{T}_N} |u|_{H^s(K)}^2,$$

respectively. Finite-dimensional space $V_N(\mathcal{D})$ for the partition $\mathcal{T}_N$ is as follows

$$V_N(\mathcal{D}) = \{u \in L^2(\mathcal{D}) : u|_K \in Q_k(K), \forall K \in \mathcal{T}_N\},$$

where $Q_k(K)$ denotes the tensor products Lagrange polynomial space of degree at most k in one variable on K.

Let $\mathcal{E}_N$ be the set of edges corresponding to the partitioning $\mathcal{T}_N$ and $\mathcal{E}_{int} \subset \mathcal{E}_N$ be the set of all edges $e \in \mathcal{E}_N$ contained in $\mathcal{D}$. Let $\Gamma_{int} = \{x \in \mathcal{D} : x \in e \text{ for some } e \in \mathcal{E}_{int}\}$. Then for each interior edge e, there exists two rectangles K and K' sharing the interface e, then we can define the jump and the mean-value of the function v on e as follows:

$$[v]_e = v|_{\partial K \cap e} - v|_{\partial K' \cap e}, \qquad \{v\}_e = \frac{1}{2}(v|_{\partial K \cap e} + v|_{\partial K' \cap e})$$

respectively, where ∂K denote the union of all open edge of the element K. With each interface $e \in \mathcal{E}_N$ we associate the unit normal vector ν pointing from K to K', if $e \subset \Gamma$,

we take ν to be the unit outward normal vector μ. Define inflow and outflow parts of ∂K by

$$\partial_- K = \{x \in \partial K : \mathbf{b}(x) \cdot \mu_K(x) < 0\},$$
$$\partial_+ K = \{x \in \partial K : \mathbf{b}(x) \cdot \mu_K(x) \geq 0\},$$

respectively, where $\mu_K(x)$ represents the unit outward normal vector to ∂K at the point $x \in \partial K$. We define the outer trace v_K^- of v on $\partial_- K \backslash \Gamma$ relative to K as the inner trace $v_{K'}^+$ relative to the element K' such that $\partial_+ K' \cap (\partial_- K \backslash \Gamma) \neq \Phi$. The jump of v across $\partial_- K \backslash \Gamma$ is defined by

$$\lfloor v \rfloor = v_K^+ - v_K^-.$$

Let $\Gamma_{int}^H(\Gamma^H)$ and $\Gamma_{int}^V(\Gamma^V)$ denote the set of all interior (boundary) horizontal and vertical edges, respectively.

Throughout this thesis, C denotes a generic positive constant that is independent of the perturbation parameters (ε, ε_d, ε_c, ε_1, ε_2) and the mesh parameters.

1.4 Model Problems

In this section, the model problems considered in this thesis are described briefly. For clarity of the presentation, we elaborately provide these model problems with suitable information on the given data at the beginning of the subsequent chapters.

The following types of model problems are considered and their concise descriptions are given below:

1.4.1 Singularly perturbed 1D reaction-diffusion BVP

Here, we consider the following singularly perturbed reaction-diffusion BVP:

$$\begin{cases} -\varepsilon^2 u''(x) + c(x)u(x) = f(x), \quad x \in \Omega = (0,\, 1), \\ u(0) = u(1) = 0, \end{cases} \tag{1.4.1}$$

where $0 < \varepsilon \ll 1$ is the perturbation parameter and the reaction coefficient satisfies $c(x) \geq \beta^2 > 0$. The reaction coefficient $c(x)$ and source function $f(x)$ are sufficiently smooth functions. We know that, solution $u(x)$ of (1.4.1) exhibits boundary layers of width $\mathcal{O}(\varepsilon \ln \varepsilon)$ at $x = 0$ and 1.

1.4.2 Singularly perturbed 1D convection-diffusion BVP

Consider the following singularly perturbed convection-diffusion BVP:

$$\begin{cases} -\varepsilon u''(x) + b(x)u'(x) + c(x)u(x) = f(x), \quad x \in \Omega, \\ u(0) = u(1) = 0, \end{cases} \tag{1.4.2}$$

with

$$b(x) \geq \beta > 0, \;\; \gamma^2 = \min_{x\in\Omega}\left(c(x) - \frac{b'(x)}{2}\right) > 0, \;\; \forall x \in \Omega,$$

where $0 < \varepsilon \ll 1$ is the perturbation parameter. The coefficients $b(x)$, $c(x)$ and the source function $f(x)$ are sufficiently smooth functions. We know that, solution $u(x)$ of (1.4.2) exhibits boundary layer of width $\mathcal{O}(\varepsilon \ln \varepsilon)$ at $x = 1$.

1.4.3 Singularly perturbed two-parameter 1D convection-diffusion-reaction BVP

Here, we consider the following two-parameter singularly perturbed two-point BVP:

$$\begin{cases} -\varepsilon_d u''(x) + \varepsilon_c b(x)u'(x) + c(x)u(x) = f(x), \quad x \in \Omega, \\ u(0) = u(1) = 0, \end{cases} \tag{1.4.3}$$

where $0 < \varepsilon_d, \varepsilon_c \ll 1$. The functions $b(x)$, $c(x)$ and $f(x)$ are assumed to be sufficiently smooth with $b(x) \geq b_0 > 0$, $c(x) \geq c_0 > 0$ and $\gamma^2 = \min\limits_{x\in\Omega}\left(c(x) - \varepsilon_c\dfrac{b'(x)}{2}\right) > 0$, where b_0, c_0 and γ are constants.

1.4.4 Singularly perturbed coupled system of 1D reaction-diffusion BVP

Here, we consider the following singularly perturbed system of reaction-diffusion BVP:

$$\begin{cases} L\vec{u} = \begin{pmatrix} -\varepsilon_1^2\dfrac{d^2}{dx^2} & 0 \\ 0 & -\varepsilon_2^2\dfrac{d^2}{dx^2} \end{pmatrix}\vec{u} + \mathcal{C}\vec{u} = \vec{f}, \quad x \in \Omega, \\ \vec{u}(0) = \vec{0}, \qquad\qquad \vec{u}(1) = \vec{0}, \end{cases} \tag{1.4.4}$$

where $\mathcal{E} = \operatorname{diag}(\varepsilon_1, \varepsilon_2)$ are the perturbation parameters, the coefficients c_{ij} and the source terms f_j are sufficiently smooth functions, and are given by

$$\mathcal{C} = \begin{pmatrix} c_{11}(x) & c_{12}(x) \\ c_{21}(x) & c_{22}(x) \end{pmatrix} \quad \text{and} \quad \vec{f} = \begin{pmatrix} f_1(x) \\ f_2(x) \end{pmatrix}.$$

We shall assume that reaction coefficient matrix $\mathcal{C} = \{c_{ij}\}_{i,j=1}^{2}$ is an L_0–matrix with

$$\min\{c_{11} + c_{12}, c_{21} + c_{22}\} > \beta^2, \tag{1.4.5}$$

i.e., $\mathcal{C}$ is an M-matrix whose inverse is bounded by β^{-2} in the maximum norm. The solution $\vec{u} = (u_1, u_2)^T$ of (1.4.4) has boundary layers of width $\mathcal{O}(\varepsilon_1 \ln \varepsilon_1)$ and $\mathcal{O}(\varepsilon_2 \ln \varepsilon_2)$ at $x = 0$ and 1.

1.4.5 Singularly perturbed 1D parabolic IBVP

We consider the following singularly perturbed parabolic convection-diffusion-reaction problem:

$$\begin{cases} u_t - \varepsilon u_{xx} + b(x)u_x + c(x)u = f(x,t), \quad (x,\, t) \in \mathcal{G} := (\Omega \times (0,\, T]), \\ u(x,\, 0) = u_0, \quad \text{for } x \in \overline{\Omega}, \\ u(0,\, t) = u(1,\, t) = 0, \quad \text{for } t \in (0,\, T], \end{cases} \tag{1.4.6}$$

here, $0 < \varepsilon \ll 1$ is a small parameter and $b(x), c(x)$ are sufficiently smooth with $b(x) > \beta > 0$. We also assume that

$$\gamma^2 = \min_{x \in \Omega} \left(c(x) - \frac{b'(x)}{2} \right) > 0, \ \ \forall x \in \Omega.$$

Solution of the IBVP (1.4.6) exhibits boundary layer at $x = 1$.

1.4.6 Singularly perturbed 2D elliptic BVP

Here, the following singularly perturbed 2D elliptic BVP is considered:

$$\begin{cases} -\varepsilon \Delta u + \mathbf{b} \cdot \nabla u + cu = f, \quad \text{in} \quad \mathcal{D} = (0,\, 1) \times (0,\, 1), \\ u = 0, \quad \text{on} \quad \Gamma = \partial \mathcal{D}, \end{cases} \tag{1.4.7}$$

where ε is a small positive parameter, and $\mathbf{b}(x,\, y) = (b_1(x,\, y),\, b_2(x,\, y)) \geq (\beta_1,\, \beta_2) \geq (\beta,\, \beta) > (0,\, 0)$, $c(x,\, y) \geq 0$ for all $(x,\, y) \in \overline{\mathcal{D}}$, and $\gamma^2 = \left(c(x,\, y) - \frac{1}{2}\nabla \cdot \mathbf{b}(x,\, y)\right) > 0$, where β and γ are constants.

1.5 General Outline of the Thesis

In this thesis, we focus on obtaining the numerical solution of SPPs in one and two-dimensions by the NIPG method.

The rest of this thesis includes six chapters and is organized as follows:

In **Chapter 2**, superconvergence properties of the NIPG method for singularly perturbed two-point BVPs of reaction-diffusion and convection-diffusion types are studied. By using piecewise polynomials of degree k on modified Shishkin mesh, superconvergence error bounds of $\mathcal{O}((N^{-1}\ln N)^{k+1})$ in the discrete energy norm are established, where N is the number of elements. Numerical experiments are carried out to validate the theoretical findings.

We applied the NIPG method to obtain the numerical solution of two-parameter singularly perturbed convection-diffusion-reaction BVPs in **Chapter 3**. In order to discretize the domain, here, we use the layer-adapted piecewise uniform Shishkin mesh, the Bakhvalov mesh and the exponentially-graded mesh. We establish a superconvergence result of the NIPG method, that is, the proposed method is parameter-uniformly convergent with the order almost $(k+1)$ on the Shishkin mesh and $(k+1)$ on the Bakhvalov mesh and on the exponentially graded mesh in the discrete energy norm, where k is the order of the polynomials. Numerical results comparing the three different types of meshes are presented at the end of the chapter supporting the theoretical error estimates.

Chapter 4 is devoted to the study of the numerical solution of singularly perturbed system of two-point BVPs of reaction-diffusion type. The solutions of these problems exhibit twin overlapping exponential boundary layers. To obtain the numerical solutions of these problems, we apply the NIPG method on layer-adapted piecewise uniform Shishkin mesh. Also, we have proved that the proposed numerical method is uniformly convergent with order k in the $\mathcal{E}$-weighted energy norm, where k is the degree of the piecewise polynomial in the finite element space. To improve the order of convergence for the interpolation error, we use piecewise Lagrange interpolation on Gauss points and discrete energy norm. Numerical results are presented to support the theoretical results.

In **Chapter 5**, parabolic convection-diffusion-reaction problem is discretized in space by the NIPG method and in time by DG method. We have shown that the superconvergence properties that is $(k+1)$–order of convergence in space and $(l+1)$–order of convergence in time, where k and l are the degree of piecewise polynomial in finite element space. Numerical results are given to verify our theoretical findings.

Chapter 6 deals with the numerical solution of singularly perturbed 2D elliptic BVPs. Here, we obtain the error estimates of the superconvergence of the NIPG method with interior penalties on layer-adapted meshes of Shishkin type. We have established the error bound in the discrete energy norm. Numerical tests support our theoretical estimates.

Finally, **Chapter 7**, contains the brief summary of the results highlighting the contribution made by this thesis. It also provides various ideas for the scope of future

investigations of the present work.

CHAPTER 2

Superconvergence Error Analysis of Discontinuous Galerkin Method with Interior Penalties for Singularly Perturbed Two-Point BVPs

This chapter presents, superconvergence properties of the NIPG method for singularly perturbed two-point BVPs of reaction-diffusion and convection-diffusion SPPs. By using piecewise polynomials of degree k on modified Shishkin mesh, superconvergence error bounds of $\mathcal{O}((N^{-1}\ln N)^{k+1})$ in the discrete energy norm are established. Finally, the convergence result is verified numerically.

2.1 Introduction

The main objective of this chapter is to propose the NIPG method for the singularly perturbed reaction-diffusion and convection-diffusion problems on layer-adapted Shishkin mesh and shows superconvergence properties of the NIPG method. To derive the theoretical error analysis, we have decompose the error into two parts that is interpolation error and discretization error. Using the piecewise Lagrange interpolation on Gauss points, we have derived the bound for interpolation error. Then by combining, with the discretization error we obtained main convergence result.

The outline of this chapter is as follows: This chapter is mainly divided into two sections. In Section 2.2, we have considered reaction-diffusion problem whereas convection-diffusion problem is considered in Section 2.3. We have applied the NIPG method to discretize the problems. Bounds for the interpolation error and discretization error are derived in Subsections 2.2.1 and 2.2.2 for reaction-diffusion problem and Subsections 2.3.1 and 2.3.2 for convection-diffusion problem, respectively. Numerical results confirming the theoretical error bounds are given in Section 2.4.

2.2 Reaction-Diffusion BVP

Here, we consider the following singularly perturbed reaction-diffusion BVP:

$$\begin{cases} -\varepsilon^2 u''(x) + c(x)u(x) = f(x), \quad x \in \Omega, \\ u(0) = u(1) = 0, \end{cases} \tag{2.2.1}$$

where $0 < \varepsilon \ll 1$ is the perturbation parameter and the reaction coefficient satisfies $c(x) \geq \beta^2 > 0$. We assume that the reaction coefficient $c(x)$ and source function $f(x)$ are sufficiently smooth functions. The exact solution $u(x)$ of (2.2.1) exhibits boundary layers of width $\mathcal{O}(\varepsilon \ln \varepsilon)$ at $x = 0$ and 1.

Lemma 2.2.1. *Let p be a positive integer and the exact solution u of the BVP (2.2.1) can be decomposed as $u = S+E$, where, S and E are smooth and layer parts, respectively. Then the bounds on the smooth and layer components are*

$$|S^{(l)}(x)| \leq C, \tag{2.2.2}$$

$$|E^{(l)}(x)| \leq C\varepsilon^{-l} D_\varepsilon(x), \quad 0 \leq l \leq p, \tag{2.2.3}$$

where $D_\varepsilon(x) = \exp((-\beta x)/\varepsilon) + \exp((-\beta(1-x))/\varepsilon)$. Here, p depends on the regularity of the coefficients of the problem (2.2.1).

Proof. The proof of this lemma can be found in [56]. ∎

To discretize the domain Ω, we use the layer-adapted piecewise uniform Shishkin mesh, which is described as follows: We divide the domain Ω into three subdomains as $\Omega = \Omega_1 \cup \Omega_2 \cup \Omega_3$, where Ω_1, Ω_2 and Ω_3 are $[0, \tau_\varepsilon]$, $[\tau_\varepsilon, 1-\tau_\varepsilon]$ and $[1-\tau_\varepsilon, 1]$, respectively. Here the transition point τ_ε is defined by

$$\tau_\varepsilon = \min\left(\frac{1}{4}, \frac{\alpha\varepsilon}{\beta}\ln N\right),$$

where, the constant α is typically chosen to accommodate the error analysis. We assume that $\tau_\varepsilon = (\alpha\varepsilon/\beta)\ln N$, otherwise N^{-1} is much smaller than ε, which is rare in practice. The mesh-width on the coarse part of the mesh is $h_i = H = 2(1-2\tau_\varepsilon)/N$, $i = N/4+1, \ldots, 3N/4$, with $1/N \leq H \leq 2/N$, whereas, on the fine part of the mesh, we have $h_i = 4\tau_\varepsilon/N, i = 1, \ldots, N/4$, and $3N/4+1, \ldots, N$.

By using the NIPG method, the finite element approximation for the reaction-diffusion problem (2.2.1) is given by

$$\begin{cases} \text{find } u_h \in V_N^k(\Omega), \text{ such that} \\ B(u_h, v_h) = l(v_h), \quad \forall v_h \in V_N^k(\Omega), \end{cases} \tag{2.2.4}$$

with $B(u,\, v) = B_1(u,\, v) + B_2(u,\, v) - B_2(v,\, u) + B_3(u,\, v)$, where

$$\begin{aligned} B_1(u,\, v) &= \varepsilon^2 \sum_{j=1}^{N} \int_{K_j} u'(x)v'(x)dx + \sum_{j=1}^{N} \int_{K_j} c(x)u(x)v(x)dx, \\ B_2(u,\, v) &= \varepsilon^2 \sum_{j=0}^{N} \{u'(x_j)\}[v(x_j)], \quad B_3(u,\, v) = \sum_{j=0}^{N} \sigma_j [u(x_j)][v(x_j)], \end{aligned}$$

and

$$l(v) = \sum_{j=1}^{N} \int_{K_j} fv dx,$$

where, $\sigma_j \geq 0$ $(j = 0, 1, \ldots, N)$ are the so-called discontinuity-penalization parameters associated with the node x_j.

Lemma 2.2.2. *Let u be the exact solution of the problem (2.2.1). Then the bilinear form $B(.,.)$ defined in (2.2.4) satisfies the Galerkin orthogonality property:*

$$B(u - u_h,\, v) = 0, \quad \forall v \in V_N^k(\Omega).$$

Proof. Since, u is the exact solution of (2.2.1), we have $[u(x_j)] = 0$, $0 \leq j \leq N$ and $[u'(x_j)] = 0$, $1 \leq j \leq N-1$. Then, for all $v \in V_N^k(\Omega)$, we easily get

$$B(u,\, v) = \sum_{j=1}^{N} \int_{K_j} (\varepsilon^2 u'(x)v'(x) + c(x)u(x)v(x))dx + \varepsilon^2 \sum_{j=0}^{N} \{u'(x_j)\}[v(x_j)].$$

By using integration by parts and the definition of jump and average, one can show that

$$\varepsilon^2 \sum_{j=1}^{N} \int_{K_j} u'(x)v'(x)dx = -\varepsilon^2 \sum_{j=1}^{N} \int_{K_j} u''(x)v(x)dx - \varepsilon^2 \sum_{j=0}^{N} \{u'(x_j)\}[v(x_j)].$$

Applying the above estimate and recalling BVP (2.2.1), we can obtain

$$B(u - u_h,\, v) = 0, \qquad \forall v \in V_N^k(\Omega),$$

which is the required result. ∎

Discrete energy norm associated with the bilinear form $B(.,.)$ is

$$|||v|||^2 = \varepsilon^2 \sum_{i=1}^{N} h_i \sum_{j=1}^{p} w_j v'(x_{ij})^2 + \sum_{i=1}^{N} \beta^2 \|v\|^2_{L^2(K_i)} + \sum_{i=0}^{N} \sigma_i [v(x_i)]^2, \tag{2.2.5}$$

where x_{ij} are the Gauss points in element $K_i = (x_{i-1}, x_i)$, $w_j > 0$ are weights for the p-point Gaussian quadrature rule and σ_i are the penalty parameters. It is easy to show

that, the bilinear form given in (2.2.4) satisfies the coercivity condition. Hence it can be verified that

$$|||u_h||| \leq \|f\|_{L^2(\Omega)},$$

which implies the uniqueness of the solution of (2.2.4). Because of the finite-dimensional space, the existence of the solution follows from its uniqueness.

Now, we perform the error analysis for the NIPG method (2.2.4). To obtain the error estimate, we decompose the error into two parts, as

$$|||u - u_h||| \leq |||u - u_I||| + |||u_I - u_h|||.$$

Let $\eta = u - u_I$ and $\xi = u_I - u_h$, where η and ξ are known as the interpolation and discretization errors, respectively.

2.2.1 Interpolation error

In this subsection, we shall estimate the error using piecewise Lagrange interpolation at the Gauss points.

Let

$$F_i(t) = \left(\frac{x_{i-1} + x_i}{2}\right) + \left(\frac{x_i - x_{i-1}}{2}\right) t.$$

Then, F_i maps the interval $[-1,\ 1]$ to $[x_{i-1},\ x_i]$. Let

$$-1 = t_0^k < t_1^k < t_2^k < \cdots < t_k^k = 1$$

be the Lobatto points in $[-1,\ 1]$, *i.e.*, the $k+1$ zeros of the polynomial

$$\Phi_{k+1}(t) = \frac{d^{k-1}}{dt^{k-1}}(t^2 - 1)^k.$$

For $i \in 1, 2, \cdots, N$, let $x_{i,j} = F_i(t_j^k)$, and u_I denote the piecewise Lagrange interpolation using $\{x_{i,j}\}_{j=0}^k$ as nodal points on each interval $[x_{i-1},\ x_i]$. Then, we have for $x \in [x_{i-1},\ x_i]$,

$$\begin{aligned}
(u - u_I)(x) &= \frac{u^{(k+1)}(x)}{(2k)!}\Phi_{i,k+1}(x) + \mathcal{O}(h_i^{k+1}) \int_{x_{i-1}}^{x_i} |u^{(k+2)}(x)|dx, \\
(u - u_I)'(x) &= \frac{u^{(k+1)}(x)}{(2k)!}\Psi_{i,k}(x) + \mathcal{O}(h_i^k) \int_{x_{i-1}}^{x_i} |u^{(k+2)}(x)|dx,
\end{aligned}$$

where

$$\Phi_{i,k+1}(x) = \frac{d^{k-1}}{dx^{k-1}}\left((x - x_{i-\frac{1}{2}})^2 - \frac{h_i^2}{4}\right)^k, \quad \Psi_{i,k}(x) = \Phi'_{i,k+1}(x).$$

Since the leading term of the above equation vanishes at the Gauss points $x = x_{ij}$, we have

$$|(u - u_I)'(x_{i,j})| \leq C h_i^k \int_{x_{i-1}}^{x_i} |u^{(k+2)}(x)|dx.$$

We know that estimate for the interpolation error $u - u_I$, for any $u \in H^{k+1}(\Omega, \mathcal{T}_N)$ is

$$\|u - u_I\|_{j,\mathcal{T}_N} \leq Ch^{k+1-j}|u|_{k+1,\mathcal{T}_N}, \ 0 \leq j \leq k+1.$$

The solution u of the BVP (2.2.1) can be decomposed as $u = S + E$ and let S_I and E_I be the interpolants of S and E on the piecewise uniform Shishkin mesh. Hence

$$|||u - u_I||| \leq |||S - S_I||| + |||E - E_I|||.$$

Theorem 2.2.3. *The following result holds true for the interpolation error corresponding to the smooth part*

$$|||S - S_I||| \leq C(N^{-1}\ln N)^{k+1}.$$

Proof. Using the definition of the discrete energy norm (2.2.5) and the fact that S_I be the interpolant of S, we have

$$|||S - S_I||| = \varepsilon^2 \sum_{i=1}^{N} h_i \sum_{j=1}^{p} w_j (S - S_I)'(x_{ij})^2 + \beta^2 \sum_{i=1}^{N} \|S - S_I\|^2_{L^2(K_i)}. \tag{2.2.6}$$

First term in the RHS of (2.2.6) satisfies

$$\begin{aligned}
\varepsilon^2 \sum_{i=1}^{N} h_i \sum_{j=1}^{p} w_j (S - S_I)'(x_{ij})^2 &\leq C \sum_{i=1}^{N} h_i h_i^{2k} \left(\int_{x_{i-1}}^{xi} |S^{(k+2)}(x)| dx \right)^2 \\
&\leq C \sum_{i=1}^{N} h_i^{2k+3} \\
&\leq C \sum_{i=1}^{N/4} h_i^{2k+3} + \sum_{i=N/4+1}^{3N/4} h_i^{2k+3} + \sum_{i=3N/4+1}^{N} h_i^{2k+3} \\
&\leq C(N^{-1}\ln N)^{2k+2},
\end{aligned} \tag{2.2.7}$$

by using

$$|(S - S_I)'(x_{ij}| \leq Ch_i^k \int_{x_{i-1}}^{x_i} |S^{(k+2)}(x)| dx.$$

The second term in the RHS of (2.2.6) can be bounded as

$$\begin{aligned}
\sum_{i=1}^{N} \|S - S_I\|_{L^2(K_i)} &\leq C \sum_{i=1}^{N} h_i^{k+1} \int_{x_{i-1}}^{xi} |S^{(k+1)}(x)| dx \\
&\leq C \sum_{i=1}^{N} h_i^{k+2} \leq C(N^{-1}\ln N)^{k+1}.
\end{aligned} \tag{2.2.8}$$

Using the estimates obtained in (2.2.7) and (2.2.8) in (2.2.6), we get the desired result. ∎

Lemma 2.2.4. *The following result holds true for interpolation error in maximum norm for the layer part:*

$$\|(E - E_I)^{(q)}\|_{L^\infty(\Omega_2)} \leq C\varepsilon^{-q} N^{-(k+1)}.$$

Proof. Here, we will derive the estimate in the maximum norm. That is,

$$\begin{aligned} \|(E - E_I)^{(q)}\|_{L^\infty(\Omega_2)} &\leq \|E^{(q)}\|_{L^\infty(\Omega_2)} + \|E_I^{(q)}\|_{L^\infty(\Omega_2)} \\ &\leq \|E^{(q)}\|_{L^\infty(\Omega_2)}, \ \big(\text{using } \|E_I^{(q)}\|_{L^\infty(\Omega_2)} \leq \|E^{(q)}\|_{L^\infty(\Omega_2)}\big), \end{aligned}$$

and

$$\begin{aligned} \|E^{(q)}\|_{L^\infty(\Omega_2)} &\leq C\varepsilon^{-q} \max_{[\tau_\varepsilon, 1-\tau_\varepsilon]} (\exp(-\beta x/\varepsilon) + \exp(-\beta(1-x)/\varepsilon)) \\ &\leq C\varepsilon^{-q} N^{-(k+1)}, \big(\text{using } \tau_\varepsilon = ((k+1)\varepsilon/\beta)\ln N\big). \end{aligned}$$

Hence, we obtain that

$$\|(E - E_I)^{(q)}\|_{L^\infty(\Omega_2)} \leq C\varepsilon^{-q} N^{-(k+1)}.$$

This completes the proof. ∎

Theorem 2.2.5. *The interpolation error for the layer part satisfy the following bound:*

$$|||E - E_I||| \leq C(N^{-1}\ln N)^{k+1}.$$

Proof. Here, we will derive the required bounds separately for fine part and coarse part of the mesh.

Case 1- (Inner-region)

For the boundary layer regions, we have

$$|||E - E_I|||^2_{\Omega_1} = \varepsilon^2 \sum_{i=1}^{N/4} h_i \sum_{j=1}^{p} w_j (E - E_I)'(x_{ij})^2 + \beta^2 \sum_{i=1}^{N/4} \|E - E_I\|^2_{L^2(K_i)}. \tag{2.2.9}$$

The first term in the RHS of the above expression satisfies

$$\begin{aligned} \varepsilon^2 \sum_{i=1}^{N/4} h_i \sum_{j=1}^{p} w_j (E - E_I)'(x_{ij})^2 &\leq C\varepsilon^2 \sum_{i=1}^{N/4} h_i h_i^{2k} \left(\int_{x_{i-1}}^{xi} |E^{(k+2)}(x)| dx \right)^2 \\ &\leq C\varepsilon^2 \sum_{i=1}^{N/4} h_i^{2k+1} \left(\int_{x_{i-1}}^{xi} |E^{(k+2)}(x)|^2 dx \right) \left(\int_{x_{i-1}}^{xi} dx \right) \\ &\leq C\varepsilon^2 \sum_{i=1}^{N/4} h_i^{2k+2} \left(\int_{x_{i-1}}^{xi} \varepsilon^{-2(k+2)} D_\varepsilon(x)^2 dx \right) \\ &\leq C\varepsilon^{-2(k+1)} h_i^{2(k+1)} \leq C(N^{-1}\ln N)^{2(k+1)}. \end{aligned}$$

Now for the second term in the RHS of (2.2.9), we have

$$\begin{aligned}\sum_{i=1}^{N/4}\|E-E_I\|^2_{L^2(K_i)} &\leq Ch_i^{2(k+1)}\|E^{(k+1)}\|^2_{L^2(K_i)}\\ &\leq Ch_i^{2(k+1)}\left(\int_{x_{i-1}}^{xi}\varepsilon^{-2(k+1)}D_\varepsilon(x)^2dx\right)\\ &\leq C(N^{-1}\ln N)^{2(k+1)}.\end{aligned}$$

Hence, we obtain that

$$|||E-E_I|||_{\Omega_1}\leq C(N^{-1}\ln N)^{(k+1)}.$$

Similarly, one can show that

$$|||E-E_I|||_{\Omega_3}\leq C(N^{-1}\ln N)^{(k+1)}.$$

Case 2- (Outer-region)

Now, we will derive the estimate on the coarse part Ω_2

$$|||E-E_I|||_{\Omega_2}=\varepsilon^2\sum_{i=N/4+1}^{3N/4}h_i\sum_{j=1}^{p}w_j(E-E_I)'(x_{ij})^2+\beta^2\sum_{i=N/4+1}^{3N/4}\|E-E_I\|^2_{L^2(K_i)}. \quad (2.2.10)$$

By using Lemma 2.2.4, the first term in the RHS of the above expression satisfies

$$\varepsilon^2\sum_{i=N/4+1}^{3N/4}h_i\sum_{j=1}^{p}w_j(E-E_I)'(x_{ij})^2 \leq \varepsilon^2\sum_{i=N/4+1}^{3N/4}h_i\varepsilon^{-2}N^{-2(k+1)}\leq CN^{-(k+1)}.$$

The second term in the RHS of (2.2.10) can be express as

$$\|E-E_I\|^2_{L^2(\Omega_2)}\leq\|E\|^2_{L^2(\Omega_2)}+\|E_I\|^2_{L^2(\Omega_2)}.$$

Here, we derive both the terms separately as follows

$$\|E\|^2_{L^2(\Omega_2)} = \sum_{i=N/4+1}^{3N/4}\|E\|^2_{L^2(I_i)}\leq C\sum_{i=N/4+1}^{3N/4}\int_{I_i}D_\varepsilon(x)^2dx\leq CN^{-2(k+1)}$$

and

$$\begin{aligned}\|E_I\|^2_{L^2(\Omega_2)} &\leq \sum_{i=N/4+1}^{3N/4}\|E_I\|^2_{L^2(I_i)}\leq\sum_{i=N/4+1}^{3N/4}\int_{x_{i-1}}^{x_i}(E_I)^2dx\\ &\leq \sum_{i=N/4+1}^{3N/4}h_i\|E_I\|^2_{L^\infty(I_i)}\leq CN^{-2(k+1)}.\end{aligned}$$

Hence, we obtain that

$$|||E-E_I|||_{L^2(\Omega_2)}\leq CN^{-(k+1)}.$$

Combining the result obtained in case 1 and case 2, we get

$$|||E - E_I||| \leq C(N^{-1} \ln N)^{k+1},$$

which is the required error bound. ∎

Theorem 2.2.6. *Let u be the solution of the problem (2.2.1) and u_I be its piecewise Lagrange interpolation at the Gauss points, then the interpolation error satisfies*

$$|||u - u_I||| \leq C(N^{-1} \ln N)^{k+1}.$$

Proof. Since, we have

$$|||u - u_I||| \leq |||S - S_I||| + |||E - E_I|||,$$

then, by combining Theorems 2.2.3 and 2.2.5, we get our desired result. ∎

2.2.2 Discretization error

We proceed with the analysis of the discretization error $\xi = u_I - u_h$. By using the coercivity and the Galerkin orthogonality, we can have

$$|||\xi|||^2 \leq B(\xi, \xi) = B(u - u_h, \xi) - B(\eta, \xi) = -B(\eta, \xi).$$

Theorem 2.2.7. *The following estimate holds true:*

$$B(\eta, \xi) \leq C(N^{-1} \ln N)^{k+1} |||\xi|||.$$

Proof. Since $\eta(x_j) = 0$, for $j = 0, 1, 2, \cdots N$, which implies that $[\eta(x_j)] = 0$. By using this we can estimate $B_2(\xi, \eta) = 0$, and $B_3(\eta, \xi) = 0$. Also $B_1(\eta, \xi)$ can be written as

$$B_1(\eta, \xi) = \sum_{j=1}^{N} \int_{K_j} \varepsilon^2 \eta'(x)\xi'(x)dx + \sum_{j=1}^{N} \int_{K_j} c(x)\eta(x)\xi(x)dx. \tag{2.2.11}$$

We proceed with separate estimates for each term that appears in the above equation, first term in the RHS of (2.2.11)

$$\begin{aligned} \sum_{j=1}^{N} \int_{K_j} \varepsilon^2 \eta'(x)\xi'(x)dx &\leq \left(\sum_{j=1}^{N} \int_{K_j} \varepsilon^2 (\eta')^2(x)dx \right)^{1/2} \left(\sum_{j=1}^{N} \int_{K_j} \varepsilon^2 (\xi')^2(x)dx \right)^{1/2} \\ &\leq C(N^{-1} \ln N)^{k+1} |||\xi|||, \end{aligned} \tag{2.2.12}$$

and for the second term in the RHS of (2.2.11)

$$\sum_{j=1}^{N} \int_{K_j} c(x)\eta(x)\xi(x)dx \leq C\|\eta\|_{L^2(\Omega)} \|\xi\|_{L^2(\Omega)} \leq C(N^{-1} \ln N)^{k+1} |||\xi|||. \tag{2.2.13}$$

Collecting (2.2.12) and (2.2.13) into (2.2.11), we get

$$B_1(\eta, \xi) \leq C(N^{-1} \ln N)^{k+1} |||\xi|||.$$

It remains to evaluate $B_2(\eta, \xi)$ that is

$$B_2(\eta, \xi) = \varepsilon^2 \sum_{j=0}^{N} \{\eta'\}_j [\xi]_j \leq C(N^{-1} \ln N)^{k+1} |||\xi|||.$$

Now combining all the above estimates, we get

$$B(\eta, \xi) = B_1(\eta, \xi) + B_2(\eta, \xi) - B_2(\xi, \eta) + B_3(\eta, \xi) \leq C(N^{-1} \ln N)^{k+1} |||\xi|||.$$

Hence, we get our desired result. ∎

Theorem 2.2.8. *Let u be the solution of the problem (2.2.1) and u_h be the solution of the problem (2.2.4), then, we have*

$$|||u - u_h||| \leq C(N^{-1} \ln N)^{k+1}.$$

Proof. Using the coercivity property and the Galerkin orthogonality, we have

$$|||\xi|||^2 \leq B(\xi, \xi) = B(u - u_h, \xi) - B(\eta, \xi) = -B(\eta, \xi).$$

From Theorem 2.2.7, we get

$$|||\xi||| \leq C(N^{-1} \ln N)^{k+1}.$$

Combining this with the interpolation error obtained in Theorem 2.2.6, we can obtain the desired result. ∎

2.3 Convection-Diffusion BVP

Consider the following singularly perturbed convection-diffusion BVP:

$$\begin{cases} -\varepsilon u''(x) + b(x)u'(x) + c(x)u(x) = f(x), \quad x \in \Omega, \\ u(0) = u(1) = 0, \end{cases} \tag{2.3.1}$$

with

$$b(x) \geq \beta > 0, \;\; \gamma^2 = \min_{x\in\Omega} \left(c(x) - \frac{b'(x)}{2} \right) > 0, \;\; \forall x \in \Omega,$$

where $0 < \varepsilon \ll 1$ is the perturbation parameter. The coefficients $b(x)$, $c(x)$ and the source function $f(x)$ are sufficiently smooth functions. We know that, solution $u(x)$ of (2.3.1) exhibits boundary layer of width $\mathcal{O}(\varepsilon \ln \varepsilon)$ at $x = 1$.

Lemma 2.3.1. *[31] The exact solution u of the BVP (2.3.1) can be decomposed as $u = S + E$, where, S and E are smooth and layer parts, respectively. Then for any positive integer p, the following bounds hold true:*

$$|S^{(l)}(x)| \leq C, \tag{2.3.2}$$

$$|E^{(l)}(x)| \leq C\varepsilon^{-l} \exp((-\beta(1-x))/\varepsilon), \quad 0 \leq l \leq p, \tag{2.3.3}$$

where p depends on the regularity of the coefficients.

Proof. For detailed proof, one can refer [56]. ∎

To discretize the domain Ω, we use the layer-adapted piecewise uniform Shishkin mesh, which is described as follows. Since, there is a boundary layer at $x = 1$, the mesh should be condensed in the neighborhood of $x = 1$. Hence, we divide the domain Ω into two subdomains as $\Omega = \Omega_1 \cup \Omega_2$, where Ω_1 and Ω_2 are $[0,\ \tau_\varepsilon]$ and $[1-\tau_\varepsilon,\ 1]$, respectively. Here, the transition point τ_ε is defined by

$$\tau_\varepsilon = \min\left(\frac{1}{2}, \frac{\alpha\varepsilon}{\beta} \ln N \right),$$

where, the constant α is typically chosen to accommodate the error analysis. Here, we will assume that $\tau_\varepsilon = (\alpha\varepsilon/\beta)\ln N$, otherwise N^{-1} is much smaller than ε, which is rare in practice. The mesh-width on the coarse part of the mesh is $h_i = H = 2(1-\tau_\varepsilon)/N,\ i = 1, \ldots, N/2$, with $1/N \leq H \leq 2/N$, whereas on the fine part of the mesh we have $h_i = 2\tau_\varepsilon/N, i = N/2+1, \ldots, N$.

By using the NIPG method, the finite element approximation for convection-diffusion problem is

$$\begin{cases} \text{find } u_h \in V_N^k(\Omega), \text{ such that} \\ B(u_h,\, v_h) = l(v_h), \forall v_h \in V_N^k(\Omega), \end{cases} \tag{2.3.4}$$

with $B(u,\, v) = B_1(u,\, v) + B_2(u,\, v) - B_2(v,\, u) + B_3(u,\, v)$, where

$$\begin{aligned} B_1(u,\, v) &= \sum_{j=1}^{N} \varepsilon \int_{K_j} u'(x)v'(x)dx + \sum_{j=1}^{N} \int_{K_j} (b(x)u'(x) + c(x)u(x))v(x)dx, \\ B_2(u,\, v) &= \sum_{j=0}^{N} \varepsilon\{u'(x_j)\}[v(x_j)], \\ B_3(u,\, v) &= \sum_{j=0}^{N} \sigma_j[u(x_j)][v(x_j)] + \sum_{j=0}^{N} b(x_j)[u(x_j)]v(x_j^-), \end{aligned}$$

and

$$l(v) = \sum_{j=1}^{N} \int_{K_j} fvdx,$$

where, $\sigma_j \geq 0$ $(j = 0, 1, \ldots, N)$ are the so-called discontinuity-penalization parameters associated with the node x_j.

Lemma 2.3.2. *Let u be the exact solution of the problem (2.3.1), then the bilinear form $B(.,.)$ defined in (2.3.4) satisfies the Galerkin orthogonality property:*

$$B(u - u_h,\, v) = 0, \quad \forall v \in V_N^k(\Omega).$$

Proof. Since u is the exact solution of (2.3.1), we have $[u(x_j)] = 0$, $0 \leq j \leq N$ and $[u'(x_j)] = 0$, $1 \leq j \leq N-1$. Then, for all $v \in V_N^k(\Omega)$, we easily get

$$B(u,\, v) = \sum_{j=1}^{N} \int_{K_j} (\varepsilon u'(x)v'(x) + b(x)u'(x)v(x) + c(x)u(x)v(x))dx + \varepsilon \sum_{j=0}^{N} \{u'(x_j)\}[v(x_j)].$$

By using integration by parts and the definition of jump and average, one can show that

$$\varepsilon \sum_{j=1}^{N} \int_{K_j} u'(x)v'(x)dx = -\varepsilon \sum_{j=1}^{N} \int_{K_j} u''(x)v(x)dx - \varepsilon \sum_{j=0}^{N} \{u'(x_j)\}[v(x_j)].$$

Applying the above estimate and recalling BVP (2.3.1), we can obtain

$$B(u - u_h,\, v) = 0, \qquad \forall v \in V_N^k(\Omega).$$

This is the required result. ∎

Discrete energy norm associated with the bilinear form $B(.,.)$ is

$$|||v|||^2 = \varepsilon \sum_{i=1}^{N} h_i \sum_{j=1}^{p} w_j v'(x_{ij})^2 + \gamma^2 \sum_{i=1}^{N} \|v\|^2_{L^2(K_i)} + \sum_{i=0}^{N} \left(\frac{1}{2} b(x_i) + \sigma_i\right) [v(x_i)]^2, \quad (2.3.5)$$

where x_{ij} are the Gauss points in element $K_i = (x_{i-1}, x_i)$, $w_j > 0$ are weights for the p-point Gaussian quadrature rule and σ_i are the penalty parameters. It is easy to show

that, the bilinear form given in (2.3.4) satisfies the coercivity condition. Hence it can be shown that

$$|||u_h||| \leq \|f\|_{L^2(\Omega)},$$

which implies the uniqueness of the solution of (2.3.4). Because of the finite-dimensional space, the existence of the solution follows from its uniqueness.

2.3.1 Interpolation error

The solution u of the BVP (2.3.1) can be decomposed as $u = S + E$ and let S_I and E_I be the interpolants of S and E on the piecewise uniform Shishkin mesh. Hence, we have

$$|||u - u_I||| \leq |||S - S_I||| + |||E - E_I|||.$$

Theorem 2.3.3. *Let u be the solution of the problem (2.3.1) and u_I be its piecewise Lagrange interpolation on the piecewise uniform Shishkin mesh, then*

$$|||u - u_I||| \leq C(N^{-1} \ln N)^{k+1}.$$

Proof. By following the approach as discussed in Theorem 2.2.6, one can derive the required result. ∎

2.3.2 Discretization error

We proceed with the analysis of the discretization error $\xi = u_I - u_h$. Using the coercivity and the Galerkin orthogonality, we can write

$$|||\xi|||^2 \leq B(\xi, \xi) = B(u - u_h, \xi) - B(\eta, \xi) = -B(\eta, \xi).$$

Theorem 2.3.4. *The following estimate holds true:*

$$|B(\eta, \xi)| \leq C(N^{-1} \ln N)^{k+1} |||\xi|||.$$

Proof. Since $\eta(x_j) = 0$, for $j = 0, 1, 2, \cdots N$, which implies that $[\eta(x_j)] = 0$. By using this we can estimate $B_2(\xi, \eta) = 0$, and $B_3(\eta, \xi) = 0$. Therefore, from the bilinear form given in (2.3.4), we have

$$\begin{aligned} B_1(\eta, \xi) = \sum_{j=1}^{N} \int_{K_j} \varepsilon \eta'(x)\xi'(x)dx &- \sum_{j=1}^{N} \int_{K_j} b(x)\eta(x)\xi'(x)dx \\ &+ \sum_{j=1}^{N} \int_{K_j} (c(x) - b'(x))\eta(x)\xi(x)dx. \quad (2.3.6) \end{aligned}$$

We proceed with separate estimate for each term that appears in the above equation, first term in the RHS of (2.3.6)

$$\begin{aligned}\sum_{j=1}^{N}\int_{K_j}\varepsilon\eta'(x)\xi'(x)dx &\leq \left(\sum_{j=1}^{N}\int_{K_j}\varepsilon(\eta')^2(x)dx\right)^{1/2}\left(\sum_{j=1}^{N}\int_{K_j}\varepsilon(\xi')^2(x)dx\right)^{1/2}\\ &\leq C(N^{-1}\ln N)^{k+1}|||\xi|||,\end{aligned}$$

bound for the second term in the RHS of (2.3.6) is

$$\begin{aligned}\left|-\sum_{j=1}^{N}\int_{K_j}b(x)\eta\xi'dx\right| &\leq C\big(\|\eta\|_{L^\infty(\Omega_1)}\|\xi'\|_{L^1(\Omega_1)}+\|\eta\|_{L^\infty(\Omega_2)}\|\xi'\|_{L^1(\Omega_2)}\big)\\ &\leq C(N^{-1}\ln N)^{k+1}|||\xi|||,\end{aligned}$$

and for the last term in the RHS of (2.3.6), we have

$$\sum_{j=1}^{N}\int_{K_j}(c(x)-b'(x))\eta(x)\xi(x)dx \leq C\|\eta\|_{L^2(\Omega)}\|\xi\|_{L^2(\Omega)} \leq C(N^{-1}\ln N)^{k+1}|||\xi|||.$$

Combining the above estimates, we get

$$B_1(\eta,\,\xi)\leq C(N^{-1}\ln N)^{k+1}|||\xi|||.$$

It remains to evaluate $B_2(\eta,\,\xi)$, that is,

$$B_2(\eta,\,\xi)=\varepsilon\sum_{j=0}^{N}\{\eta'\}_j[\xi]_j \leq C(N^{-1}\ln N)^{k+1}|||\xi|||.$$

Now combining all the above estimates, we obtain that

$$B(\eta,\,\xi)=B_1(\eta,\,\xi)+B_2(\eta,\,\xi)-B_2(\xi,\,\eta)+B_3(\eta,\,\xi)\leq C(N^{-1}\ln N)^{k+1}|||\xi|||.$$

Hence we get our desired result. ∎

Theorem 2.3.5. *Let u be the solution of the problem (2.3.1) and u_h be the solution of the problem (2.3.4), then*

$$|||u-u_h|||\leq C(N^{-1}\ln N)^{k+1}.$$

Proof. We know that

$$|||\xi|||^2 \leq B(\xi,\,\xi)=B(u-u_h,\,\xi)-B(\eta,\,\xi)=-B(\eta,\,\xi).$$

By using Theorem 2.3.4, we get

$$|||\xi||| \leq C(N^{-1}\ln N)^{k+1},$$

combining this with the interpolation error given in Theorem 2.3.3, we get the required estimate. ∎

2.4 Numerical Result

Here, we experimentally verify the convergence results by considering the numerical solution of the following two-point BVPs.

2.4.1 For reaction-diffusion BVP

Example 2.4.1. *Consider the singularly perturbed reaction-diffusion BVP on* $(0, 1)$*:*

$$\begin{cases} -\varepsilon^2 u''(x) + u(x) = x, \\ u(0) = u(1) = 0. \end{cases} \tag{2.4.1}$$

The exact solution is

$$u(x) = x - \frac{e^{(x-1)/\varepsilon} - e^{-(x+1)/\varepsilon}}{1 - e^{-2/\varepsilon}}.$$

To visualize the appearance of the boundary layer, we have given plots of the exact and numerical solutions and their corresponding error (error=|exact solution − numerical solution|) for Example 2.4.1 for $\varepsilon = 10^{-2}$ with $N = 32$.

We calculate the error in the discrete energy norm as defined in (2.2.5) also in L^2-norm and maximum norm. The order of convergence is computed by using the formula $r = \ln(e_N/e_{2N})/\ln 2$, where, e_N is the computational error with N number of intervals. Tables 2.1, 2.2 and 2.3 provide the numerical results in discrete energy norm, L^2-norm and maximum norm respectively, with the linear finite element space. Tables 2.4, 2.5 and 2.6 provide the numerical results in discrete energy norm, L^2-norm and maximum norm respectively, with the quadratic finite element space. To visualize the order of convergence of the numerical solutions, we have given the loglog plot for $\varepsilon = 10^{-6}$. Figure 2.2(a) and 2.2(b) depict the order of convergence in the discrete energy norm, L^2-norm and maximum norm in the loglog scale using the NIPG method for Example 2.4.1 with linear and quadratic finite element space, respectively.

2.4.2 For convection-diffusion BVP

Example 2.4.2. *Consider the following singularly perturbed BVP:*

$$\begin{cases} -\varepsilon u''(x) + u'(x) + u(x) = f(x), \quad x \in \Omega, \\ u(0) = u(1) = 0, \end{cases} \tag{2.4.2}$$

where, $f(x)$ is chosen such that

$$u(x) = (1 - \exp((x-1)/\varepsilon)) \sin x,$$

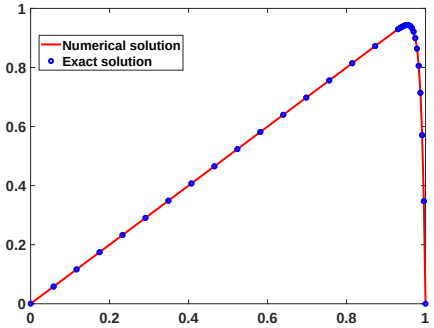

(a) Solution

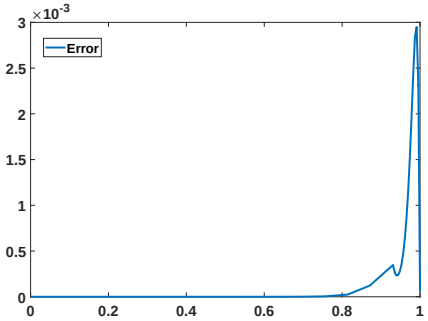

(b) Error

Figure 2.1: Solution and corresponding error for Example 2.4.1 for $\varepsilon = 10^{-2}$ with $N = 32$.

Table 2.1: *Error in the discrete energy norm and order of convergence for Example 2.4.1 for* $k = 1$.

ε	Number of mesh intervals N					
	32	64	128	256	512	1024
1	4.4398e-04	1.5788e-04	5.5980e-05	1.9820e-05	7.0125e-06	2.4802e-06
	1.4916	1.4959	1.4979	1.4990	1.4995	
10^{-2}	3.1340e-03	1.0709e-03	3.5022e-04	1.1086e-04	3.4222e-05	1.0352e-05
	1.5491	1.6125	1.6594	1.6958	1.7250	
10^{-4}	3.1325e-03	1.0696e-03	3.4963e-04	1.1065e-04	3.4138e-05	1.0305e-05
	1.5503	1.6132	1.6598	1.6966	1.7280	
10^{-6}	8.6189e-03	3.1327e-03	1.0696e-03	3.4935e-04	1.1011e-04	3.0472e-05
	1.4601	1.5504	1.6143	1.6657	1.8534	

is the exact solution of (2.4.2).

Exact and numerical solutions and their corresponding error (error=|exact solution − numerical solution|) for Example 2.4.2 for $\varepsilon = 10^{-2}$ with $N = 32$ are shown in Figure 2.3.

We calculate the error in the discrete energy norm as defined in (2.3.5) also in L^2-norm and maximum norm. The order of convergence is computed by using the formula $r = \ln(e_N/e_{2N})/\ln 2$, where, e_N is the computation error with N number of intervals. Tables 2.7, 2.8 and 2.9 provide the numerical result in discrete energy norm, L^2-norm and maximum norm, respectively, with the linear finite element space. Tables 2.10, 2.11 and 2.12 provide the numerical result in discrete energy norm, L^2-norm and maximum norm, respectively, with the quadratic finite element space. To visualize the order of convergence of the numerical solutions, we have given the loglog plot for $\varepsilon = 10^{-6}$. Figure 2.4(a) and 2.4(b) depict the order of convergence in the discrete energy norm, L^2-norm

Table 2.2: *Error in the L^2-norm and the order of convergence for Example 2.4.1 for $k = 1$.*

ε	Number of mesh intervals N					
	32	64	128	256	512	1024
1	2.1538e-04	5.3950e-05	1.3500e-05	3.3764e-06	8.4429e-07	2.1109e-07
	1.9972	1.9987	1.9994	1.9997	1.9998	
10^{-2}	4.0898e-04	1.4330e-04	4.8468e-05	1.5788e-05	4.9889e-06	1.5384e-06
	1.5130	1.5639	1.6182	1.6621	1.6973	
10^{-4}	1.7552e-04	3.3094e-05	7.0615e-06	1.7951e-06	5.1528e-07	1.5393e-07
	2.4070	2.2285	1.9759	1.8006	1.7431	
10^{-6}	1.7266e-04	3.0544e-05	5.4139e-06	9.6548e-07	1.7517e-07	3.4206e-08
	2.4990	2.4962	2.4873	2.4625	2.3564	

Table 2.3: *Error in the maximum norm and the order of convergence for Example 2.4.1 for $k = 1$.*

ε	Number of mesh intervals N					
	32	64	128	256	512	1024
1	4.7398e-04	1.2029e-04	3.0295e-05	7.6016e-06	1.9039e-06	4.7640e-07
	1.9784	1.9893	1.9947	1.9974	1.9987	
10^{-2}	2.9491e-03	1.0530e-03	3.5583e-04	1.1611e-04	3.6705e-05	1.1319e-05
	1.4858	1.5652	1.6157	1.6615	1.6972	
10^{-4}	2.9023e-03	1.0415e-03	3.5254e-04	1.1507e-04	3.6406e-05	1.1224e-05
	1.4785	1.5628	1.6152	1.6603	1.6976	
10^{-6}	2.9018e-03	1.0414e-03	3.5245e-04	1.1474e-04	3.5913e-05	7.9545e-06
	1.4784	1.5631	1.6191	1.6757	2.1747	

and maximum norm in the loglog scale using the NIPG method for Example 2.4.2 with linear and quadratic finite element space, respectively.

2.5 Conclusions

In this chapter, superconvergence of the NIPG method is proposed and analyzed for singularly perturbed BVPs on piecewise uniform Shishkin meshes. Theoretically, we proved that the proposed method is uniformly convergent of order $(k + 1)$ in the ε–weighted discrete energy norm, where k is the degree of the piecewise polynomial in the finite element space. Predicted order of convergence is observed through numerical experiments.

Table 2.4: *Error in the discrete energy norm and order of convergence for Example 2.4.1 for* $k = 2$.

ε	Number of mesh intervals N					
	32	64	128	256	512	1024
10^{-2}	3.2918e-04	8.3991e-05	1.9586e-05	4.3922e-06	9.6152e-07	2.0600e-07
	1.9706	2.1004	2.1568	2.1915	2.2226	
10^{-4}	9.2741e-06	2.0485e-06	3.7809e-07	6.1839e-08	9.3475e-09	1.3503e-09
	2.1786	2.4378	2.6121	2.7259	2.7913	
10^{-6}	8.9554e-07	1.9619e-07	3.5727e-08	5.7146e-09	8.3278e-10	1.1344e-10
	2.1905	2.4572	2.6443	2.7786	2.8760	
10^{-8}	8.9522e-08	1.9610e-08	3.5708e-09	5.7111e-10	8.7109e-11	1.2976e-11
	2.1907	2.4572	2.6444	2.7129	2.7470	

Table 2.5: *Error in the* L^2*-norm and the order of convergence for Example 2.4.1 for* $k = 2$.

ε	Number of mesh intervals N					
	32	64	128	256	512	1024
10^{-2}	2.6544e-04	5.9434e-05	1.0872e-05	1.7242e-06	2.4751e-07	3.3114e-08
	2.1590	2.4506	2.6566	2.8004	2.9020	
10^{-4}	2.2274e-05	4.8846e-06	8.9153e-07	1.4273e-07	2.0801e-08	2.8298e-09
	2.1891	2.4539	2.6430	2.7786	2.8778	
10^{-6}	2.2305e-06	4.8865e-07	8.9140e-08	1.4268e-08	2.0791e-09	2.8278e-10
	2.1905	2.4546	2.6433	2.7787	2.8782	
10^{-8}	2.2305e-07	4.8864e-08	8.9143e-09	1.4258e-09	2.0823e-10	4.5696e-11
	2.1905	2.4546	2.6443	2.7755	2.1880	

Table 2.6: *Error in the maximum norm and the order of convergence for Example 2.4.1 for* $k = 2$.

ε	Number of mesh intervals N					
	32	64	128	256	512	1024
10^{-2}	1.7904e-03	5.2178e-04	1.4240e-04	3.9047e-05	1.0687e-05	2.9281e-06
	1.7788	1.8736	1.8666	1.8693	1.8678	
10^{-4}	3.8497e-03	9.4966e-04	2.3107e-04	5.4715e-05	1.2272e-05	2.4725e-06
	2.0192	2.0391	2.0783	2.1566	2.3113	
10^{-6}	3.9057e-03	9.7629e-04	2.4401e-04	6.0969e-05	1.5226e-05	3.7981e-06
	2.0002	2.0004	2.0008	2.0016	2.0031	
10^{-8}	3.9062e-03	9.7656e-04	2.4414e-04	6.1034e-05	1.5258e-05	3.8145e-06
	2.0000	2.0000	2.0000	2.0000	2.0001	

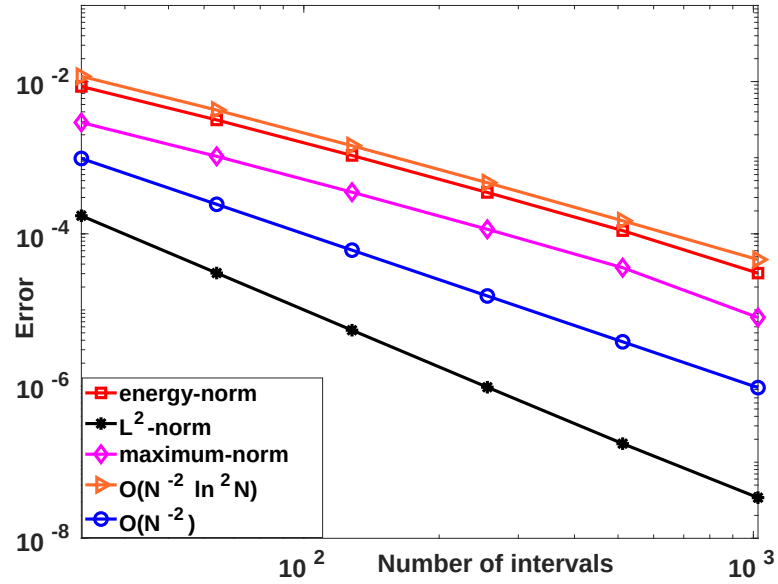

(a) For linear elements.

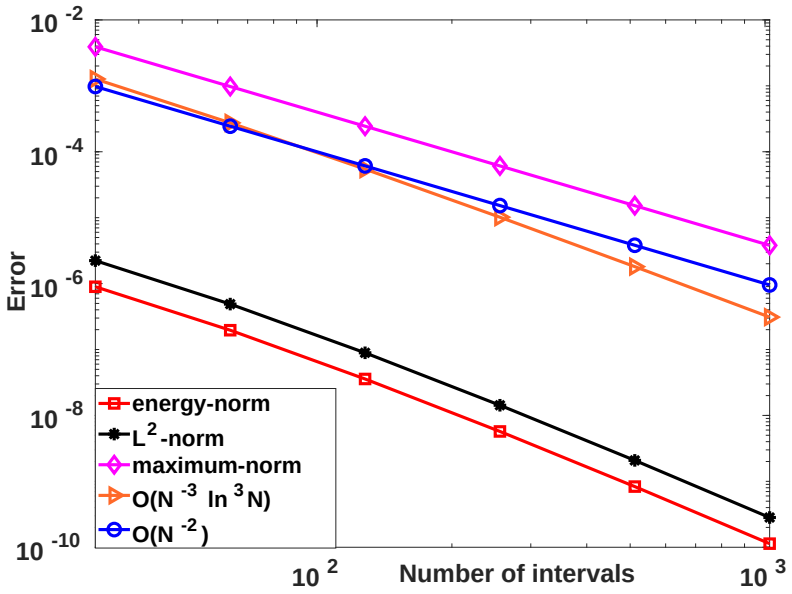

(b) For quadratic elements.

Figure 2.2: Visualization of the order of convergence through loglog plot for Example 2.4.1 for $\varepsilon = 10^{-6}$.

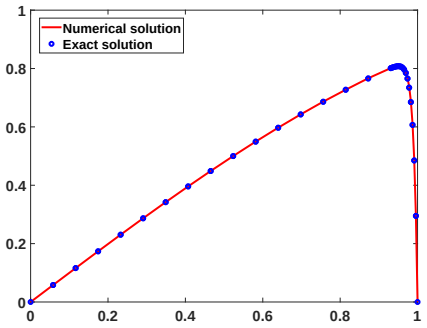

(a) Solution

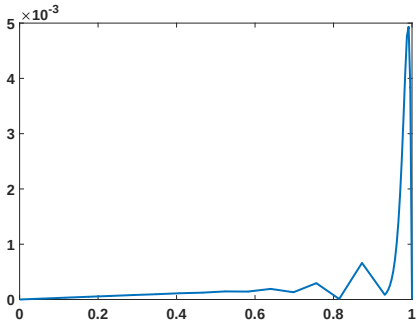

(b) Error

Figure 2.3: Solution and corresponding error for Example 2.4.2 for $\varepsilon = 10^{-2}$ with $N = 32$.

Table 2.7: *Error in the discrete energy norm and the order of convergence for Example 2.4.2 for* $k = 1$.

ε	Number of mesh intervals N					
	32	64	128	256	512	1024
1	3.6274e-03	1.4486e-03	5.8297e-04	2.3663e-04	9.6818e-05	3.9878e-05
	1.3243	1.3131	1.3008	1.2893	1.2797	
10^{-2}	3.7665e-04	1.4848e-04	5.5020e-05	1.9709e-05	6.9542e-06	2.4467e-06
	1.3429	1.4323	1.4811	1.5029	1.5070	
10^{-4}	1.1892e-04	4.6877e-05	1.7368e-05	6.2208e-06	2.1949e-06	7.7231e-07
	1.3431	1.4324	1.4813	1.5029	1.5069	
10^{-6}	1.1890e-07	4.6894e-08	1.7296e-08	6.3432e-09	2.3781e-09	7.6642e-10
	1.3423	1.4389	1.4472	1.4154	1.6336	

Table 2.8: *Error in* L^2*-norm and the order of convergence for Example 2.4.2 for* $k = 1$.

ε	Number of mesh intervals N					
	32	64	128	256	512	1024
1	6.1967e-04	1.6536e-04	4.4740e-05	1.2290e-05	3.4261e-06	9.6805e-07
	1.9059	1.8859	1.8641	1.8428	1.8234	
10^{-2}	4.2479e-04	1.2437e-04	3.7754e-05	1.1501e-05	3.4749e-06	1.0387e-06
	1.7722	1.7199	1.7149	1.7267	1.7422	
10^{-4}	3.2333e-04	7.7302e-05	1.9558e-05	5.1767e-06	1.4077e-06	3.8773e-07
	2.0644	1.9828	1.9177	1.8787	1.8602	
10^{-6}	3.1020e-04	7.0275e-05	1.6411e-05	3.9374e-06	9.6220e-07	2.3768e-07
	2.1421	2.0983	2.0594	2.0328	2.0173	

Table 2.9: *Error in maximum norm and the order of convergence for Example 2.4.2 for* $k = 1$.

ε	Number of mesh intervals N					
	32	64	128	256	512	1024
1	1.4984e-03	5.2544e-04	1.8433e-04	6.4748e-05	2.2775e-05	8.0210e-06
	1.5118	1.5112	1.5094	1.5074	1.5056	
10^{-2}	9.8797e-03	3.2485e-03	9.8393e-04	2.8717e-04	8.5487e-05	2.5248e-05
	1.6047	1.7232	1.7767	1.7481	1.7595	
10^{-4}	9.8682e-03	3.2446e-03	9.8269e-04	2.8673e-04	8.5335e-05	2.5196e-05
	1.6048	1.7232	1.7771	1.7485	1.7600	
10^{-6}	9.8664e-03	3.2400e-03	9.9500e-04	2.6672e-04	6.1770e-05	2.5878e-05
	1.6065	1.7032	1.8994	2.1104	1.2551	

Table 2.10: *Error in the discrete energy norm and the order of convergence for Example 2.4.2 for* $k = 2$.

ε	Number of mesh intervals N					
	32	64	128	256	512	1024
10^{-2}	2.0739e-04	4.4246e-05	7.9400e-06	1.2581e-06	1.8215e-07	2.4672e-08
	2.2287	2.4783	2.6579	2.7880	2.8841	
10^{-4}	2.1819e-05	4.5411e-06	7.8949e-07	1.2337e-07	1.7846e-08	2.4173e-09
	2.2645	2.5240	2.6780	2.7893	2.8841	
10^{-6}	2.1973e-06	4.6470e-07	8.3916e-08	1.3567e-08	2.0087e-09	2.6211e-10
	2.2413	2.4693	2.6288	2.7558	2.9380	
10^{-8}	2.1765e-07	4.7009e-08	8.7525e-09	1.4767e-09	2.3294e-10	4.8426e-11
	2.2110	2.4252	2.5673	2.6644	2.2661	

Table 2.11: *Error in* L^2*-norm and the order of convergence for Example 2.4.2 for* $k = 2$.

ε	Number of mesh intervals N					
	32	64	128	256	512	1024
10^{-2}	1.9188e-04	4.2009e-05	7.6547e-06	1.2243e-06	1.7832e-07	2.4254e-08
	2.1914	2.4563	2.6444	2.7794	2.8782	
10^{-4}	2.0267e-05	4.2682e-06	7.5899e-07	1.2031e-07	1.7511e-08	2.3814e-09
	2.2475	2.4915	2.6574	2.7804	2.8783	
10^{-6}	2.0376e-06	4.3157e-07	7.7368e-08	1.2257e-08	1.7729e-09	2.3945e-10
	2.2392	2.4798	2.6581	2.7895	2.8883	
10^{-8}	2.0849e-07	4.3924e-08	7.8455e-09	1.2407e-09	1.8077e-10	3.7921e-11
	2.2469	2.4851	2.6607	2.7789	2.2531	

Table 2.12: *Error in maximum norm and the order of convergence for Example 2.4.2 for* $k = 2$.

ε	Number of mesh intervals N					
	32	64	128	256	512	1024
10^{-2}	2.2168e-04	6.2157e-05	1.7370e-05	4.8279e-06	1.3330e-06	3.6569e-07
	1.8345	1.8393	1.8472	1.8567	1.8660	
10^{-4}	2.9253e-03	7.6550e-04	2.2164e-04	6.2179e-05	1.7379e-05	4.8293e-06
	1.9341	1.7882	1.8337	1.8391	1.8475	
10^{-6}	2.9599e-03	7.8299e-04	2.2165e-04	6.2184e-05	1.7380e-05	4.8301e-06
	1.9185	1.8207	1.8337	1.8391	1.8473	
10^{-8}	2.9602e-03	7.8317e-04	2.2164e-04	6.2274e-05	1.7525e-05	4.5276e-06
	1.9183	1.8211	1.8315	1.8292	1.9526	

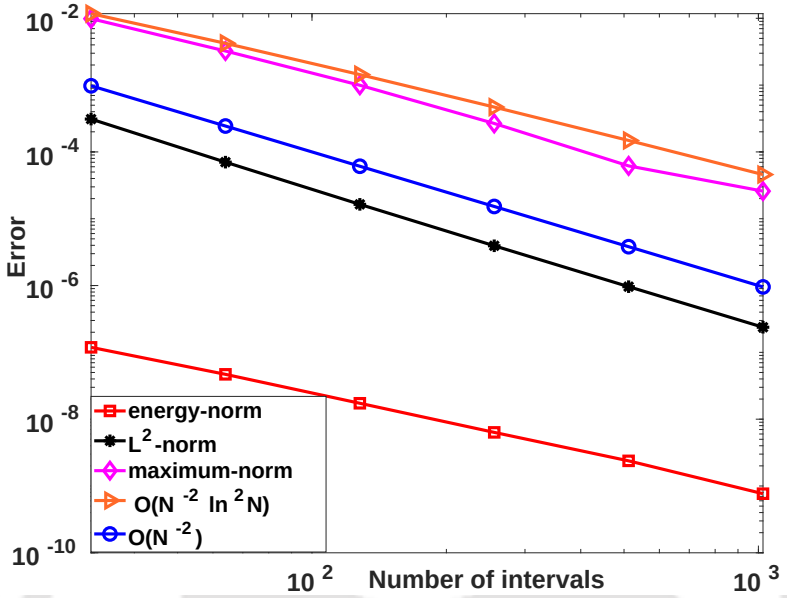

(a) For linear elements.

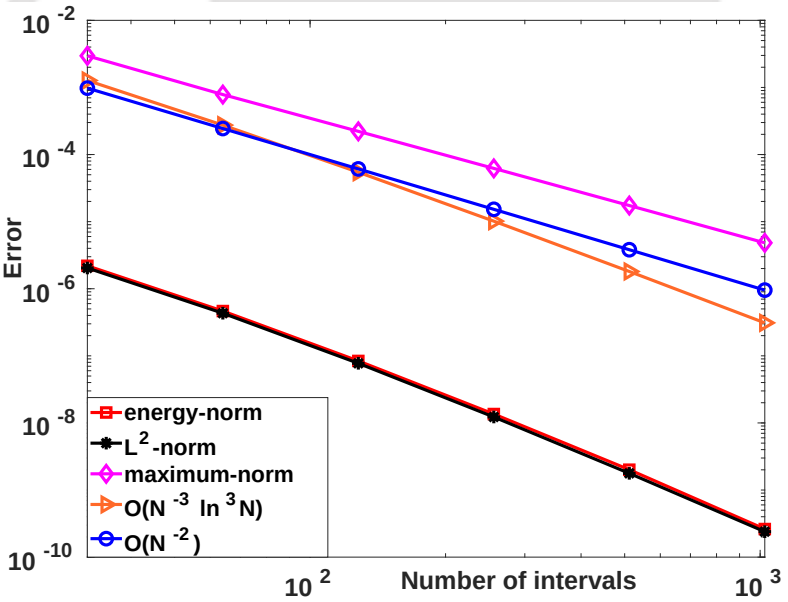

(b) For quadratic elements.

Figure 2.4: Visualization of the order of convergence through loglog plot for Example 2.4.2 for $\varepsilon = 10^{-6}$.

CHAPTER 3

Superconvergence Properties of the NIPG Method for Two–Parameter Singular Perturbation Problems on Several Layer-Adapted Grids

In this chapter, we apply the NIPG method to obtain the numerical solution of two-parameter singularly perturbed convection-diffusion-reaction BVP. In order to discretize the domain, here, we use the layer-adapted piecewise uniform Shishkin mesh, the Bakhvalov mesh and the exponentially-graded mesh. We establish a superconvergence result of the NIPG method, that is, the proposed method is parameter-uniformly convergent with the order almost $(k+1)$ on the Shishkin mesh and $(k+1)$ on the Bakhvalov mesh and on the exponentially graded mesh in the discrete energy norm, where k is the order of the polynomials. Numerical results comparing various types of meshes are presented at the end of the chapter supporting the theoretical error estimates.

3.1 Introduction

In this chapter, we consider the following two-parameter singularly perturbed two-point BVP:

$$\begin{cases} -\varepsilon_d u''(x) + \varepsilon_c b(x)u'(x) + c(x)u(x) = f(x), \quad x \in \Omega, \\ u(0) = u(1) = 0, \end{cases} \tag{3.1.1}$$

where $0 < \varepsilon_d, \varepsilon_c \ll 1$. The functions $b(x)$, $c(x)$ and $f(x)$ are assumed to be sufficiently smooth with $b(x) \geq b_0 > 0$, $c(x) \geq c_0 > 0$ and $\gamma^2 = \min\limits_{x\in\Omega}\left(c(x) - \varepsilon_c \dfrac{b'(x)}{2}\right) > 0$, where b_0, c_0 and γ are constants.

Therefore, in this chapter, we apply the NIPG method to solve singularly perturbed two-parameter BVP, on the Shishkin mesh, the Bakhvalov mesh and the exponentially graded mesh. Further, we have shown the superconvergence properties of the NIPG

method.

The rest of the chapter is organized in the following way: Bounds for the solution of the continuous problem are given in Section 3.2. Numerical discretizations are introduced in Section 3.3. Further, Section 3.4 is divided into three subsections. Error analysis on the Shishkin, Bakhvalov and exponentially graded meshes are described in Subsections 3.4.1, 3.4.2 and 3.4.3, respectively. Section 3.5 provides some numerical examples to validate the theoretical results. And the chapter ends with the conclusions.

3.2 Bound for the Solution of the Continuous Problem

Here, we present some standard results for the solution of the continuous problem (3.1.1), and bounds for the smooth and layer components of the solution. As we know that the solution of the reduced problem of (3.1.1), in general, does not satisfy both the boundary conditions, therefore, there exist boundary layers at both the boundaries, $x = 0$ and $x = 1$. To describe the layers, let r_0 and r_1 be the two solutions of the characteristic equation:

$$-\varepsilon_d r^2(x) + \varepsilon_c b(x) r(x) + c(x) = 0.$$

Here, $r_0(x) < 0$, $r_1(x) > 0$ describe the boundary layers at $x = 0$ and $x = 1$, respectively. Set

$$\mu_\ell = -\max_{x\in[0,\,1]} r_0(x) \qquad \mu_r = \min_{x\in[0,\,1]} r_1(x),$$

where μ_ℓ and μ_r are defined as

$$\mu_\ell = \min_{x\in[0,\,1]} \frac{-\varepsilon_c b(x) + \sqrt{\varepsilon_c^2 b^2(x) + 4\varepsilon_d c(x)}}{2\varepsilon_d}, \quad \mu_r = \min_{x\in[0,\,1]} \frac{\varepsilon_c b(x) + \sqrt{\varepsilon_c^2 b^2(x) + 4\varepsilon_d c(x)}}{2\varepsilon_d}.$$

Depending on the values of the perturbation parameters, we can classify the problem (3.1.1) into the following three categories:

Case 1. When $\varepsilon_d \ll \varepsilon_c = 1$, then $\mu_\ell = \mathcal{O}(\varepsilon_d^{-1})$ and $\mu_r = \mathcal{O}(1)$, this case is similar to convection-diffusion equation.

Case 2. When $\varepsilon_d \ll \varepsilon_c^2 \ll 1$, then $\mu_\ell = \mathcal{O}(\varepsilon_c \varepsilon_d^{-1})$ and $\mu_r = \mathcal{O}(\varepsilon_d^{-1})$. Here μ_r is larger than μ_ℓ, and hence the boundary layer at $x = 1$ is stronger than the boundary layer at $x = 0$.

Case 3. When $\varepsilon_c^2 \ll \varepsilon_d \ll 1$, then μ_ℓ and μ_r will be of order $\mathcal{O}(\varepsilon_d^{-1/2})$ and layers are similar to the reaction-diffusion equation.

Theorem 3.2.1. *([33]) Let $p, k \in (0, 1)$ be arbitrary and assume that*

$$\varepsilon_c\, q\|b'\|_{L^\infty(\Omega)} \leq k(1-p).$$

Then, the derivatives of the solution of the BVP (3.1.1) satisfy

$$|u^{(k)}(x)| \leq C(1+\mu_\ell^k e^{-p\mu_\ell x} + \mu_r^k e^{-p\mu_r(1-x)}), \quad x \in \Omega, \quad \text{for } 0 \leq k \leq q,$$

where q depends on the smoothness of the data. Further, the smooth and layer components of the solution $u = S + E_\ell + E_r$ satisfy the following bounds:

$$\begin{aligned} |S^{(k)}(x)| &\leq C, \\ |E_\ell^{(k)}(x)| &\leq C\mu_\ell^k e^{-p\mu_\ell x}, \\ |E_r^{(k)}(x)| &\leq C\mu_r^k e^{-p\mu_r(1-x)}, \end{aligned}$$

for $x \in \Omega$ and $0 \leq k \leq q$.

3.3 The NIPG Method

The finite element approximation using the NIPG method for the convection-diffusion-reaction problem (3.1.1) is given by

$$\begin{cases} \text{find } u_h \in V_N^k(\Omega), \text{ such that} \\ B(u_h, v_h) = l(v_h), \quad \forall v_h \in V_N^k(\Omega), \end{cases} \tag{3.3.1}$$

with $B(u, v) = B_1(u, v) + B_2(u, v) - B_2(v, u) + B_3(u, v)$, where

$$\begin{aligned} B_1(u, v) &= \sum_{j=1}^{N} \left(\varepsilon_d \int_{K_j} u'(x)v'(x)dx + \varepsilon_c \int_{K_j} b(x)u'(x)v(x)dx + \int_{K_j} c(x)u(x)v(x)dx \right), \\ B_2(u, v) &= \sum_{j=0}^{N} \varepsilon_d \{u'(x_j)\}[v(x_j)], \\ B_3(u, v) &= \sum_{j=0}^{N} \sigma_j [u(x_j)][v(x_j)] + \varepsilon_c \sum_{j=0}^{N} b(x_j)[u(x_j)]v(x_j^-), \end{aligned}$$

and

$$l(v) = \sum_{j=1}^{N} \int_{K_j} fv dx.$$

here, σ_j are the penalty parameters at the grid points x_j for $j = 0, 1, \ldots, N$.

Discrete energy norm can be defined as

$$|||v|||^2 = \varepsilon_d \sum_{i=1}^{N} h_i \sum_{j=1}^{p} w_j v'(x_{ij})^2 + \gamma^2 \sum_{i=1}^{N} \|v\|^2_{L^2(K_i)} + \sum_{i=0}^{N} \left(\frac{1}{2} b(x_i) + \sigma_i \right) [v(x_i)]^2, \tag{3.3.2}$$

where x_{ij} are the Gauss points in element $K_i = (x_{i-1}, x_i)$, $w_j > 0$ are the weights for the p-points Gaussian quadrature rule. With simple calculations, one can show that (3.3.1) satisfies the coercivity condition. Using the coercivity condition it is easy to show that

$$|||u_h||| \leq \|f\|_{L^2(\Omega)}. \tag{3.3.3}$$

Further, using inequality (3.3.3), we can show the uniqueness of the solution of (3.3.1). Because of the Rank-Nullity Theorem in finite-dimensional space and using the uniqueness of the solution we can be prove its existence.

Lemma 3.3.1. *Let u and u_h be the solutions of the continuous problem (3.1.1) and the discrete problem (3.3.1), respectively. Then the Galerkin orthogonality property can be stated as:*

$$B(u - u_h, v) = 0, \quad \forall v \in V_N^k(\Omega).$$

Proof. This can be proved by using the ideas given in Lemma 2.3.2 of Chapter 2. ∎

Here we use the piecewise Lagrange interpolation at the Gauss points. Let u_I denote the piecewise Lagrange interpolation using $\{x_{ij}\}_{j=0}^k$ as nodal points on each interval $[x_{i-1}, x_i]$. Then, we have for $x \in [x_{i-1}, x_i]$,

$$(u - u_I)(x) = \frac{u^{(k+1)}(x)}{(2k)!}\Phi_{i,k+1}(x) + \mathcal{O}(h_i^{k+1}) \int_{x_{i-1}}^{x_i} |u^{(k+2)}(x)|dx, \tag{3.3.4}$$

$$(u - u_I)'(x) = \frac{u^{(k+1)}(x)}{(2k)!}\Psi_{i,k}(x) + \mathcal{O}(h_i^{k}) \int_{x_{i-1}}^{x_i} |u^{(k+2)}(x)|dx, \tag{3.3.5}$$

where

$$\Phi_{i,k+1}(x) = \frac{d^{k-1}}{dx^{k-1}}\left(\left(x - x_{i-\frac{1}{2}}\right)^2 - \frac{h_i^2}{4}\right)^k, \quad \Psi_{i,k}(x) = \Phi'_{i,k+1}(x),$$

and

$$x_{i-\frac{1}{2}} = \frac{(x_{i-1} + x_i)}{2}.$$

The first term of Equation (3.3.5) will be zero at the Gauss points $x = x_{ij}$, using this, we can show that

$$|(u - u_I)'(x_{ij})| \leq C h_i^k \int_{x_{i-1}}^{x_i} |u^{(k+2)}(x)|dx. \tag{3.3.6}$$

It is well-known that the interpolation error $u - u_I$, for any $u \in H^{k+1}(\Omega, \mathcal{T}_N)$ satisfies

$$\|u - u_I\|_{j,\mathcal{T}_N} \leq C h^{k+1-j} |u|_{k+1,\mathcal{T}_N}, \quad 0 \leq j \leq k+1. \tag{3.3.7}$$

We decompose the solution u of the BVP (3.1.1) as $u = S + E_\ell + E_r$, where S is the smooth component, E_ℓ and E_r represent the layer components at $x = 0$ and $x = 1$, respectively. And, therefore, we have

$$|||u - u_I||| \leq |||S - S_I||| + |||E_\ell - E_{\ell,I}||| + |||E_r - E_{r,I}|||, \tag{3.3.8}$$

where S_I, $E_{\ell,I}$ and $E_{r,I}$ are respectively the interpolants of S, E_ℓ and E_r.

3.4 Error Estimates

3.4.1 On the Shishkin mesh

In this subsection, first, the Shishkin mesh for the BVP (3.1.1) is introduced, and then the NIPG method is applied on the Shishkin mesh. On Ω, the Shishkin mesh of N intervals is constructed as follows: The domain Ω is divided into three subdomains as $\Omega = \Omega_\ell \cup \Omega_o \cup \Omega_r$, here

$$\Omega_\ell = [0, \tau_0], \qquad \Omega_o = [\tau_0, 1-\tau_1], \qquad \Omega_r = [1-\tau_1, 1]$$

for some τ_0 and τ_1, where

$$\tau_0 = \min\left\{\frac{1}{4}, \frac{\tau}{\mu_\ell}\ln N\right\}, \quad \text{and} \quad \tau_1 = \min\left\{\frac{1}{4}, \frac{\tau}{\mu_r}\ln N\right\},$$

here $\tau \geq 1$ is a user chosen parameter. The step-size in each of the subdomain is given by

$$h_i = \begin{cases} \dfrac{4}{N}\dfrac{\tau}{\mu_\ell}\ln N, & \text{for } \Omega_\ell, \\ \dfrac{2(1-\tau_1-\tau_0)}{N}, & \text{for } \Omega_o, \\ \dfrac{4}{N}\dfrac{\tau}{\mu_r}\ln N, & \text{for } \Omega_r. \end{cases}$$

The following bounds on the step-size can be easily obtained

$$h_i \leq \begin{cases} C(N^{-1}\ln N)\mu_\ell^{-1}, & \text{for } \Omega_\ell, \\ CN^{-1}, & \text{for } \Omega_o, \\ C(N^{-1}\ln N)\mu_r^{-1}, & \text{for } \Omega_r. \end{cases}$$

Theorem 3.4.1. *Let S_I denotes the piecewise Lagrange interpolation of the smooth part S of the solution u of (3.1.1), then we have*

$$|||S - S_I||| \leq CN^{-(k+1)}.$$

Proof. From the definition of the discrete energy norm (3.3.2), one can have

$$|||S - S_I|||^2 = \varepsilon_d \sum_{i=1}^{N} h_i \sum_{j=1}^{p} w_j (S - S_I)'(x_{ij})^2 + \gamma^2 \sum_{i=1}^{N} \|S - S_I\|^2_{L^2(K_i)}. \tag{3.4.1}$$

We will derive the bounds separately for both the terms in the RHS of (3.4.1). The first

term can be bounded by

$$\begin{aligned}\varepsilon_d \sum_{i=1}^{N} h_i \sum_{j=1}^{p} w_j (S - S_I)'(x_{ij})^2 &\leq C \sum_{j=1}^{N} h_i h_i^{2k} \left(\int_{x_{i-1}}^{x_i} |S^{(k+2)}(x)| dx \right)^2 \\ &\leq C \sum_{i=1}^{N} h_i^{2k+3} \\ &\leq C \sum_{i=1}^{N/4} h_i^{2k+3} + \sum_{i=N/4+1}^{3N/4} h_i^{2k+3} + \sum_{i=3N/4+1}^{N} h_i^{2k+3} \\ &\leq C(N(N^{-1}\ln N)^{2k+3} {\mu_\ell}^{-(2k+3)} + N^{-2(k+1)}), \quad (3.4.2)\end{aligned}$$

where, we have used the inequality given in (3.3.6), and $\mu_r^{-1} \leq \mu_\ell^{-1}$ and the values of the step-size. Bound for the second term in the RHS of (3.4.1) is given by

$$\begin{aligned}\sum_{i=1}^{N} \|S - S_I\|_{L^2(K_i)} &\leq C \sum_{i=1}^{N} h_i^{k+1} \int_{x_{i-1}}^{xi} |S^{(k+1)}(x)| dx \\ &\leq C \sum_{i=1}^{N} h_i^{k+2} \leq C(N(N^{-1}\ln N)^{(k+2)} {\mu_\ell}^{-(k+2)} + N^{-(k+1)}) \quad (3.4.3)\end{aligned}$$

By using (3.4.2) and (3.4.3), in Equation (3.4.1), we can obtain

$$|||S - S_I||| \leq C N^{-(k+1)},$$

here, we have used the inequality $\mu_\ell^{-1} \leq N^{-1}$. ∎

Lemma 3.4.2. *Let $E_{\ell,I}$ denotes the piecewise Lagrange interpolation of the left layer component E_ℓ of the solution u of (3.1.1), then we have*

$$\|(E_\ell - E_{\ell,I})^{(q)}\|_{L^\infty(\Omega_o \cup \Omega_r)} \leq C \mu_\ell^q N^{-(k+1)}.$$

Proof. Using the Cauchy–Schwarz inequality, we can express

$$\begin{aligned}\|(E_\ell - E_{\ell,I})^{(q)}\|_{L^\infty(\Omega_o \cup \Omega_r)} &\leq \|E_\ell^{(q)}\|_{L^\infty(\Omega_o \cup \Omega_r)} + \|E_{\ell,I}^{(q)}\|_{L^\infty(\Omega_o \cup \Omega_r)} \\ &\leq \|E_\ell^{(q)}\|_{L^\infty(\Omega_o \cup \Omega_r)}, \ \left(\text{using } \|E_{\ell,I}^{(q)}\|_{L^\infty(\Omega_o \cup \Omega_r)} \leq \|E_\ell^{(q)}\|_{L^\infty(\Omega_o \cup \Omega_r)}\right),\end{aligned}$$

and, we have

$$\begin{aligned}\|E_\ell^{(q)}\|_{L^\infty(\Omega_o \cup \Omega_r)} &\leq C \mu_\ell^q \max_{[\tau_0, 1]} (e^{-p\mu_\ell x}) \\ &\leq C \mu_\ell^q e^{-p\tau \ln N}, \quad \left(\text{using } \tau_0 = \frac{\tau}{\mu_\ell} \ln N\right), \\ &\leq C \mu_\ell^q N^{-(p\tau)} \leq C \mu_\ell^q N^{-(k+1)}, \quad (\text{using } p\,\tau \geq k+1),\end{aligned}$$

which is the required estimate. ∎

Lemma 3.4.3. *Let $E_{r,I}$ denotes the piecewise Lagrange interpolation of the right layer part E_r of the solution u of (3.1.1), then we have*

$$\|(E_r - E_{r,I})^{(q)}\|_{L^\infty(\Omega_\ell \cup \Omega_o)} \leq C\mu_r^q N^{-(k+1)}.$$

Proof. Following the idea given in the above Lemma 3.4.2, we can derive the required result. ∎

Let $E = E_\ell + E_r$ and $E_I = E_{\ell,I} + E_{r,I}$, then by combining the errors for the left and right layer components, we can obtain following result.

Theorem 3.4.4. *Let E_I denotes the piecewise Lagrange interpolation of the layer component E, then the interpolation error for the layer component satisfies*

$$|||E - E_I||| \leq C(N^{-1} \ln N)^{k+1}.$$

Proof. We can express the errors in terms of the left and right layer components, *i.e.,* corresponding to $x = 0$ and $x = 1$ as

$$|||E - E_I||| \leq |||E_\ell - E_{\ell,I}||| + |||E_r - E_{r,I}|||. \tag{3.4.4}$$

We will derive the bounds for both the terms in the RHS of the inequality (3.4.4), separately. First, we will estimate on the subdomain Ω_ℓ, that is, on the fine mesh region in the LHS of the domain:

$$|||E_\ell - E_{\ell,I}|||^2_{\Omega_\ell} = \varepsilon_d \sum_{i=1}^{N/4} h_i \sum_{j=1}^{p} w_j (E_\ell - E_{\ell,I})'(x_{ij})^2 + \gamma^2 \sum_{i=1}^{N/4} \|E_\ell - E_{\ell,I}\|^2_{L^2(K_i)}. \tag{3.4.5}$$

Bound for the first term in the RHS of the above equation is obtained as

$$\begin{aligned}
\varepsilon_d \sum_{i=1}^{N/4} h_i \sum_{j=1}^{p} w_j (E_\ell - E_{\ell,I})'(x_{ij})^2 &\leq C\varepsilon_d \sum_{i=1}^{N/4} h_i h_i^{2k} \left(\int_{x_{i-1}}^{x_i} |E_\ell^{(k+2)}(x)| dx \right)^2 \\
&\leq C\varepsilon_d \sum_{i=1}^{N/4} h_i^{2k+1} \left(\int_{x_{i-1}}^{x_i} |E_\ell^{(k+2)}(x)|^2 dx \right) \left(\int_{x_{i-1}}^{x_i} dx \right) \\
&\leq C\varepsilon_d \sum_{i=1}^{N/4} h_i^{2k+2} \left(\int_{x_{i-1}}^{x_i} \mu_\ell^{2(k+2)} e^{-2p\mu_\ell x} dx \right) \\
&\leq C(N^{-1} \ln N)^{2(k+1)}, \qquad (3.4.6)
\end{aligned}$$

where we have used the inequality (3.3.6) and $\varepsilon_d \, \mu_\ell \leq C$.

Second term in the RHS of the (3.4.5) can be bounded by

$$\begin{aligned}\sum_{i=1}^{N/4}\|E_\ell - E_{\ell,I}\|^2_{L^2(K_i)} &\leq C\sum_{i=1}^{N/4} h_i^{2(k+1)}\|E_\ell^{(k+1)}\|^2_{L^2(K_i)}\\ &\leq C\sum_{i=1}^{N/4} h_i^{2(k+1)}\left(\int_{x_{i-1}}^{xi}\mu_\ell^{2(k+1)}e^{-2p\mu_\ell x}dx\right)\\ &\leq C(N^{-1}\ln N)^{2(k+1)}, \end{aligned} \tag{3.4.7}$$

here, we have used inequality (3.3.7). Using (3.4.7) and (3.4.6) in (3.4.5), we can obtain

$$|||E_\ell - E_{\ell,I}|||_{\Omega_\ell} \leq C(N^{-1}\ln N)^{k+1}. \tag{3.4.8}$$

Similarly, we can show that

$$|||E_r - E_{r,I}|||_{\Omega_r} \leq C(N^{-1}\ln N)^{k+1}. \tag{3.4.9}$$

On the domain $\Omega_o \cup \Omega_r$, we can derive the bound using the maximum norm bound and the triangle inequality. Consider the interpolation error for E_ℓ in $\Omega_o \cup \Omega_r$:

$$|||E_\ell - E_{\ell,I}|||^2_{\Omega_o\cup\Omega_r} = \varepsilon_d \sum_{i=N/4+1}^{N} h_i \sum_{j=1}^{p} w_j (E_\ell - E_{\ell,I})'(x_{ij})^2 + \gamma^2 \sum_{i=N/4+1}^{N}\|E_\ell - E_{\ell,I}\|^2_{L^2(K_i)}. \tag{3.4.10}$$

Bound for the first term in the RHS of the above equation is

$$\begin{aligned}\varepsilon_d \sum_{i=N/4+1}^{N} h_i \sum_{j=1}^{p} w_j (E_\ell - E_{\ell,I})'(x_{ij})^2 &\leq C\varepsilon_d \sum_{i=N/4+1}^{N} h_i\mu_0^2 N^{-2(k+1)} \text{(using Lemma 3.4.2)}\\ &\leq CN^{-2(k+1)},\end{aligned}$$

and bound for the second term in the RHS of Equation (3.4.10) is given as

$$\|E_\ell - E_{\ell,I}\|^2_{L^2(\Omega_o\cup\Omega_r)} \leq \|E_\ell\|^2_{L^2(\Omega_o\cup\Omega_r)} + \|E_{\ell,I}\|^2_{L^2(\Omega_o\cup\Omega_r)}. \tag{3.4.11}$$

Now, we obtain the bounds for both the terms in the RHS of the above inequality separately. Bound for the first term in the RHS of inequality (3.4.11) is

$$\begin{aligned}\|E_\ell\|^2_{L^2(\Omega_o\cup\Omega_r)} &= \sum_{i=N/4+1}^{N}\|E_\ell\|^2_{L^2(I_i)} \leq C\sum_{i=N/4+1}^{N}\int_{I_i}(e^{-p\mu_\ell x})^2 dx\\ &\leq CN^{-2(k+1)}.\end{aligned}$$

The second term in the RHS of inequality (3.4.11) is bounded by

$$\begin{aligned}\|E_{\ell,I}\|^2_{L^2(\Omega_o\cup\Omega_r)} &= \sum_{i=N/4+1}^{N}\|E_{\ell,I}\|^2_{L^2(I_i)} \leq C\sum_{i=N/4+1}^{N}\int_{I_i}(E_{\ell,I})^2 dx\\ &\leq C\sum_{i=N/4+1}^{N} h_i\|E_{\ell,I}\|^2_{L^\infty(I_i)} \leq CN^{-2(k+1)}, (\text{ using } \|E_{\ell,I}\|_{L^\infty(I_i)} \leq C\|E_\ell\|_{L^\infty(I_i)}).\end{aligned}$$

Combining both the inequalities and (3.4.11), we have

$$|||E_\ell - E_{\ell,I}|||^2_{\Omega_o \cup \Omega_r} \leq CN^{-2(k+1)}. \tag{3.4.12}$$

Similarly, we can prove that

$$|||E_r - E_{r,I}|||^2_{\Omega_\ell \cup \Omega_o} \leq CN^{-2(k+1)}. \tag{3.4.13}$$

By combining the inequalities (3.4.4) (3.4.8) (3.4.9) (3.4.12) and (3.4.13), we can obtain the desired result. ∎

Theorem 3.4.5. *Let u_I be the piecewise Lagrange interpolation of the solution u of (3.1.1) at the Gauss points. Then the interpolation error satisfies*

$$|||u - u_I||| \leq C(N^{-1} \ln N)^{k+1}.$$

Proof. From the solution decomposition, we know that

$$|||u - u_I||| \leq |||S - S_I||| + |||E - E_I|||.$$

Using the results from Theorems 3.4.1 and 3.4.4, we can obtain the required estimate. ∎

Now it remains to prove the bound for the discretization error $\xi = u_I - u_h$. To prove discretization error, we use the coercivity and the Galerkin orthogonality properties of the bilinear form.

Theorem 3.4.6. *Let u and u_h be the solution of the continuous problem (3.1.1) and the discrete problem (3.3.1), respectively and let u_I be the piecewise Lagrange interpolation of the solution u, then the discretization error $\xi = u_I - u_h$ satisfies*

$$|||\xi||| \leq C(N^{-1} \ln N)^{k+1}.$$

Proof. Using the coercivity and the Galerkin orthogonality, we can write

$$|||\xi|||^2 \;\leq\; B(\xi, \xi) = B(u - u_h, \xi) - B(\eta, \xi) = -B(\eta, \xi). \tag{3.4.14}$$

By the definition of the interpolation, we have $\eta(x_j) = 0,\ j = 0, 1, \cdots, N$, which implies that $[\eta(x_j)] = 0$. Using this in the bilinear form (3.3.1), we get $B_2(\xi, \eta) = 0$ and $B_3(\eta, \xi) = 0$. Further, we will estimate the bounds separately for the nonzero terms of $B_1(\eta, \xi)$ and $B_2(\eta, \xi)$. We have

$$\begin{aligned} B_1(\eta, \xi) \;=\; & \sum_{j=1}^{N} \int_{K_j} \varepsilon_d \eta'(x)\xi'(x)dx + \varepsilon_c \sum_{j=1}^{N} \int_{K_j} b(x)\eta'(x)\xi(x)dx \\ & + \sum_{j=1}^{N} \int_{K_j} c(x)\eta(x)\xi(x)dx. \end{aligned} \tag{3.4.15}$$

Using integration by parts for the second term in the RHS of above equation, we get

$$\begin{aligned} B_1(\eta,\,\xi) &= \sum_{j=1}^{N}\int_{K_j}\varepsilon_d\eta'(x)\xi'(x)dx+\varepsilon_c\sum_{j=1}^{N}\int_{K_j}b(x)\eta(x)\xi'(x)dx \\ &\quad+\sum_{j=1}^{N}\int_{K_j}(c(x)-\varepsilon_c b'(x))\eta(x)\xi(x)dx. \end{aligned} \tag{3.4.16}$$

Using the Cauchy–Schwarz inequality and the bound for the interpolation error, we can derive the bound for each of the term of (3.4.16), separately. The first term in the RHS of Equation (3.4.16) can be bounded as

$$\begin{aligned} \left|\sum_{j=1}^{N}\int_{K_j}\varepsilon_d\eta'(x)\xi'(x)dx\right| &\le \left(\sum_{j=1}^{N}\int_{K_j}\varepsilon_d(\eta')^2(x)dx\right)^{1/2}\left(\sum_{j=1}^{N}\int_{K_j}\varepsilon_d(\xi')^2(x)dx\right)^{1/2} \\ &\le C(N^{-1}\ln N)^{k+1}|||\xi|||. \end{aligned}$$

To bound the second term in the RHS of (3.4.16), we use the bound of the interpolation error in the maximum norm. That is, we obtain

$$\begin{aligned} \left|\sum_{j=1}^{N}\int_{K_j}\varepsilon_c b(x)\eta(x)\xi'(x)dx\right| &\le C\big(\|\eta\|_{L^\infty(\Omega_\ell)}\|\xi'\|_{L^1(\Omega_\ell)}+\|\eta\|_{L^\infty(\Omega_o)}\|\xi'\|_{L^1(\Omega_o)} \\ &\quad+\|\eta\|_{L^\infty(\Omega_r)}\|\xi'\|_{L^1(\Omega_r)}\big) \\ &\le C(N^{-1}\ln N)^{k+1}|||\xi|||, \end{aligned}$$

here, we have used $||\xi'||_{L^1(\Omega_\ell)} \le C(\mu_\ell^{-1}\ln N)^{1/2}\|\xi'\|_{L^2(\Omega_\ell)} \le C(\varepsilon_d^{-1}\mu_\ell^{-1}\ln N)^{1/2}|||\xi|||$. And for the third term in the RHS of (3.4.16), we have

$$\left|\sum_{j=1}^{N}\int_{K_j}(c(x)-\varepsilon_c b'(x))\eta(x)\xi(x)dx\right| \le C\|\eta\|_{L^2(\Omega)}\|\xi\|_{L^2(\Omega)} \le C(N^{-1}\ln N)^{k+1}|||\xi|||.$$

Finally, we derive the bound for $B_2(\eta,\,\xi)$ as

$$\begin{aligned} |B_2(\eta,\,\xi)| &\le \left(\sum_{j=0}^{N}\frac{\varepsilon_d^2}{\sigma_j}\{\eta'\}_j^2\right)^{1/2}\left(\sum_{j=0}^{N}\sigma_j[\xi]_j^2\right)^{1/2} \\ &\le C(N^{-1}\ln N)^{k+1}|||\xi|||, \end{aligned}$$

here, we have used $\sigma_j = N$, $j = 0, 1, \cdots, N$. Now combining all the above estimates with the bilinear form (3.3.1), we get

$$|B(\eta,\,\xi)| \le C(N^{-1}\ln N)^{k+1}|||\xi|||. \tag{3.4.17}$$

Combining inequalities (3.4.14) and (3.4.17), we can obtain the required result. ∎

Theorem 3.4.7. *Let u and u_h be the solution of the continuous problem (3.1.1) and the discrete problem (3.3.1), respectively. Then the error satisfies the following bound in the discrete energy norm:*

$$|||u - u_h||| \leq C(N^{-1} \ln N)^{k+1}.$$

Proof. From the triangle inequality, we have

$$|||u - u_h||| \leq |||u - u_I||| + |||u_I - u_h|||,$$

using the estimates obtained in the Theorem 3.4.5 and Theorem 3.4.6 in the above inequality, we get the required result. ∎

3.4.2 On the Bakhvalov mesh

Let $N \in \mathbb{N}$, $N \geq 8$, be divisible by 4 and the mesh generating functions ϕ_0 and ϕ_1 are given by

$$\begin{cases} \phi_0(t) = -\ln(1 - 4(1 - \mu_\ell^{-1})t), \\ \phi_1(t) = -\ln(1 - 4(1 - \mu_r^{-1})(1 - t)), \end{cases}$$

which are piecewise continuously differentiable. The grid points for the Bakhvalov-type mesh are defined as

$$x_i = \begin{cases} \dfrac{\tau}{p\mu_\ell}\phi_0(t_i), & \text{for } i = 0, 1, \cdots, \frac{N}{4}, \\ \tau_0 + 2(t_i - \frac{1}{4})(1 - \tau_0 - \tau_1), & \text{for } i = \frac{N}{4}, \frac{N}{4} + 1, \cdots, \frac{3N}{4}, \\ 1 - \dfrac{\tau}{p\mu_r}\phi_1(t_i), & \text{for } i = \frac{3N}{4}, \frac{3N}{4} + 1, \cdots, N, \end{cases} \tag{3.4.18}$$

where $t_i = i/N$, $i = 0, 1, \cdots, N$. One can easily see the following bounds on the step-size:

$$h_i \leq \begin{cases} C\mu_\ell^{-1}, & \text{for } \Omega_\ell, \\ CN^{-1}, & \text{for } \Omega_o, \\ C\mu_r^{-1}, & \text{for } \Omega_r. \end{cases}$$

Interpolation error for the smooth part will be the same as derived in the case of the Shishkin mesh, whereas for the layer components there will not be any logarithmic term. We can have the following result for the interpolation error for the layer components.

Theorem 3.4.8. *Let E_I be the piecewise Lagrange interpolation of the layer component E, then the corresponding interpolation error satisfies*

$$|||E - E_I||| \leq CN^{-(k+1)}.$$

Discretization error can be obtained as we proved in the case of the Shishkin mesh. Hence the error estimate in the discrete energy norm on Bakhvalov-type mesh is given in the following theorem.

Theorem 3.4.9. *Let u be the solution of the continuous problem (3.1.1) and u_h be the solution of the discrete problem (3.3.1) obtained on the Bakhvalov-type mesh (3.4.18), then we have the following error bound:*

$$|||u - u_h||| \leq CN^{-(k+1)}.$$

3.4.3 On exponentially graded mesh

Let $N \in \mathbb{N}$, $N \geq 8$, be divisible by 4 and $\tau \geq 1$. The mesh generating functions ϕ_0 and ϕ_1, for the exponentially graded (eXp) mesh are given by

$$\begin{cases} \phi_0(t) = -\ln(1 - 4\theta_0 t), \\ \phi_1(t) = -\ln(1 - 4\theta_1(1-t)). \end{cases}$$

The constants θ_0 and θ_1 are defined as

$$\theta_0 = 1 - \exp\left(\frac{-p\mu_\ell}{\tau(k+1)}\right), \qquad \theta_1 = 1 - \exp\left(\frac{-p\mu_r}{\tau(k+1)}\right).$$

The grid points for the eXp mesh are defined as

$$x_i = \begin{cases} \dfrac{\tau}{2p\mu_\ell}(k+1)\phi_0(t_i), & \text{for } i = 0, 1, \cdots, \frac{N}{4} - 1, \\ x_{N/4-1} + \left(\dfrac{x_{3N/4+1} - x_{N/4-1}}{N/2+2}\right)(i - N/4 + 1), & \text{for } i = \frac{N}{4}, \frac{N}{4}+1, \cdots, \frac{3N}{4}, \\ 1 - \dfrac{\tau}{2p\mu_r}(k+1)\phi_1(t_i), & \text{for } i = \frac{3N}{4}+1, \frac{3N}{4}+2, \cdots, N, \end{cases} \tag{3.4.19}$$

where $t_i = i/N$, $i = 0, 1, \cdots, N$. Here on the domain $\Omega_\ell = [0, x_{N/4-1}]$ and $\Omega_r = [x_{3N/4+1,1}]$ the mesh points are gradually distributed while on $\Omega_o = [x_{N/4-1}, x_{3N/4+1}]$ mesh points are equidistant. Further, one can have the following bound on the step-sizes:

$$h_i \leq \begin{cases} C\mu_\ell^{-1}, & \text{for } \Omega_\ell, \\ CN^{-1}, & \text{for } \Omega_o, \\ C\mu_r^{-1}, & \text{for } \Omega_r. \end{cases}$$

We can derive alternate width of the mesh in the layer region, by introducing the mesh characteristic functions $\psi_j = \exp(-\phi_j)$, $j = 0, 1$. For $i \in \Omega_\ell$, we have

$$h_i \leq \frac{\tau}{2p\mu_\ell}(k+1)N^{-1}\max|\psi_0'|e^{\phi_0(t_i)} \leq C\mu_\ell^{-1}N^{-1}\exp\left(\frac{2p\mu_\ell x_i}{\tau(k+1)}\right). \tag{3.4.20}$$

For $i \in \Omega_r$, we have

$$h_i \leq \frac{\tau}{2p\mu_r}(k+1)N^{-1}\max|\psi_1'|e^{\phi_1(t_{i-1})} \leq C\mu_r^{-1}N^{-1}\exp\left(\frac{2p\mu_r(1-x_{i-1})}{\tau(k+1)}\right), \quad (3.4.21)$$

and

$$\begin{aligned} x_{N/4-1} &= \frac{\tau}{2p\mu_\ell}(k+1)\phi_0(1/4-1/N) \\ &= -\frac{\tau}{2p\mu_\ell}(k+1)\ln(1-\theta_0+4N^{-1}\theta_0) \\ &= 4N^{-1}+(1-4N^{-1})\exp\left(\frac{-p\mu_\ell}{\tau(k+1)}\right). \end{aligned}$$

Hence, we have

$$\begin{aligned} e^{-p\mu_\ell x_{N/4-1}} &\leq e^{\tau(k+1)/2\ln(1-\theta_0+4N^{-1}\theta_0)} \\ &\leq C(1-\theta_0+4N^{-1}\theta_0)^{\tau(k+1)/2} \\ &\leq CN^{-\tau(k+1)/2}. \end{aligned}$$

Similarly, we can show that

$$e^{-p\mu_r(1-x_{3N/4+1})} \leq CN^{-\tau(k+1)/2}.$$

The interpolation error for the smooth component can be derived as we have done in the case of Shishkin mesh. Hence, we have the following bound for the smooth component of the solution:

$$|||S-S_I||| \leq CN^{-(k+1)}. \quad (3.4.22)$$

To derive the interpolation error for the layer components, we will use Lemma 3.4.2 and length of the step-sizes from inequality (3.4.20) and (3.4.21). Using the definition of the discrete energy norm (3.3.2), we have

$$|||E_\ell - E_{\ell,I}|||_{\Omega_\ell}^2 = \varepsilon_d\sum_{i=1}^{N/4}h_i\sum_{j=1}^{p}w_j(E_\ell-E_{\ell,I})'(x_{ij})^2 + \gamma^2\sum_{i=1}^{N/4}\|E_\ell-E_{\ell,I}\|_{L^2(K_i)}^2. \quad (3.4.23)$$

The first term in the RHS of the (3.4.23) can be bounded by

$$\begin{aligned} \varepsilon_d\sum_{i=1}^{N/4}h_i\sum_{j=1}^{p}w_j(E_\ell-E_{\ell,I})'(x_{ij})^2 &\leq C\varepsilon_d\sum_{i=1}^{N/4}h_ih_i^{2k}\left(\int_{x_{i-1}}^{x_i}|E_\ell^{(k+2)}(x)|dx\right)^2 \\ &\leq C\varepsilon_d\sum_{i=1}^{N/4}h_i^{2k+1}\left(\int_{x_{i-1}}^{x_i}|E_\ell^{(k+2)}(x)|^2dx\right)\left(\int_{x_{i-1}}^{x_i}dx\right) \\ &\leq C\varepsilon_d\sum_{i=1}^{N/4}h_i^{2k+2}\left(\int_{x_{i-1}}^{x_i}\mu_\ell^{2(k+2)}e^{-2p\mu_\ell x}dx\right) \\ &\leq CN^{-2(k+1)}, \end{aligned} \quad (3.4.24)$$

here we have used $\varepsilon_d\mu_\ell \leq C$ and $h_i = C\mu_\ell^{-1}N^{-1}\exp\left(\frac{2p\mu_\ell x_i}{\tau(k+1)}\right)$.

The bound for the second term in the RHS of the (3.4.23) can be derived by

$$\begin{aligned}\sum_{i=1}^{N/4}\|E_\ell - E_{\ell,I}\|^2_{L^2(K_i)} &\leq C\sum_{i=1}^{N/4} h_i^{2(k+1)}\|E_\ell^{(k+1)}\|^2_{L^2(K_i)}\\ &\leq C\sum_{i=1}^{N/4} h_i^{2(k+1)}\left(\int_{x_{i-1}}^{xi}\mu_\ell^{2(k+1)}e^{-2p\mu_\ell x}dx\right)\\ &\leq CN^{-2(k+1)}. \end{aligned} \tag{3.4.25}$$

Using (3.4.24) and (3.4.25) in (3.4.23), we obtain

$$|||E_\ell - E_{\ell,I}|||_{\Omega_\ell} \leq CN^{-(k+1)}. \tag{3.4.26}$$

Similarly, we can show that

$$|||E_r - E_{r,I}|||_{\Omega_r} \leq CN^{-(k+1)}. \tag{3.4.27}$$

Now on the domain $\Omega_o \cup \Omega_r$, we have

$$|||E_\ell - E_{\ell,I}|||^2_{\Omega_o\cup\Omega_r} = \varepsilon_d \sum_{i=N/4+1}^{N} h_i \sum_{j=1}^{p} w_j (E_\ell - E_{\ell,I})'(x_{ij})^2 + \gamma^2 \sum_{i=N/4+1}^{N}\|E_\ell - E_{\ell,I}\|^2_{L^2(K_i)}. \tag{3.4.28}$$

The first term in the RHS of (3.4.28) satisfies

$$\begin{aligned}\varepsilon_d \sum_{i=N/4+1}^{N} h_i \sum_{j=1}^{p} w_j (E_\ell - E_{\ell,I})'(x_{ij})^2 &\leq C\varepsilon_d \sum_{i=N/4+1}^{N} h_i\mu_\ell^2 N^{-2(k+1)} \text{ (using Lemma 3.4.2)}\\ &\leq CN^{-2(k+1)}.\end{aligned}$$

Second term in the RHS of (3.4.28), can be bounded by

$$\|E_\ell - E_{\ell,I}\|^2_{L^2(\Omega_o\cup\Omega_r)} \leq \|E_\ell\|^2_{L^2(\Omega_o\cup\Omega_r)} + \|E_{\ell,I}\|^2_{L^2(\Omega_o\cup\Omega_r)}. \tag{3.4.29}$$

Now we obtain the bounds for both the terms in the above inequality separately. We get the following bound for the first term in the RHS of (3.4.29)

$$\begin{aligned}\|E_\ell\|^2_{L^2(\Omega_o\cup\Omega_r)} &= \sum_{i=N/4+1}^{N}\|E_\ell\|^2_{L^2(I_i)} \leq C\sum_{i=N/4+1}^{N}\int_{I_i}(e^{-p\mu_\ell x})^2dx\\ &\leq CN^{-2(k+1)}.\end{aligned}$$

Second term in the RHS of (3.4.29) can be bounded as

$$\begin{aligned}\|E_{\ell,I}\|^2_{L^2(\Omega_o\cup\Omega_r)} &= \sum_{i=N/4+1}^{N}\|E_{\ell,I}\|^2_{L^2(I_i)} \leq C\sum_{i=N/4+1}^{N}\int_{I_i}(E_{\ell,I})^2dx\\ &\leq \sum_{i=N/4+1}^{N} h_i\|E_{\ell,I}\|^2_{L^\infty(I_i)} \leq CN^{-2(k+1)}.\end{aligned}$$

Combining the above inequalities with (3.4.29), we have the following estimate:

$$|||E_\ell - E_{\ell,I}|||^2_{\Omega_o \cup \Omega_r} \leq CN^{-2(k+1)}. \tag{3.4.30}$$

Similarly, we can prove that

$$|||E_r - E_{r,I}|||^2_{\Omega_\ell \cup \Omega_o} \leq CN^{-2(k+1)}. \tag{3.4.31}$$

Now, we are in a position to provide the following theorem, which shows the bounds for the interpolation error.

Theorem 3.4.10. *If u is the solution of the convection-diffusion-reaction problem (3.1.1) and u_I is its Lagrange interpolants, then*

$$|||u - u_I||| \leq CN^{-(k+1)}.$$

Proof. From inequality (3.3.8), we have

$$|||u - u_I||| \leq |||S - S_I||| + |||E_\ell - E_{\ell,I}||| + |||E_r - E_{r,I}|||. \tag{3.4.32}$$

From inequality (3.4.22), bound for the interpolation error for the smooth component of the solution (3.1.1) is given by

$$|||S - S_I||| \leq CN^{-(k+1)}.$$

To obtain the bound for the second term in the RHS of the inequality (3.4.32), we express the term as

$$|||E_\ell - E_{\ell,I}|||^2 = |||E_\ell - E_{\ell,I}|||^2_{\Omega_\ell} + |||E_\ell - E_{\ell,I}|||^2_{\Omega_o \cup \Omega_r},$$

using inequalities (3.4.26) and (3.4.30) in the above equation, we get

$$|||E_\ell - E_{\ell,I}||| \leq CN^{-(k+1)}.$$

Similarly, for the third term in the RHS of the inequality (3.4.32), we have

$$|||E_r - E_{r,I}|||^2 = |||E_r - E_{r,I}|||^2_{\Omega_r} + |||E_r - E_{r,I}|||^2_{\Omega_\ell \cup \Omega_o},$$

using inequalities (3.4.27) and (3.4.31) in the above equation, we get

$$|||E_r - E_{r,I}||| \leq CN^{-(k+1)}.$$

Using all the above inequalities in (3.4.32), we can obtain the desired result. ∎

Discretization error can be derived in a similar way as we have done in the case of Shishkin mesh. Hence error in the discrete energy norm on exponentially graded mesh is given in the following theorem.

Theorem 3.4.11. *Let u be the solution of the continuous problem (3.1.1) and u_h be the solution of the discrete problem (3.3.1) obtained on the exponentially graded mesh (3.4.19), then we have the following error bound:*

$$|||u - u_h||| \leq CN^{-(k+1)}.$$

3.5 Numerical Experiments

In this section, in order to validate the theoretical error estimates derived in the previous section, we perform some numerical experiments with a test problem. Here, we have considered two examples one with variable coefficients and other with constant coefficients. Numerical results are given for the NIPG method and the standard FEM on all three types of meshes namely the Shishkin mesh, the Bakhvalov mesh and the exponentially graded mesh.

Example 3.5.1. *Consider the following two-parameter singularly perturbed two-point BVP:*

$$\begin{cases} -\varepsilon_d u''(x) + \varepsilon_c(1+x)u'(x) + u(x) = f(x), \quad x \in \Omega, \\ u(0) = u(1) = 0, \end{cases} \tag{3.5.1}$$

where $f(x)$ is chosen such that

$$u(x) = a\cos\pi x + b\sin\pi x + Ae^{-\mu_\ell x} + Be^{-\mu_r(1-x)},$$

is the exact solution of (3.5.1). Here

$$a = \frac{\varepsilon_d\pi^2 + 1}{\varepsilon_c^2\pi^2 + (\varepsilon_d\pi^2+1)^2}, \qquad b = \frac{\varepsilon_c\pi}{\varepsilon_c^2\pi^2 + (\varepsilon_d\pi^2+1)^2},$$

$$A = -a\frac{1+e^{-\mu_r}}{1-e^{-\mu_\ell-\mu_r}}, \qquad B = a\frac{1+e^{-\mu_\ell}}{1-e^{-\mu_\ell-\mu_r}}, \qquad \mu_{\ell,r} = \frac{\mp\varepsilon_c + \sqrt{\varepsilon_c^2+4\varepsilon_d}}{2\varepsilon_d}.$$

Example 3.5.2. *Consider the two-parameter singularly perturbed convection-diffusion-reaction BVP:*

$$\begin{cases} -\varepsilon_d u''(x) - \varepsilon_c u'(x) + u(x) = e^{(1-x)}, \quad x \in \Omega, \\ u(0) = u(1) = 0. \end{cases} \tag{3.5.2}$$

The exact solution is given by

$$u(x) = \frac{e^{(m_2+1)}-1}{D}e^{m_1x} + \frac{1-e^{(m_1+1)}}{D}e^{m_2x} - \frac{e^{(1-x)}}{\varepsilon(m_1+1)(m_2+1)},$$

where,

$$D = \varepsilon(e^{m_2} - e^{m_1})(m_1+1)(m_2+1),$$

$$m_1 = \frac{-\varepsilon_c - \sqrt{\varepsilon_c^2+4\varepsilon_d}}{2\varepsilon_d}, \qquad m_2 = \frac{-\varepsilon_c + \sqrt{\varepsilon_c^2+4\varepsilon_d}}{2\varepsilon_d}.$$

The exact and numerical solutions and the corresponding error for different values of the perturbation parameters are given in Figures 3.1, 3.2 and Figures 3.3, 3.4 for

Example 3.5.1 and Example 3.5.2, respectively. We can observe from the Figure 3.1 and Figure 3.3 that whenever $\varepsilon_c^2 \ll \varepsilon_d \ll 1$, the appearance of the boundary layers will be similar to the reaction-diffusion BVPs for both the examples. Whereas, if $\varepsilon_d \ll \varepsilon_c^2 \ll 1$, then the boundary layers at $x = 1$ is sharper than the boundary layer at $x = 0$ for Example 3.5.1 and boundary layer at $x = 0$ is sharper than the boundary layer at $x = 1$ for Example 3.5.2 which can be seen in Figure 3.2 and Figure 3.4, respectively.

The numerical results are given in the form of tables and figures. Table 3.1 shows the discrete energy norm error and the order of convergence for Example 3.5.1 using the NIPG method for $k = 1$ on all the three layer-adapted meshes discussed in this chapter. Whereas Table 3.2 shows the discrete energy norm error and the order of convergence for Example 3.5.1 using the standard FEM for $k = 1$. In the same way discrete energy norm error and the order of convergence using the NIPG method and the standard FEM for Example 3.5.2 for $k = 1$ are given in Tables 3.3 and 3.4, respectively. Tables 3.5 and 3.6 provide the numerical result in discrete energy norm for Example 3.5.2 with the quadratic finite element space. In all the tables, the singular perturbation parameters take values from the set $\mathcal{S} = \{(\varepsilon_d, \varepsilon_c) | \varepsilon_d = 10^{-5}, \varepsilon_c = 10^{-1}, 10^{-2}, \cdots, 10^{-10}\}$.

In order to reveal the numerical order of convergence, we have plotted the error in the loglog scale. Figures 3.5(a) and 3.5(b) depict the order of convergence in the discrete energy norm in the loglog scale for the NIPG method and the standard FEM for $k = 1$ for Example 3.5.1, respectively. Figures 3.6(a) and 3.6(b) represent the loglog plot of the error in discrete energy norm for the NIPG method and the standard FEM for $k = 1$ for Example 3.5.2, respectively. Figures 3.7(a) and 3.7(b) depict the order of convergence through loglog plot for $k = 2$ using the NIPG method for Example 3.5.1 and Example 3.5.2, respectvely.

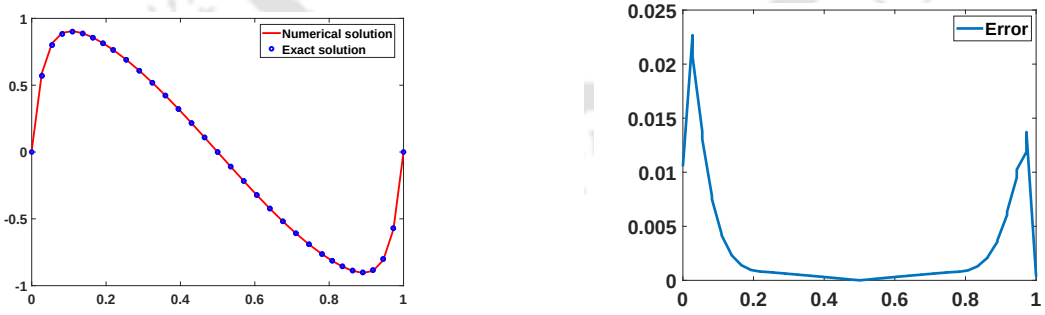

(a) Solution (b) Error

Figure 3.1: Solution and corresponding error for Example 3.5.1 for $\varepsilon_d = 10^{-3}$ and $\varepsilon_c = 10^{-6}$ with $N = 32$.

Table 3.1: *Comparison of error on different types of meshes using the NIPG method for Example 3.5.1 for $k = 1$ on the set $\mathcal{S}$.*

	Number of mesh intervals N					
	32	64	128	256	512	1024
S-mesh	6.5975e-01	2.4282e-01	8.3020e-02	2.7094e-02	8.5619e-03	2.6264e-03
	1.4447	1.5525	1.6224	1.6707	1.7421	
B-mesh	1.0798e-02	2.8729e-03	7.4219e-04	1.8658e-04	4.6557e-05	1.1615e-05
	1.9102	1.9527	1.9920	2.0027	2.0030	
eXp-mesh	2.8838e-03	7.4581e-04	1.8738e-04	4.6677e-05	1.1611e-05	2.8947e-06
	1.9511	1.9928	2.0052	2.0073	2.0057	

Table 3.2: *Comparison of error on different types of meshes using standard FEM for Example 3.5.1 for $k = 1$ on the set $\mathcal{S}$.*

	Number of mesh intervals N					
	32	64	128	256	512	1024
S-mesh	2.7007e-02	1.6925e-02	1.0260e-02	6.0141e-03	3.4428e-03	1.9377e-03
	0.67420	0.72210	0.77061	0.80477	0.82921	
B-mesh	2.1486e-02	1.0717e-02	5.3517e-03	2.6725e-03	1.3330e-03	6.6483e-04
	1.0034	1.0019	1.0018	1.0035	1.0036	
eXp-mesh	2.1464e-02	1.0678e-02	5.3233e-03	2.6590e-03	1.3296e-03	6.6585e-04
	1.0073	1.0043	1.0014	0.99987	0.99776	

Table 3.3: *Comparison of error on different types of meshes using the NIPG method for Example 3.5.2 for $k = 1$ on the set $\mathcal{S}$.*

	Number of mesh intervals N					
	32	64	128	256	512	1024
S-mesh	1.6905e-04	6.3357e-05	2.1893e-05	7.1877e-06	2.2784e-06	7.0360e-07
	1.4159	1.5330	1.6069	1.6575	1.6952	
B-mesh	9.1020e-03	2.3817e-03	6.0275e-04	1.5191e-04	3.8662e-05	9.9885e-06
	1.9342	1.9823	1.9884	1.9742	1.9526	
eXp-mesh	9.1495e-03	2.3944e-03	6.0546e-04	1.5181e-04	3.8035e-05	9.7304e-06
	1.9340	1.9836	1.9957	1.9969	1.9668	

Table 3.4: *Comparison of error on different types of meshes using standard FEM for Example 3.5.2 for $k = 1$ on the set $\mathcal{S}$.*

	Number of mesh intervals N					
	32	64	128	256	512	1024
S-mesh	6.9305e-02	4.3323e-02	2.5225e-02	1.4082e-02	7.7124e-03	4.1965e-03
	0.67783	0.78030	0.84093	0.86865	0.87800	
B-mesh	5.5507e-02	2.5993e-02	1.2166e-02	5.7930e-03	2.8100e-03	1.3812e-03
	1.0946	1.0953	1.0704	1.0438	1.0246	
eXp-mesh	5.5695e-02	2.6082e-02	1.2207e-02	5.8120e-03	2.8190e-03	1.3856e-03
	1.0945	1.0954	1.0705	1.0438	1.0247	

Table 3.5: *Comparison of error on different types of meshes using the NIPG method for Example 3.5.1 for $k = 2$ on the set $\mathcal{S}$.*

	Number of mesh intervals N					
	32	64	128	256	512	1024
S-mesh	1.9260e-04	3.8753e-05	6.5889e-06	9.9586e-07	1.3865e-07	1.8218e-08
	2.3132	2.5562	2.7260	2.8445	2.9280	
B-mesh	1.6590e-03	1.9058e-04	1.9370e-05	1.8382e-06	1.6834e-07	1.5155e-08
	3.1218	3.2985	3.3975	3.4489	3.4735	
eXp-mesh	1.9278e-04	1.9652e-05	1.8740e-06	1.7317e-07	1.5854e-08	1.4628e-09
	3.2942	3.3905	3.4358	3.4493	3.4381	

Table 3.6: *Comparison of error on different types of meshes using the NIPG method for Example 3.5.2 for $k = 2$ on the set $\mathcal{S}$.*

	Number of mesh intervals N					
	32	64	128	256	512	1024
S-mesh	1.0235e-04	2.0141e-05	3.3956e-06	5.1209e-07	7.1345e-08	9.4000e-09
	2.3453	2.5684	2.7292	2.8435	2.9241	
B-mesh	1.9084e-04	1.9447e-05	1.8541e-06	1.7132e-07	1.5685e-08	1.4476e-09
	3.2948	3.3907	3.4359	3.4492	3.4377	
eXp-mesh	1.9281e-04	1.9655e-05	1.8743e-06	1.7320e-07	1.5857e-08	1.4631e-09
	3.2942	3.3905	3.4358	3.4493	3.4380	

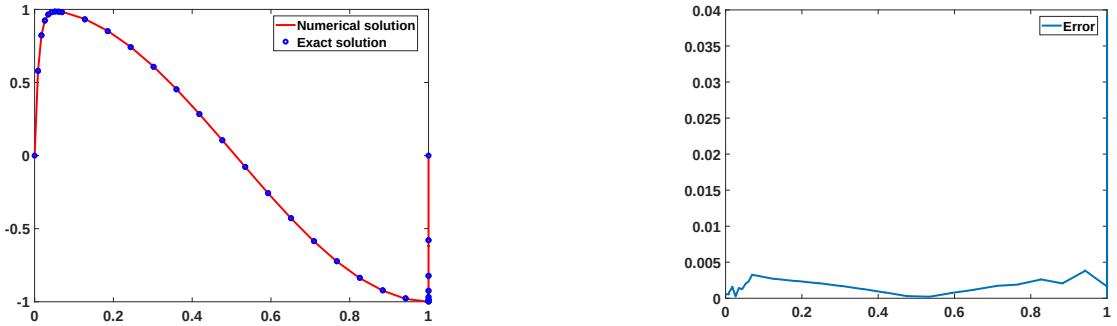

(a) Solution (b) Error

Figure 3.2: Solution and corresponding error for Example 3.5.1 for $\varepsilon_d = 10^{-12}$ and $\varepsilon_2 = 10^{-2}$ with $N = 32$.

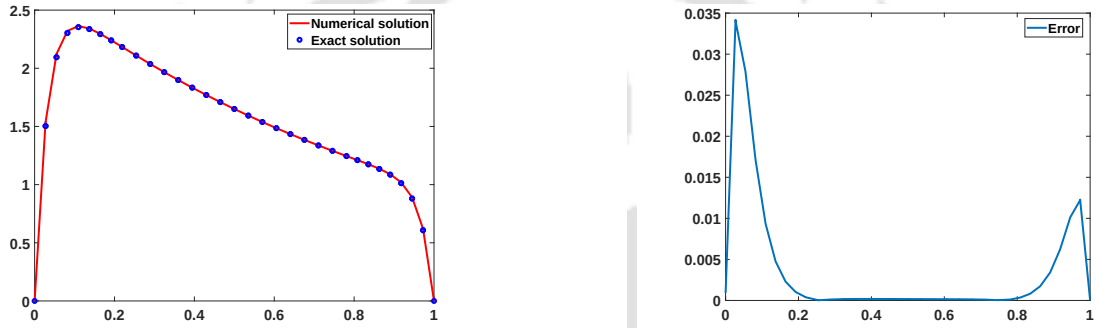

(a) Solution (b) Error

Figure 3.3: Solution and corresponding error for Example 3.5.2 for $\varepsilon_d = 10^{-3}$ and $\varepsilon_c = 10^{-6}$ with $N = 32$.

3.6 Conclusions

In this chapter, we have applied the NIPG method to obtain the numerical solution of two-parameter singularly perturbed two-point BVP, on the Shishkin, Bakhvalov and exponentially graded meshes. Further, we have studied the superconvergence of the NIPG method on these layer-adapted meshes and obtained almost $(k+1)$–order of convergence on the Shishkin mesh and exactly $\mathcal{O}(k+1)$ on the Bakhvalov and exponentially graded meshes. Numerical experiments are carried out to validate the theoretical error bounds derived in this chapter.

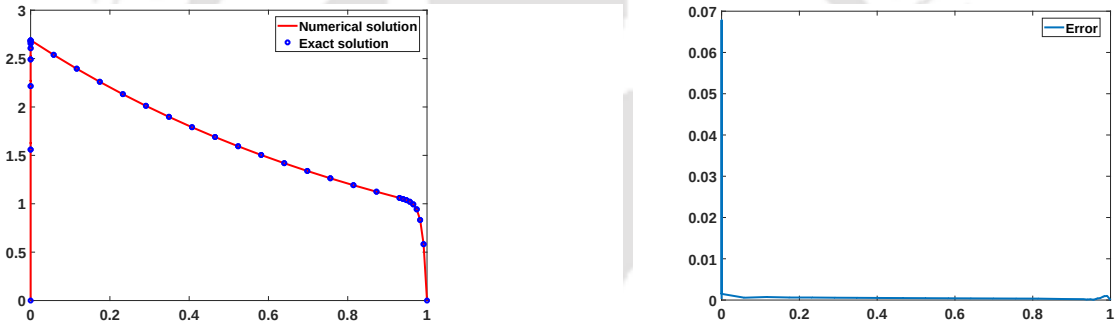

(a) Solution (b) Error

Figure 3.4: Solution and corresponding error for Example 3.5.2 for $\varepsilon_d = 10^{-12}$ and $\varepsilon_c = 10^{-2}$ with $N = 32$.

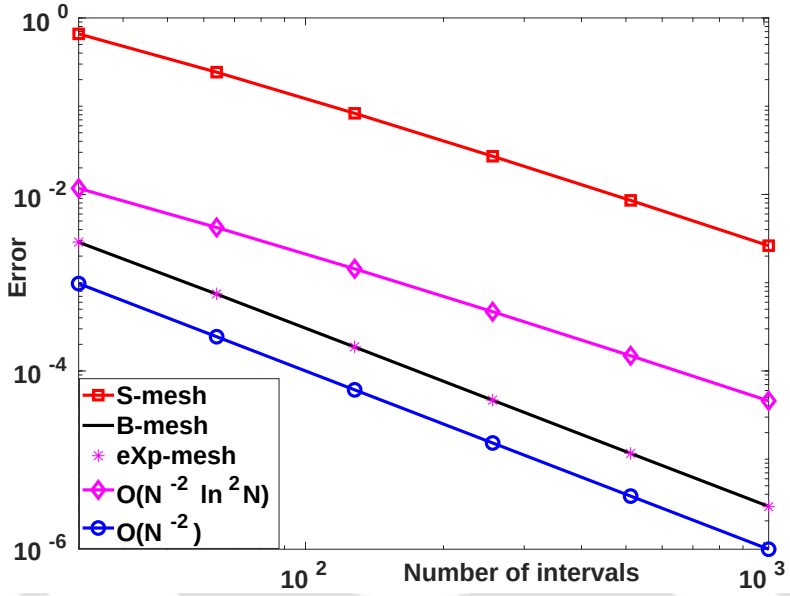

(a) For NIPG method.

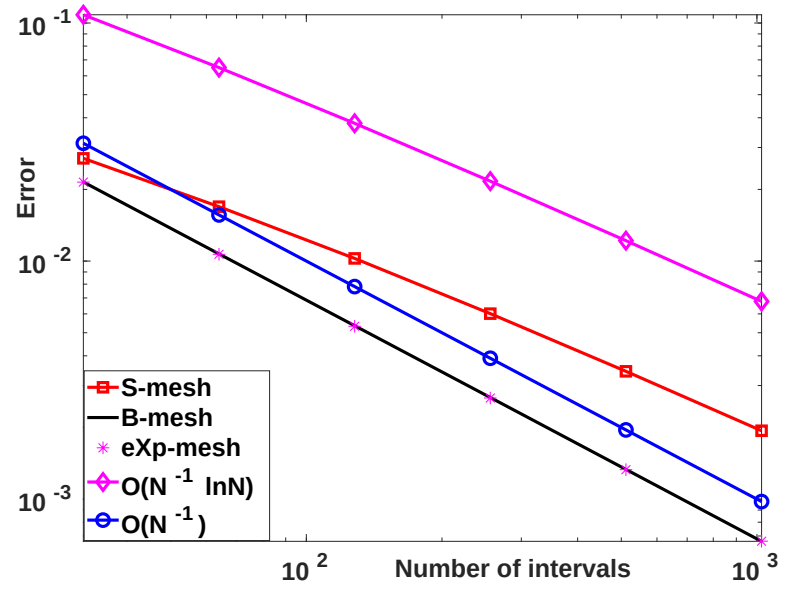

(b) For standard FEM.

Figure 3.5: Visualization of the order of convergence through loglog plot for Example 3.5.1 for $k = 1$.

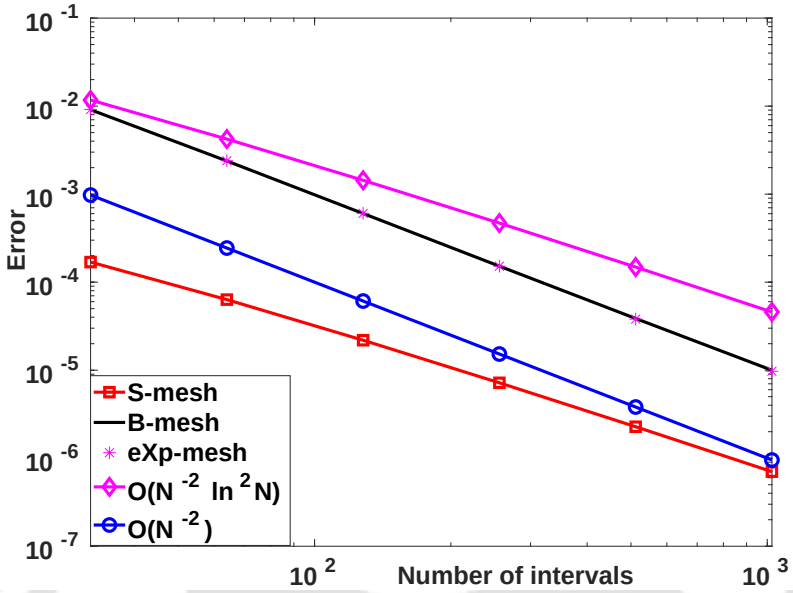

(a) For NIPG method.

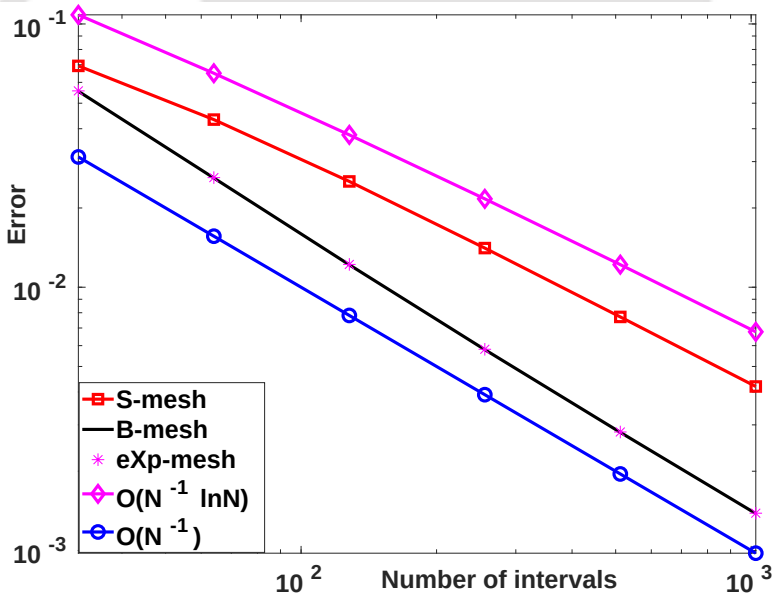

(b) For standard FEM.

Figure 3.6: Visualization of the order of convergence through loglog plot for Example 3.5.2 for $k = 1$.

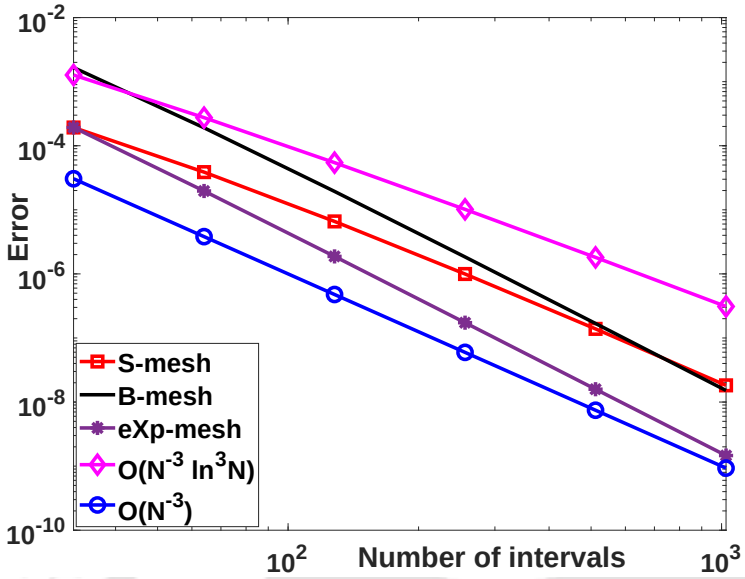

(a) For Example 3.5.1.

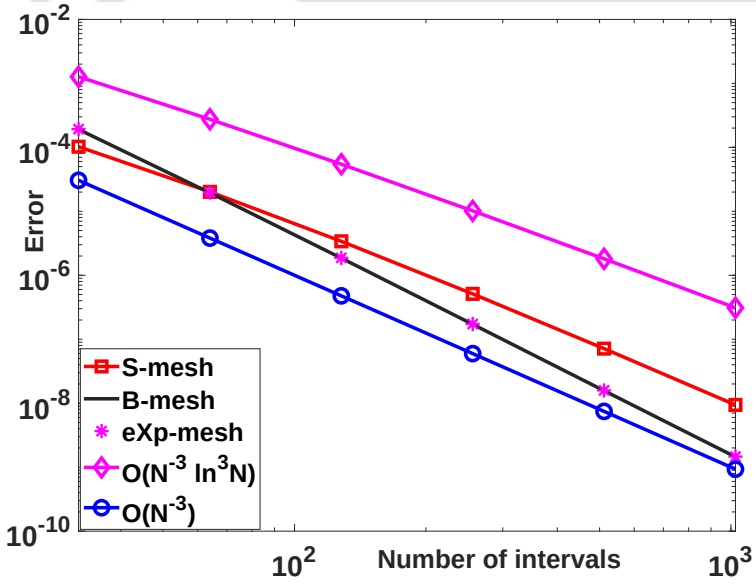

(b) For Example 3.5.2.

Figure 3.7: Visualization of the order of convergence through loglog plot for $k = 2$ using NIPG method.

CHAPTER 4

Parameter-Uniform Numerical Scheme for a Coupled System of Singularly Perturbed Reaction-Diffusion Equations

Here, we study the numerical solution of singularly perturbed system of two-point BVPs of reaction-diffusion type. The solutions of these problems exhibit twin overlapping exponential boundary layers. To obtain the numerical solutions of these problems, we apply the NIPG method on layer-adapted piecewise uniform Shishkin mesh. Also, we have proved that the proposed method is uniformly convergent with order k in the $\mathcal{E}$-weighted energy norm, where k is the degree of the piecewise polynomial in the finite element space. Numerical results are presented to support the theoretical results.

4.1 Introduction

Here, we consider the following singularly perturbed system of reaction-diffusion BVP:

$$\begin{cases} L\vec{u} = \begin{pmatrix} -\varepsilon_1^2 \dfrac{d^2}{dx^2} & 0 \\ 0 & -\varepsilon_2^2 \dfrac{d^2}{dx^2} \end{pmatrix} \vec{u} + \mathcal{C}\vec{u} = \vec{f}, \quad x \in \Omega, \\ \vec{u}(0) = \vec{0}, \qquad\qquad \vec{u}(1) = \vec{0}, \end{cases} \tag{4.1.1}$$

where $\mathcal{E} = \text{diag}(\varepsilon_1, \varepsilon_2)$, $0 < \varepsilon_1 \leq \varepsilon_2 \ll 1$ are the perturbation parameters, the coefficients c_{ij} and the source terms f_j are sufficiently smooth functions, and are given by

$$\mathcal{C} = \begin{pmatrix} c_{11}(x) & c_{12}(x) \\ c_{21}(x) & c_{22}(x) \end{pmatrix} \quad \text{and} \quad \vec{f} = \begin{pmatrix} f_1(x) \\ f_2(x) \end{pmatrix}.$$

We shall assume that reaction coefficient matrix $\mathcal{C} = \{c_{ij}\}_{i,j=1}^2$ is an L_0–matrix with

$$\min\{c_{11} + c_{12}, c_{21} + c_{22}\} > \beta^2, \tag{4.1.2}$$

i.e., $\mathcal{C}$ is an M-matrix whose inverse is bounded by β^{-2} in the maximum norm. The solution $\vec{u} = (u_1,\, u_2)^T$ of (4.1.1) has boundary layers of width $\mathcal{O}(\varepsilon_1 \ln \varepsilon_1)$ and $\mathcal{O}(\varepsilon_2 \ln \varepsilon_2)$ at $x = 0$ and 1, see [39] for more details.

This chapter is organized in the following style: Section 4.2 has divided into two subsections. In Subsection 4.2.1, bounds for the smooth and layer parts of the solution are given. Piecewise uniform Shishkin mesh is defined in Subsection 4.2.2. We introduce the NIPG method for system of SPPs and prove its existence and uniqueness in Section 4.3. Parameter-uniform error estimate is derived in Section 4.4. Further, superconvergence error analysis are carried out in Section 4.5. Section 4.6 contains the results of numerical experiments in order to illustrate the theoretical bounds. We shall also assume that $\varepsilon_1 \le CN^{-1}$ and $\varepsilon_2 \le CN^{-1}$ as is generally the case.

4.2 Solution Decomposition and Domain Discretization

Here, in the section, first, we study the properties of the analytical solution of the system (4.1.1). In particular, we obtain the bounds for the smooth and singular components of the solution and its derivatives. Later, we introduce the piecewise uniform Shishkin mesh for discretization of the domain.

4.2.1 Solution decomposition

The solution $\vec{u}$ of the BVP (4.1.1) can be decomposed as $\vec{u} = \vec{S} + \vec{E}$, where $\vec{S}$ and $\vec{E}$ are respectively the solutions of the following BVPs:

$$L\vec{S} = \vec{f} \quad \text{on} \quad \Omega \qquad \text{and} \quad \vec{S} = A^{-1}\vec{f} \quad \text{on} \quad \partial\Omega = \{0,\, 1\}, \tag{4.2.1}$$

and

$$L\vec{E} = \vec{0} \quad \text{on} \quad \Omega \qquad \text{and} \quad \vec{E} = \vec{u} - \vec{S} \quad \text{on} \quad \partial\Omega. \tag{4.2.2}$$

Here, $\vec{S}$ and $\vec{E}$ are the smooth and layer parts of the solution $\vec{u}$.

Lemma 4.2.1. *For a positive integer p the derivatives of the smooth and layer components $\vec{S}$ and $\vec{E}$ satisfy the following bounds:*

$$\begin{aligned}
|S_i^{(l)}(x)| &\le C, \qquad \textit{for} \quad i = 1, 2,\\
|E_1^{(l)}(x)| &\le C(\varepsilon_1^{-l} D_{\varepsilon_1}(x) + \varepsilon_2^{-l} D_{\varepsilon_2}(x)), \qquad 0 \le l \le p,\\
|E_2^{(l)}(x)| &\le C(\varepsilon_2^{-l} D_{\varepsilon_2}(x)), \qquad 0 \le l \le 2,\\
|E_2^{(l)}(x)| &\le C(\varepsilon_1^{-l} D_{\varepsilon_1}(x) + \varepsilon_2^{-l} D_{\varepsilon_2}(x)), \qquad 3 \le l \le p,
\end{aligned} \tag{4.2.3}$$

where $D_\nu(x) = \exp((-\beta x)/\nu) + \exp((-\beta(1-x))/\nu)$. *Here,* p *depends on the regularity of the solutions.*

Proof. The proof of this lemma can be seen in [39]. ∎

4.2.2 Piecewise uniform Shishkin mesh

To discretize the domain Ω, we use the layer-adapted piecewise uniform Shishkin mesh, which is described in the following. We divide the domain $\Omega = (0, 1)$ into five subdomains as $\Omega = \Omega_1 \cup \Omega_2 \cup \Omega_3 \cup \Omega_4 \cup \Omega_5$, where Ω_1, Ω_2, Ω_3, Ω_4 and Ω_5 are $[0, \tau_{\varepsilon_1}]$, $[\tau_{\varepsilon_1}, \tau_{\varepsilon_2}]$, $[\tau_{\varepsilon_2}, 1-\tau_{\varepsilon_2}]$, $[1-\tau_{\varepsilon_2}, 1-\tau_{\varepsilon_1}]$ and $[1-\tau_{\varepsilon_1}, 1]$, respectively. Which can be seen in Figure 4.1. Here, the transition point τ_{ε_1} and τ_{ε_2} are defined by

$$\tau_{\varepsilon_2} = \min\left(\frac{1}{4}, \frac{\alpha\varepsilon_2}{\beta}\ln N\right), \qquad \tau_{\varepsilon_1} = \min\left(\frac{1}{2}\tau_{\varepsilon_2}, \frac{\alpha\varepsilon_1}{\beta}\ln N\right).$$

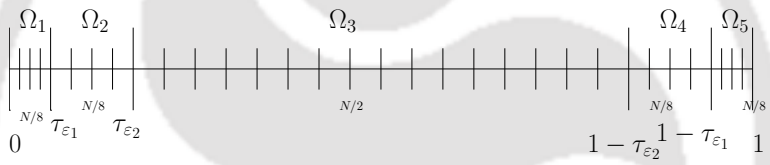

Figure 4.1: Domain discretization and piecewise uniform mesh

Where α is user chosen constant and we shall assume that $\tau_{\varepsilon_2} = (\alpha\varepsilon_2/\beta)\ln N$ as the case $\tau_{\varepsilon_2} = 1/4$ occurs only when N is exponentially large relative to ε_2, which is rare in practice.

The step-size in each of the subdomain is given by

$$h_i = \begin{cases} 8\tau_{\varepsilon_1}/N, & \text{for } \Omega_1 \text{ and } \Omega_5, \\ 8(\tau_{\varepsilon_2} - \tau_{\varepsilon_1})/N, & \text{for } \Omega_2 \text{ and } \Omega_4, \\ 2(1 - 2\tau_{\varepsilon_2})/N, & \text{for } \Omega_3. \end{cases}$$

4.3 Problem Discretization: The NIPG Method

The finite element problem corresponds to the system of BVP (4.1.1) by the NIPG method is given by

$$\begin{cases} \text{find } \vec{u}_h \in V_N^k(\Omega)^2, \text{ such that} \\ B(\vec{u}_h, \vec{v}_h) = L(\vec{v}_h), \quad \forall \vec{v}_h \in V_N^k(\Omega)^2, \end{cases} \tag{4.3.1}$$

with $B(\vec{u}, \vec{v}) = B_1(\vec{u}, \vec{v}) + B_2(\vec{u}, \vec{v})$, where

$$\begin{aligned} B_1(\vec{u}, \vec{v}) &= {\varepsilon_1}^2 \sum_{j=1}^{N} \int_{K_j} u_1'(x)v_1'(x)dx + {\varepsilon_1}^2 \sum_{j=0}^{N} (\{u_1'(x_j)\}[v_1(x_j)] - \{v_1'(x_j)\}[u_1(x_j)]) \\ &\quad + \sum_{j=0}^{N} \sigma_j [u_1(x_j)][v_1(x_j)] + \sum_{j=1}^{N} \int_{K_j} (c_{11}(x)u_1(x) + c_{12}(x)u_2(x))v_1(x)dx, \\ B_2(\vec{u}, \vec{v}) &= {\varepsilon_2}^2 \sum_{j=1}^{N} \int_{K_j} u_2'(x)v_2'(x)dx + {\varepsilon_2}^2 \sum_{j=0}^{N} (\{u_2'(x_j)\}[v_2(x_j)] - \{v_2'(x_j)\}[u_2(x_j)]) \\ &\quad + \sum_{j=0}^{N} \sigma_j [u_2(x_j)][v_2(x_j)] + \sum_{j=1}^{N} \int_{K_j} (c_{21}(x)u_1(x) + c_{22}(x)u_2(x))v_2(x)dx, \end{aligned}$$

and

$$L(\vec{v}) = \sum_{j=1}^{N} \int_{K_j} (f_1 v_1 + f_2 v_2)dx,$$

here, σ_j $(j = 0, 1, \ldots, N)$ are the so-called discontinuity-penalization parameters associated with the node x_j, which are nonnegative constants.

Lemma 4.3.1. *The bilinear form $B(., .)$ defined in (4.3.1) satisfies the Galerkin orthogonality property:*

$$B(\vec{u} - \vec{u}_h, \vec{v}) = 0, \quad \forall \vec{v} \in V_N^k(\Omega)^2.$$

Proof. Since $\vec{u}$ is the exact solution of (4.1.1), we have $[u_1(x_j)] = [u_2(x_j)] = 0$, $0 \le j \le N$ and $[u_1'(x_j)] = [u_2'(x_j)] = 0$, $1 \le j \le N-1$. Then, for all $\vec{v} \in V_N^k(\Omega)^2$, we easily get

$$\begin{aligned} B_1(\vec{u}, \vec{v}) &= {\varepsilon_1}^2 \sum_{j=1}^{N} \int_{K_j} u_1'(x)v_1'(x)dx + {\varepsilon_1}^2 \sum_{j=0}^{N} (\{u_1'(x_j)\}[v_1(x_j)]) \\ &\quad + \sum_{j=1}^{N} \int_{K_j} c_{11}(x)u_1(x)v_1(x)dx + \sum_{j=1}^{N} \int_{K_j} c_{12}(x)u_2(x)v_1(x)dx. \end{aligned}$$

Similarly, we can write for $B_2(\vec{u}, \vec{v})$. Using integration by parts and the definition of the jump and the average, one can show that

$${\varepsilon_1}^2 \sum_{j=1}^{N} \int_{K_j} u_1'(x)v_1'(x)dx = -{\varepsilon_1}^2 \sum_{j=1}^{N} \int_{K_j} u_1''(x)v_1(x)dx - {\varepsilon_1}^2 \sum_{j=0}^{N} (\{u_1'(x_j)\}[v_1(x_j)]),$$

and

$${\varepsilon_2}^2 \sum_{j=1}^{N} \int_{K_j} u_2'(x)v_2'(x)dx = -{\varepsilon_2}^2 \sum_{j=1}^{N} \int_{K_j} u_2''(x)v_2(x)dx - {\varepsilon_2}^2 \sum_{j=0}^{N} (\{u_2'(x_j)\}[v_2(x_j)]).$$

Using the above estimates and recalling (4.1.1), we can obtain that

$$B(\vec{u},\, \vec{v}) = L(\vec{v}), \qquad \forall \vec{v} \in V_N^k(\Omega)^2. \tag{4.3.2}$$

By subtracting (4.3.2) from (4.3.1), we get

$$B(\vec{u} - \vec{u}_h,\, \vec{v}) = 0, \qquad \forall \vec{v} \in V_N^k(\Omega)^2. \qquad \blacksquare$$

A natural norm associated with the bilinear form $B(.,.)$ is the $\mathcal{E}-$weighted energy norm

$$\begin{aligned} |||\vec{v}|||_{\mathcal{E}}^2 &= \sum_{j=1}^{N} \left({\varepsilon_1}^2 \|v_1'\|_{L^2(K_j)}^2 + {\varepsilon_2}^2 \|v_2'\|_{L^2(K_j)}^2 \right) + \beta^2 \sum_{j=1}^{N} \left(\|v_1\|_{L^2(K_j)}^2 + \|v_2\|_{L^2(K_j)}^2 \right) \\ &\quad + \sum_{j=0}^{N} \sigma_j [v_1(x_j)]^2 + \sum_{j=0}^{N} \sigma_j [v_2(x_j)]^2, \end{aligned} \tag{4.3.3}$$

where σ_j are the penalty parameters and β is such that it satisfies $\min\{c_{11} + c_{12}, c_{21} + c_{22}\} > \beta^2$.

It is easy to show that, the bilinear form given in (4.3.1) satisfies the coercivity condition, and hence it can be shown that

$$|||\vec{u_h}|||_{\mathcal{E}} \leq \|f\|_{L^2(\Omega)},$$

which implies the uniqueness of the solution of (4.3.1). Because $V_N^k(\Omega)^2$ is a finite-dimensional space, the existence of the solution follows from its uniqueness.

4.4 Error Analysis

In this section, we perform the error analysis for the NIPG method (4.3.1). We will show that the NIPG method possesses optimal order of convergence. Following the idea given in [60], we introduce a special interpolant on each element K_j, for any $w \in C(K_j)$, we define $k+1$ nodal functional N_l by

$$N_0(w) = w(x_{j-1}),\ N_k(w) = w(x_j),$$

$$N_l(w) = \frac{1}{(x_j - x_{j-1})^l} \int_{x_{j-1}}^{x_j} (x - x_{j-1})^{l-1} w(x)dx, \quad l = 1, \ldots, k-1.$$

Now the local interpolation $w_I|_k \in P^k(K_j)$ is defined by $N_l(w_I - w) = 0, l = 0, \ldots, k$.

Lemma 4.4.1. *[60] Let w_I be the interpolant of w, then we have the following properties:*

$$\begin{aligned} |w - w_I|_{l,K_j} &\leq C h_j^{k+1-l} |w|_{k+1,K_j}, l = 0, 1, \ldots, k+1, \forall w \in H^{k+1}(K_j), \\ \|w - w_I\|_{L^\infty(K_j)} &\leq C h_j^{k+1} |w|_{k+1,\infty,K_j}, \forall w \in W^{k+1,\infty}(K_j), \end{aligned}$$

where K_j is any element of the partition $\mathcal{T}_N$ and h_j is the length of element K_j.

Lemma 4.4.2. *Let $\vec{S}_I$ and $\vec{E}_I$ be the interpolants of $\vec{S}$ and $\vec{E}$, respectively, on the piecewise uniform Shishkin mesh. Then, we have $\vec{u}_I = \vec{S}_I + \vec{E}_I$ and for $m = 1, 2$ the following estimates hold true:*

$$\begin{aligned}
\|u_m - u_{m,I}\|_{L^\infty(\Omega_i)} &\leq C(N^{-1}\ln N)^{k+1}, \text{for } i = 1, 2, 4, 5, && (4.4.1)\\
\|(S_m - S_{m,I})^{(l)}\|_{L^2(\Omega)} &\leq CN^{l-(k+1)}, \text{ for } l = 0, 1, 2, \ldots, k, && (4.4.2)\\
\|E_m\|_{L^\infty(\Omega_3)} + {\varepsilon_2}^{-1/2}\|E_m\|_{L^2(\Omega_3)} &\leq CN^{-\alpha}, && (4.4.3)\\
\|E_m^{(l)}\|_{L^2(\Omega_3)} &\leq C{\varepsilon_2}^{1/2-l}N^{-\alpha}, \text{ for } l = 0, 1, \cdots, k, && (4.4.4)\\
N^{-1}\|E'_{m,I}\|_{L^2(\Omega_3)} + \|E_{m,I}\|_{L^2(\Omega_3)} &\leq C({\varepsilon_2}^{1/2}N^{-\alpha} + N^{-(1/2+\alpha)}), && (4.4.5)\\
\|u_m - u_{m,I}\|_{L^\infty(\Omega_3)} &\leq C(N^{-(k+1)} + N^{-\alpha}). && (4.4.6)
\end{aligned}$$

Proof. The linearity of the interpolation operator implies $\vec{u_I} = (\vec{S} + \vec{E})_I = \vec{S}_I + \vec{E}_I$. From Lemma 4.4.1, we can have

$$\|u_m - u_{m,I}\|_{L^\infty(\Omega_i)} \leq Ch_j^{k+1}|u_m^{(k+1)}|_{L^\infty(\Omega_i)}, \tag{4.4.7}$$

using the solution decomposition and the bounds on the smooth and the layer components given in (4.2.3), we can obtain that

$$|u_1^{(k+1)}|_{L^\infty(\Omega_i)} \leq |S_1^{(k+1)}|_{L^\infty(\Omega_i)} + |E_1^{(k+1)}|_{L^\infty(\Omega_i)} \leq C({\varepsilon_1}^{-(k+1)}D_{\varepsilon_1}(x) + {\varepsilon_2}^{-(k+1)}D_{\varepsilon_2}(x)).$$

We know that the interval length of the mesh in the subdomains Ω_1 and Ω_5 is given by $h_i = (8\alpha\varepsilon_1/\beta)N^{-1}\ln N$. From (4.4.7) and the above inequality, we obtain

$$\|u_1 - u_{1,I}\|_{L^\infty(\Omega_i)} \leq C(N^{-1}\ln N)^{k+1}, \quad \text{for} \quad i = 1, 5.$$

In a similar way, we can show that

$$|u_2^{(k+1)}|_{L^\infty(\Omega_i)} \leq C{\varepsilon_2}^{-(k+1)}|D_{\varepsilon_2}(x)|,$$

now from the inequality (4.4.7) and the above inequality, we can obtain that

$$\|u_2 - u_{2,I}\|_{L^\infty(\Omega_i)} \leq C(N^{-1}\ln N)^{k+1}, \text{ for } i = 1, 5.$$

Next, we will prove inequality (4.4.1) in the subdomains Ω_2 and Ω_4, as we know that the interval length of the mesh in the subdomains Ω_2 and Ω_4 is given by $h_i = 8(\tau_{\varepsilon_2} - \tau_{\varepsilon_1})/N$. Using inequality (4.4.7) and the value of $h_i = \frac{8\alpha}{\beta}(\varepsilon_2 - \varepsilon_1)N^{-1}\ln N$ in Ω_2 and Ω_4, we can obtain that

$$\|u_m - u_{m,I}\|_{L^\infty(\Omega_i)} \leq C(N^{-1}\ln N)^{k+1}, \text{ for } i = 2, 4 \text{ and } m = 1, 2.$$

Next by using Lemma 4.4.1 for the smooth part of the solution and the bounds on the smooth part given in (4.2.3), we get

$$\|(S_m - S_{m,I})^{(l)}\|_{L^2(\Omega)} \leq CN^{l-(k+1)}|S_m|_{k+1,K_j} \leq CN^{l-(k+1)}.$$

To prove (4.4.3), we need to show that

$$\begin{aligned}
\|E_m\|_{L^\infty(\Omega_3)} &\leq C \max_{[\tau_{\varepsilon_2},1-\tau_{\varepsilon_2}]}(D_{\varepsilon_1}(x) + D_{\varepsilon_2}(x)) \\
&\leq C \max_{[\tau_{\varepsilon_2},1-\tau_{\varepsilon_2}]}(\exp(-\beta x/\varepsilon_2) + \exp(-\beta(1-x)/\varepsilon_2)) \\
&\leq CN^{-\alpha}, \quad (\text{using } \tau_{\varepsilon_2} = (\alpha\varepsilon_2/\beta)\ln N),
\end{aligned}$$

here, we have used $D_{\varepsilon_1}(x) \leq D_{\varepsilon_2}(x)$. From the definition of the L^2–norm and the value of τ_{ε_2}, we obtain that

$$\begin{aligned}
\|E_m\|^2_{L^2(\Omega_3)} &\leq C \int_{\tau_{\varepsilon_2}}^{1-\tau_{\varepsilon_2}} (D_{\varepsilon_1}(x) + D_{\varepsilon_2}(x))^2 dx \\
&\leq C \int_{\tau_{\varepsilon_2}}^{1-\tau_{\varepsilon_2}} (\exp(-2\beta x/\varepsilon_2) + \exp(-2\beta(1-x)/\varepsilon_2))dx \\
&\leq C\varepsilon_2 N^{-2\alpha}.
\end{aligned}$$

By adding the above two inequalities, we can get

$$\|E_m\|_{L^\infty(\Omega_3)} + {\varepsilon_2}^{-1/2}\|E_m\|_{L^2(\Omega_3)} \leq CN^{-\alpha}.$$

In order to prove (4.4.4), we need to show that

$$\begin{aligned}
\|E_m^{(l)}\|^2_{L^2(\Omega_3)} &\leq C \int_{\tau_{\varepsilon_2}}^{1-\tau_{\varepsilon_2}} |E_m^{(l)}(x)|^2 dx \\
&\leq C{\varepsilon_2}^{-2l} \int_{\tau_{\varepsilon_2}}^{1-\tau_{\varepsilon_2}} (\exp(-2\beta x/\varepsilon_2) + \exp(-2\beta(1-x)/\varepsilon_2))dx \\
&\leq C{\varepsilon_2}^{1-2l} N^{-2\alpha},
\end{aligned}$$

here, we used ${\varepsilon_1}^{-k} D_{\varepsilon_1}(x) \leq {\varepsilon_2}^{-k} D_{\varepsilon_2}(x)$ and by taking the square root, we get the required result

$$\|E_m^{(l)}\|_{L^2(\Omega_3)} \leq C{\varepsilon_2}^{1/2-l} N^{-\alpha}.$$

An inverse inequality yields

$$N^{-1}\|E'_{m,I}\|_{L^2(\Omega_3)} + \|E_{m,I}\|_{L^2(\Omega_3)} \leq C\|E_{m,I}\|_{L^2(\Omega_3)}.$$

In order to prove (4.4.5) it remains to bound $\|E_{m,I}\|_{L^2(\Omega_3)}$. Consider the element $K_j = (x_{j-1}, x_j)$. The local nodal functionals can be estimated by

$$|N_i(E_m)| \leq C(\exp(-\beta x_{j-1}/\varepsilon_2) + \exp(-\beta(1-x_j)/\varepsilon_2)),$$

thus, we have from the local representation,

$$E_{m,I}|_{K_j} = \sum_{i=0}^{k} N_i(E_m)\phi_i,$$

the estimate

$$\begin{aligned} ||E_{m,I}||^2_{L^2(K_j)} &\leq \sum_{i=0}^{k} |N_i(E_m)|^2 ||\phi_i||^2_{L^2(K)} \\ &\leq CN^{-1}(\exp(-2\beta x_{j-1}/\varepsilon_2) + \exp(-2\beta(1-x_j)/\varepsilon_2)), \end{aligned} \tag{4.4.8}$$

where we have used $||\phi_i||_{L^2(K_j)} \leq CN^{-1}$, summing up, we get,

$$\sum_{K_j \in \Omega_3} ||E_{m,I}||^2_{L^2(K_j)} \leq CN^{-1} \sum_{j=N/4+1}^{3N/4} (\exp(-2\beta x_{j-1}/\varepsilon_2) + \exp(-2\beta(1-x_j)/\varepsilon_2)).$$

Recall that the mesh size on the coarse mesh has been denoted by H and satisfies $1/N \leq H \leq 2/N$. The RHS of the above inequality becomes,

$$\begin{aligned} \exp(-2\beta x_{j-1}/\varepsilon_2) + \exp(-2\beta(1-x_j)/\varepsilon_2) &= \exp\left((-2\beta x_{j-1} + 2\beta x_j - 2\beta x_j)/\varepsilon_2\right) \\ &\quad + \exp\left((-2\beta(1-x_j) + 2\beta x_{j-1} - 2\beta x_{j-1})/\varepsilon_2\right) \\ &\leq \exp(2\beta H/\varepsilon_2)(\exp\left(-2\beta x/\varepsilon_2\right) + \exp\left(-2\beta(1-x)/\varepsilon_2\right)), \text{ for } x \in (x_{j-1},\, x_j). \end{aligned}$$

Integrating the above inequality over (x_{j-1}, x_j), we obtain that

$$\begin{aligned} N^{-1}(\exp\left(-2\beta x_{j-1}/\varepsilon_2\right) + \exp\left(-2\beta(1-x_j)/\varepsilon_2\right)) \leq \exp(2\beta H/\varepsilon_2) \times \\ \int_{x_{j-1}}^{x_j} (\exp(-2\beta x/\varepsilon_2) + \exp(-2\beta(1-x)/\varepsilon_2))dx, \end{aligned}$$

and summing up for $j = N/4+1, \ldots, 3N/4-1$, we have

$$N^{-1} \sum_{j=N/4+1}^{3N/4-1} (\exp(-2\beta x_{j-1}/\varepsilon_2) + \exp(-2\beta(1-x_j)/\varepsilon_2)) \leq C\varepsilon_2 N^{-2\alpha}.$$

For the last interval $(x_{3N/4-1},\, x_{3N/4})$, we get from inequality (4.4.8) that

$$||E_{m,I}||^2_{L^2(K_j)} \leq CN^{-(1+2\alpha)}.$$

Combining the above two estimates, we get our desired result, *i.e.*,

$$N^{-1}\|E'_{m,I}\|_{L^2(\Omega_3)} + \|E_{m,I}\|_{L^2(\Omega_3)} \leq C({\varepsilon_2}^{1/2}N^{-\alpha} + N^{-(1/2+\alpha)}),$$

using the solution decomposition and the triangle inequality, we can get

$$\begin{aligned}\|u_m - u_{m,I}\|_{L^\infty(\Omega_3)} &\leq \|S_m - S_{m,I}\|_{L^\infty(\Omega_3)} + \|E_m\|_{L^\infty(\Omega_3)} + \|E_{m,I}\|_{L^\infty(\Omega_3)} \\ &\leq C(N^{-(k+1)} + N^{-\alpha}).\end{aligned}$$

■

To obtain the error estimate of the NIPG method, we decompose the error in two parts, as

$$|||\vec{u} - \vec{u}_h|||_\varepsilon \leq |||\vec{u} - \vec{u}_I|||_\varepsilon + |||\vec{u}_I - \vec{u}_h|||_\varepsilon.$$

Let $\vec{\eta} = \vec{u} - \vec{u}_I$ and $\vec{\xi} = \vec{u}_I - \vec{u}_h$. For proving the error estimates for the interpolation on the element boundaries, we need the following multiplicative trace inequality.

Lemma 4.4.3. *[70] For any $w \in H^1(K_j)$, we have*

$$|w(x_j)|^2 \leq 2(h_j^{-1}\|w\|^2_{L^2(K_j)} + \|w\|_{L^2(K_j)}\|w'\|_{L^2(K_j)}),\ x_j \in K_j.$$

Lemma 4.4.4. *For $\alpha = k+1$, $\{\eta'_m\}$ satisfies*

$$\{\eta'_m(x_j)\}^2 \leq \begin{cases} C{\varepsilon_2}^{-2}(N^{-1}\ln N)^{2k}, & \text{for } x_j \in \Omega \setminus \Omega_3, \\ C{\varepsilon_2}^{-2}N^{-(2k+1)}, & \text{for } x_j \in \Omega_3, \end{cases}$$

where $\eta_m = u_m - u_{m,I}$, for $m = 1, 2$.

Proof. From the definition of the average, and Lemma 4.4.3, we can write

$$\begin{aligned}\{\eta'_m(x_j)\}^2 &= \frac{1}{4}(\eta'_m(x_j^-) + \eta'_m(x_j^+))^2 \leq \frac{1}{2}(\eta'_m(x_j^-)^2 + \eta'_m(x_j^+)^2) \\ &\leq h_j^{-1}\|\eta'_m\|^2_{L^2(K_j)} + \|\eta'_m\|_{L^2(K_j)}\|\eta''_m\|_{L^2(K_j)} + h_{j+1}^{-1}\|\eta'_m\|^2_{L^2(K_{j+1})} \\ &\quad + \|\eta'_m\|_{L^2(K_{j+1})}\|\eta''_m\|_{L^2(K_{j+1})}.\end{aligned}$$

Now, we have to estimate $\|\eta'_m\|_{L^2(K_j)}$ and $\|\eta''_m\|_{L^2(K_j)}$, separately. From (4.4.2), we can have

$$\begin{aligned}\|(S_m - S_{m,I})'\|_{L^2(K_j)} &\leq CN^{-k}, \\ \|(S_m - S_{m,I})''\|_{L^2(K_j)} &\leq CN^{-k+1}, \quad \text{for all } K_j \in \Omega.\end{aligned}$$

In order to obtain the bounds for $\|\eta'_m\|_{L^2(K_j)}$ and $\|\eta''_m\|_{L^2(K_j)}$, it remains to estimate $\|(E_m - E_{m,I})'\|_{L^2(K_j)}$ and $\|(E_m - E_{m,I})''\|_{L^2(K_j)}$ inside and outside the boundary layer regions.

First, we will estimate $\|(E_m - E_{m,I})'\|_{L^2(K_j)}$ and $\|(E_m - E_{m,I})''\|_{L^2(K_j)}$ outside the boundary layer region, that is, for $K_j \in \Omega_3$. From (4.4.4) and (4.4.5) and using the fact that $\varepsilon_2 \leq CN^{-1}$, $\alpha = k+1$, we can obtain

$$\|(E_m - E_{m,I})'\|_{L^2(K_j)} \leq \|E_m'\|_{L^2(K_j)} + \|E_{m,I}'\|_{L^2(K_j)} \leq C{\varepsilon_2}^{-1/2} N^{-(k+1)}.$$

Similarly, using the inverse inequality and the fact that $\varepsilon_2 \leq CN^{-1}$, $\alpha = k+1$, we can have

$$\begin{aligned} \|(E_m - E_{m,I})''\|_{L^2(K_j)} &\leq \|E_m''\|_{L^2(K_j)} + \|E_{m,I}''\|_{L^2(K_j)} \\ &\leq \|E_m''\|_{L^2(K_j)} + Ch_j^{-1}\|E_{m,I}'\|_{L^2(K_j)} \\ &\leq C{\varepsilon_2}^{-3/2} N^{-(k+1)}. \end{aligned}$$

Now we will estimate $\|(E_m - E_{m,I})'\|_{L^2(K_j)}$ and $\|(E_m - E_{m,I})''\|_{L^2(K_j)}$ inside the boundary layer regions, that is, $K_j \in \Omega \setminus \Omega_3$. From Lemmas 4.4.1 and 4.2.1, for $l = 1, 2$, we have

$$\begin{aligned} \|(E_m - E_{m,I})^{(l)}\|_{L^2(K_j)} &\leq Ch_j^{k+1-l} \left(\int_{K_j} {\varepsilon_2}^{-2(k+1)} B_{\varepsilon_2}^2(x)dx \right)^{1/2} \\ &\leq C{\varepsilon_2}^{1/2-l} (N^{-1} \ln N)^{k+3/2-l}. \end{aligned}$$

From the triangle inequality and the above estimate, we can obtain

$$\|\eta_m'\|_{L^2(K_j)} \leq \begin{cases} C{\varepsilon_2}^{-1/2} (N^{-1} \ln N)^{k+1/2}, & \text{for } K_j \in \Omega \setminus \Omega_3, \\ C{\varepsilon_2}^{-1/2} N^{-k} ({\varepsilon_2}^{1/2} + N^{-1}), & \text{for } K_j \in \Omega_3, \end{cases}$$

and

$$\|\eta_m''\|_{L^2(K_j)} \leq \begin{cases} C{\varepsilon_2}^{-3/2} (N^{-1} \ln N)^{k-1/2}, & \text{for } K_j \in \Omega \setminus \Omega_3, \\ C{\varepsilon_2}^{-3/2} N^{1-k} ({\varepsilon_2}^{3/2} + N^{-2}), & \text{for } K_j \in \Omega_3. \end{cases}$$

By combining all the above estimates we can get the desired result. ∎

Theorem 4.4.5. *For $\alpha = k+1$, we have following interpolation error bound:*

$$|||\vec{\eta}|||_{\varepsilon} \leq C(N^{-1} \ln N)^k,$$

where $\vec{\eta} = \vec{u} - \vec{u}_I$.

Proof. Since $\vec{u} - \vec{u}_I$ is continuous in Ω, we have $[\eta_1]_j = [\eta_2]_j = 0$, $j = 0, \ldots, N$. Then

$$|||\vec{\eta}|||_{\mathcal{E}}^2 = \sum_{j=1}^{N} ({\varepsilon_1}^2 \|\eta_1'\|_{L^2(K_j)}^2 + {\varepsilon_2}^2 \|\eta_2'\|_{L^2(K_j)}^2) + \beta^2 \sum_{j=1}^{N} (\|\eta_1\|_{L^2(K_j)}^2 + \|\eta_2\|_{L^2(K_j)}^2).$$

From Lemma 4.4.2, we can easily conclude that

$$\begin{aligned}
\|u_m - u_{m,I}\|_{L^2(\Omega)} &\leq |\Omega_1|^{1/2}\|u_m - u_{m,I}\|_{L^\infty(\Omega_1)} + |\Omega_2|^{1/2}\|u_m - u_{m,I}\|_{L^\infty(\Omega_2)} + \\
&\quad |\Omega_3|^{1/2}\|u_m - u_{m,I}\|_{L^\infty(\Omega_3)} + |\Omega_4|^{1/2}\|u_m - u_{m,I}\|_{L^\infty(\Omega_4)} + \\
&\quad |\Omega_5|^{1/2}\|u_m - u_{m,I}\|_{L^\infty(\Omega_5)} \\
&\leq \tau_{\varepsilon_1}^{1/2}\|u_m - u_{m,I}\|_{L^\infty(\Omega_1)} + (\tau_{\varepsilon_2} - \tau_{\varepsilon_1})^{1/2}\|u_m - u_{m,I}\|_{L^\infty(\Omega_2)} + \\
&\quad (1 - 2\tau_{\varepsilon_2})^{1/2}\|u_m - u_{m,I}\|_{L^\infty(\Omega_3)} + (\tau_{\varepsilon_2} - \tau_{\varepsilon_1})^{1/2}\|u_m - u_{m,I}\|_{L^\infty(\Omega_4)} + \\
&\quad (\tau_{\varepsilon_1})^{1/2}\|u_m - u_{m,I}\|_{L^\infty(\Omega_5)} \\
&\quad \leq C(N^{-1}\ln N)^k, \quad \text{for } m = 1, 2.
\end{aligned}$$

Similarly, we can show that

$$\varepsilon_1 |u_m - u_{m,I}|_{1,\Omega} \leq C(N^{-1}\ln N)^k, \text{ and } \varepsilon_2 |u_m - u_{m,I}|_{1,\Omega} \leq C(N^{-1}\ln N)^k.$$

Hence, we have

$$|||\vec{\eta}|||_{\mathcal{E}} \leq C(N^{-1}\ln N)^k,$$

which is the required result. ∎

Theorem 4.4.6. *Let $\vec{\xi} = \vec{u}_h - \vec{u}_I$. Then $\vec{\xi}$ satisfies the following error bound:*

$$|||\vec{\xi}|||_{\mathcal{E}} \leq C(N^{-1}\ln N)^k.$$

Proof. From the bilinear form given in (4.3.1), for the first term of $B_1(\vec{\eta}, \vec{\xi})$, we have

$$\begin{aligned}
\sum_{j=1}^{N} \int_{K_j} {\varepsilon_1}^2 \eta_1'(x)\xi_1'(x)dx &\leq \left(\sum_{j=1}^{N} \int_{K_j} {\varepsilon_1}^2 (\eta_1')^2(x)dx\right)^{1/2} \left(\sum_{j=1}^{N} \int_{K_j} {\varepsilon_1}^2 (\xi_1')^2(x)dx\right)^{1/2} \\
&\leq \varepsilon_1 \|\eta_1'\|_{L^2(\Omega)} |||\vec{\xi}|||_{\mathcal{E}} \leq C(N^{-1}\ln N)^k |||\vec{\xi}|||_{\mathcal{E}},
\end{aligned}$$

and using the fact that $[\eta_1]_j = 0$, $j = 0, \ldots, N$, bound for the second term of $B_1(\vec{\eta}, \vec{\xi})$ is

$$\begin{aligned}
\sum_{j=0}^{N} {\varepsilon_1}^2 (\{\eta_1'(x_j)\}[\xi_1(x_j)]) &\leq \left(\sum_{j=0}^{N} \frac{{\varepsilon_1}^2}{\sigma_j} \{\eta_1'\}_j^2\right)^{1/2} \left(\sum_{j=0}^{N} \sigma_j [\xi_1]_j^2\right)^{1/2} \\
&\leq C(N^{-1}\ln N)^k |||\vec{\xi}|||_{\mathcal{E}},
\end{aligned}$$

where σ_j is defined by

$$\sigma_j = \begin{cases} N, & \text{for } K_j \in \Omega \setminus \Omega_3, \\ 1, & \text{for } K_j \in \Omega_3. \end{cases}$$

Again using the fact that $[\eta_1]_j = 0$, $j = 0, \ldots, N$, third term will vanish and we can show that the fourth term of the bilinear form $B_1(\vec{\eta}, \vec{\xi})$ given in (4.3.1) satisfy

$$\begin{aligned} \sum_{j=1}^{N} \int_{K_j} c_{11}(x)\eta_1(x)\xi_1(x)dx &\leq C(N^{-1}\ln N)^k |||\vec{\xi}|||_{\mathcal{E}}, \\ \sum_{j=1}^{N} \int_{K_j} c_{12}(x)\eta_2(x)\xi_1(x)dx &\leq C(N^{-1}\ln N)^k |||\vec{\xi}|||_{\mathcal{E}}. \end{aligned}$$

Similarly, we can show that the bound for the bilinear form $B_2(\vec{\eta}, \vec{\xi})$ is

$$B_2(\vec{\eta}, \vec{\xi}) \leq C(N^{-1}\ln N)^k |||\vec{\xi}|||_{\mathcal{E}}.$$

Using Galerkin orthogonality and coercivity of bilinear form, we have $|||\vec{\xi}|||_{\mathcal{E}} \leq C(N^{-1}\ln N)^k$. ∎

From Theorems 4.4.5 and 4.4.6, we can obtain the parameter-uniform error estimate for the NIPG method, which is given in the following theorem.

Theorem 4.4.7. *Let $\vec{u}$ and $\vec{u}_h$ be respectively the solutions of the continuous problem (4.1.1) and the discrete problem (4.3.1). Then, we have the following error bound:*

$$|||\vec{u} - \vec{u}_h|||_{\mathcal{E}} \leq C(N^{-1}\ln N)^k.$$

4.5 Remarks on the Superconvergence Error Analysis

In our error analysis, we separated the error into two parts, namely, the interpolation error and the discretization error. And we find the bound of the discretization error using the bound on the interpolation error. For the superconvergence, one has to improve the order of convergence of the interpolation error. To improve the order of convergence for the interpolation error, we use piecewise Lagrange interpolation on Gauss points and discrete energy norm. Here, we will derive theoretical error bound for the interpolation error and discretization error. Using the interpolation result from Chapter 2, we have following result.

Let u_I denote the piecewise Lagrange interpolation using $\{x_{i,j}\}_{j=0}^{k}$ as nodal points on each interval $[x_{i-1}, x_i]$. Then

$$|(u - u_I)'(x_{i,j})| \leq Ch_i^k \int_{x_{i-1}}^{x_i} |u^{(k+2)}(x)|dx.$$

And discrete energy norm is defined as

$$\begin{aligned}|||\vec{v}|||^2 &= \varepsilon_1^2\sum_{i=1}^{N}h_i\sum_{j=1}^{p}w_j v_1'(x_{ij})^2+\varepsilon_2^2\sum_{i=1}^{N}h_i\sum_{j=1}^{p}w_j v_2'(x_{ij})^2+\beta^2\sum_{i=1}^{N}(\|v_1\|^2_{L^2(K_i)}+\|v_2\|^2_{L^2(K_i)})\\ &+ \sum_{i=0}^{N}\sigma_i[v_1(x_i)]^2+\sum_{i=0}^{N}\sigma_i[v_2(x_i)]^2. \qquad (4.5.1)\end{aligned}$$

Theorem 4.5.1. *Let $\vec{u}$ be the solution of (4.1.1) and $\vec{u}_I$ denotes the piecewise Lagrange interpolation on Gauss points, then we have*

$$|||\vec{u}-\vec{u}_I|||\le C(N^{-1}\ln N)^{k+1}.$$

Proof. Since $\vec{u}-\vec{u}_I$ is continuous in Ω, we have $[\eta_1]_j=[\eta_2]_j=0$, $j=0,\dots,N$. Then

$$\begin{aligned}|||\vec{\eta}|||^2 &= \varepsilon_1^2\sum_{i=1}^{N}h_i\sum_{j=1}^{p}w_j\eta_1'(x_{ij})^2+\varepsilon_2^2\sum_{i=1}^{N}h_i\sum_{j=1}^{p}w_j\eta_2'(x_{ij})^2\\ &+\beta^2\sum_{i=1}^{N}(\|\eta_1\|^2_{L^2(K_i)}+\|\eta_2\|^2_{L^2(K_i)}). \qquad (4.5.2)\end{aligned}$$

From Lemma 4.4.2, we can easily conclude that

$$\begin{aligned}\|u_m-u_{m,I}\|_{L^2(\Omega)} &\le |\Omega_1|^{1/2}\|u_m-u_{m,I}\|_{L^\infty(\Omega_1)}+|\Omega_2|^{1/2}\|u_m-u_{m,I}\|_{L^\infty(\Omega_2)}+\\ &\quad |\Omega_3|^{1/2}\|u_m-u_{m,I}\|_{L^\infty(\Omega_3)}+|\Omega_4|^{1/2}\|u_m-u_{m,I}\|_{L^\infty(\Omega_4)}+\\ &\quad |\Omega_5|^{1/2}\|u_m-u_{m,I}\|_{L^\infty(\Omega_5)}\\ &\le \tau_{\varepsilon_1}^{1/2}\|u_m-u_{m,I}\|_{L^\infty(\Omega_1)}+(\tau_{\varepsilon_2}-\tau_{\varepsilon_1})^{1/2}\|u_m-u_{m,I}\|_{L^\infty(\Omega_2)}+\\ &\quad (1-2\tau_{\varepsilon_2})^{1/2}\|u_m-u_{m,I}\|_{L^\infty(\Omega_3)}+(\tau_{\varepsilon_2}-\tau_{\varepsilon_1})^{1/2}\|u_m-u_{m,I}\|_{L^\infty(\Omega_4)}+\\ &\quad (\tau_{\varepsilon_1})^{1/2}\|u_m-u_{m,I}\|_{L^\infty(\Omega_5)}\\ &\le C(N^{-1}\ln N)^{k+1},\quad \text{for } m=1,2.\end{aligned}$$

Now, we will derive bound for the first term in the RHS of (4.5.2)

$$\begin{aligned}\varepsilon_1^2\sum_{i=1}^{N}h_i\sum_{j=1}^{p}w_j\eta_1'(x_{ij})^2 &= \varepsilon_1^2\sum_{i=1}^{N}h_i\sum_{j=1}^{p}w_j(u_1-u_{1,I})'(x_{ij})^2\\ &= \varepsilon_1^2\sum_{i=1}^{N}h_i\sum_{j=1}^{p}w_j(S_1-S_{1,I})'(x_{ij})^2+\varepsilon_1^2\sum_{i=1}^{N}h_i\sum_{j=1}^{p}w_j(E_1-E_{1,I})'(x_{ij})^2.\end{aligned} \qquad (4.5.3)$$

First term in the RHS of (4.5.3) can be bounded as

$$\begin{aligned}\varepsilon_1^2\sum_{i=1}^{N}h_i\sum_{j=1}^{p}w_j(S_1-S_{1,I})'(x_{ij})^2 &\leq C\sum_{i=1}^{N}h_ih_i^{2k}\bigg(\int_{x_{i-1}}^{xi}|S_1^{(k+2)}(x)|dx\bigg)^2\\ &\leq C\sum_{i=1}^{N}h_i^{2k+3}\\ &\leq C(N^{-1}\ln N)^{2k+2}. \qquad (4.5.4)\end{aligned}$$

We derive bound for the second term in the RHS of (4.5.3) separately, for inside and outside of the boundary layer. For subdomain Ω_1

$$\begin{aligned}\varepsilon_1^2\sum_{i=1}^{N/8}h_i\sum_{j=1}^{p}w_j(E_1-E_{1,I})'(x_{ij})^2 &\leq C\varepsilon_1^2\sum_{i=1}^{N/8}h_ih_i^{2k}\bigg(\int_{x_{i-1}}^{xi}|E_1^{(k+2)}(x)|dx\bigg)^2\\ &\leq C\varepsilon_1^2\sum_{i=1}^{N/8}h_i^{2k+1}\bigg(\int_{x_{i-1}}^{xi}|E_1^{(k+2)}(x)|^2dx\bigg)\bigg(\int_{x_{i-1}}^{xi}dx\bigg)\\ &\leq C(N^{-1}\ln N)^{2(k+1)}.\end{aligned}$$

Similarly using the mesh size on other subdomain, we can derive bound for the subdomain Ω_2, Ω_4, and Ω_5. Now, we will derive bound outside boundary layer that is the subdomain Ω_3

$$\varepsilon_1^2\sum_{i=N/4+1}^{3N/4}h_i\sum_{j=1}^{p}w_j(E_1-E_{1,I})'(x_{ij})^2\leq\varepsilon_1^2\sum_{i=N/4+1}^{3N/4}h_i\varepsilon_2^{-2}N^{-2(k+1)}\leq CN^{-2(k+1)},$$

where, we have used

$$\|(E_1-E_{1,I})^{(q)}\|_{L^\infty(\Omega_3)}\leq C\varepsilon_2^{-q}N^{-(k+1)}.$$

And above inequality can be proved by

$$\begin{aligned}\|(E_1-E_{1,I})^{(q)}\|_{L^\infty(\Omega_3)} &\leq \|E_1^{(q)}\|_{L^\infty(\Omega_3)}+\|E_{1,I}^{(q)}\|_{L^\infty(\Omega_3)}\\ &\leq \|E_1^{(q)}\|_{L^\infty(\Omega_3)},\ \big(\text{using } \|E_{1,I}^{(q)}\|_{L^\infty(\Omega_3)}\leq\|E_1^{(q)}\|_{L^\infty(\Omega_3)}\big),\end{aligned}$$

and

$$\begin{aligned}\|E_1^{(q)}\|_{L^\infty(\Omega_3)} &\leq C\varepsilon_2^{-q}\max_{[\tau_{\varepsilon_2},1-\tau_{\varepsilon_2}]}(\exp(-\beta x/\varepsilon_2)+\exp(-\beta(1-x)/\varepsilon_2))\\ &\leq C\varepsilon_2^{-q}N^{-(k+1)},\big(\text{using } \tau_{\varepsilon_2}=((k+1)\varepsilon_2/\beta)\ln N\big).\end{aligned}$$

Hence, we obtain that

$$\|(E_1-E_{1,I})^{(q)}\|_{L^\infty(\Omega_3)}\leq C\varepsilon_2^{-q}N^{-(k+1)}.$$

Similarly, bound for the second term in the RHS of (4.5.2) is

$$\varepsilon_2^2 \sum_{i=1}^{N} h_i \sum_{j=1}^{p} w_j \eta_2'(x_{ij})^2 \leq C N^{-2(k+1)}.$$

Hence, we have

$$|||\vec{\eta}||| \leq C(N^{-1} \ln N)^{k+1},$$

which is the required result. ∎

Theorem 4.5.2. *Let $\vec{u}_h$ denotes the solution of (4.3.1), then bound for the discretization error $\vec{\xi} = \vec{u}_h - \vec{u}_I$ is:*

$$|||\vec{\xi}||| \leq C(N^{-1} \ln N)^{k+1}.$$

Proof. By following the approach as discussed in Theorem 4.4.6, and using interpolation error from Theorem 4.5.1, one can derive the require result. ∎

Theorem 4.5.3. *Let $\vec{u}$ be the solution of the BVP (4.1.1) and $\vec{u_h}$ be the solution of the NIPG method defined in (4.3.1). Then error of the scheme satisfies*

$$|||\vec{u} - \vec{u}_h||| \leq C(N^{-1} \ln N)^{k+1}.$$

Proof. Combining Theorem 4.5.1 and Theorem 4.5.2, we get required result.

4.6 Numerical Results

In this section, we verify experimentally the convergence results obtained in Sections 4.4 and 4.5, by considering the numerical solution of a constant coefficient problem.

Example 4.6.1. *Consider the following singularly perturbed system of BVP:*

$$\begin{cases} -{\varepsilon_1}^2 u_1''(x) + 2u_1(x) - u_2(x) = f_1(x), \quad x \in \Omega, \\ -{\varepsilon_2}^2 u_2''(x) - u_1(x) + 2u_2(x) = f_2(x), \\ u_1(0) = u_2(0) = u_1(1) = u_2(1) = 0, \end{cases} \tag{4.6.1}$$

where $f_1(x)$, $f_2(x)$ are chosen such that

$$\begin{aligned} u_1(x) &= \frac{(\exp(-x/\varepsilon_1) + \exp(-(1-x)/\varepsilon_1))}{(1+\exp(-1/\varepsilon_1))} + \frac{(\exp(-x/\varepsilon_2) + \exp(-(1-x)/\varepsilon_2))}{(1+\exp(-1/\varepsilon_2))} - 2, \\ u_2(x) &= \frac{(\exp(-x/\varepsilon_2) + \exp(-(1-x)/\varepsilon_2))}{(1+\exp(-1/\varepsilon_2))} - 1, \end{aligned}$$

are the exact solution of the system of BVP (4.6.1).

We know that both the solutions of Example 4.6.1 have exponential layers of width $\mathcal{O}(\varepsilon_2 \ln \varepsilon_2)$, whereas only $u_1(x)$ has an additional sublayer of width $\mathcal{O}(\varepsilon_1 \ln \varepsilon_1)$. This can be seen in Figure 4.2 for the solution of Example 4.6.1 with $\varepsilon_1 = 10^{-6}$ and $\varepsilon_2 = 10^{-4}$.

Figure 4.3 and Figure 4.4 depict the plot of the exact and numerical solutions for $u_1(x)$ and $u_2(x)$ and their corresponding error (error=|exact solution − numerical solution|) for Example 4.6.1 for $\varepsilon_1 = 10^{-6}$ and $\varepsilon_2 = 10^{-4}$ with $N = 64$.

We calculate the error in the $\mathcal{E}-$weighted energy norm as defined in (4.3.3) and as well as in discrete energy norm defined in (4.5.1). Table 4.1 provides the numerical results with the finite element polynomials of degree $k = 1, 2$ in the $\mathcal{E}-$weighted energy norm as well as in the maximum norm. For our experiments, the singular perturbation parameters take values on the set $\mathcal{S} = \{(\varepsilon_1, \varepsilon_2) | \varepsilon_2 = 10^{-2}, \ldots, 10^{-8}, \varepsilon_1 = 10^{-1}\varepsilon_2\}$.

Figure 4.5 represents the log-log plot of the error in the the $\mathcal{E}-$weighted energy norm and maximum norm and for the NIPG method with linear and quadratic elements with $\varepsilon_1 = 10^{-6}$ and $\varepsilon_2 = 10^{-4}$. Further, Figure 4.5(a) depicts first-order of convergence in $\mathcal{E}-$weighted energy norm and second-order of convergence in maximum norm for linear finite elements space, whereas Figure 4.5(b) represents second-order of convergence in both the norms for quadratic finite elements space.

Table 4.2 shows the numerical results with the finite element polynomials of degree $k = 1, 2$ in the discrete energy norm. Figure 4.6 represents the log-log plot of the error in the discrete energy norm for the NIPG method with linear and quadratic elements with $\varepsilon_1 = 10^{-6}$ and $\varepsilon_2 = 10^{-4}$. Superconvergence properties of the NIPG method can be observed in Table 4.2 and Figure 4.6.

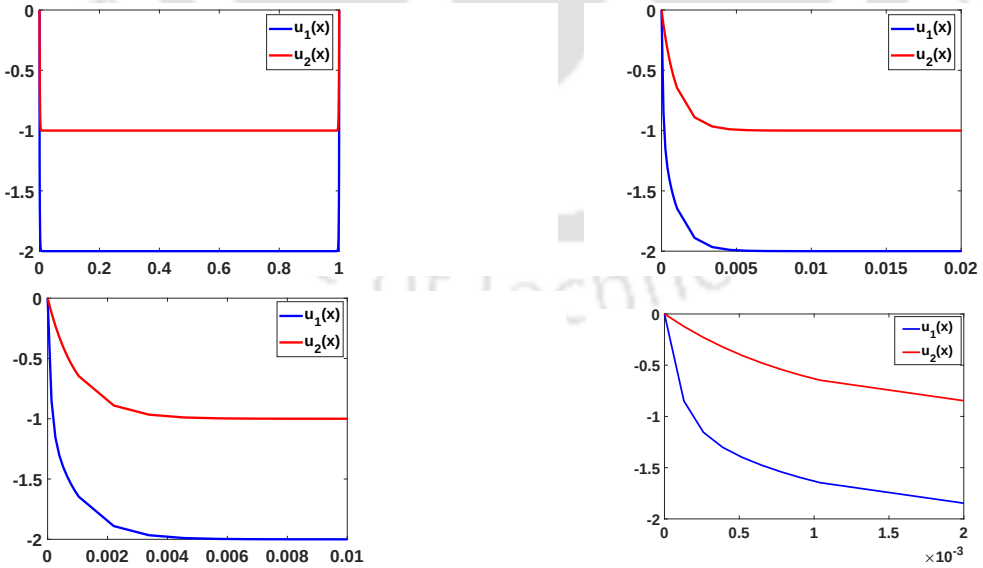

Figure 4.2: Overlapping boundary layers for Example 4.6.1 for $\varepsilon_1 = 10^{-6}$ and $\varepsilon_2 = 10^{-4}$ with $N = 64$.

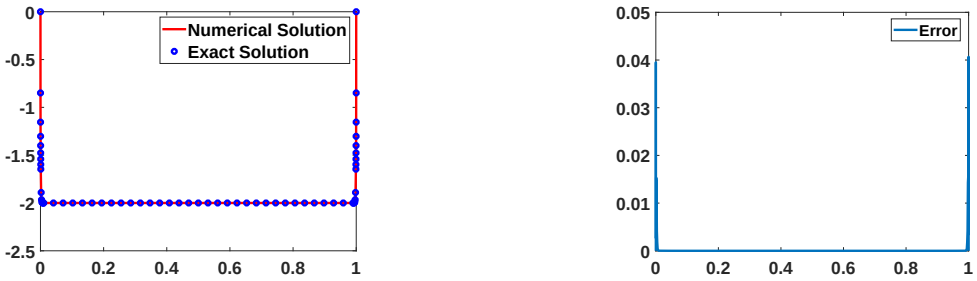

(a) Solution for $u_1(x)$. (b) Error for $u_1(x)$.

Figure 4.3: Solution $u_1(x)$ and corresponding error for Example 4.6.1 for $\varepsilon_1 = 10^{-6}$ and $\varepsilon_2 = 10^{-4}$ with $N = 64$.

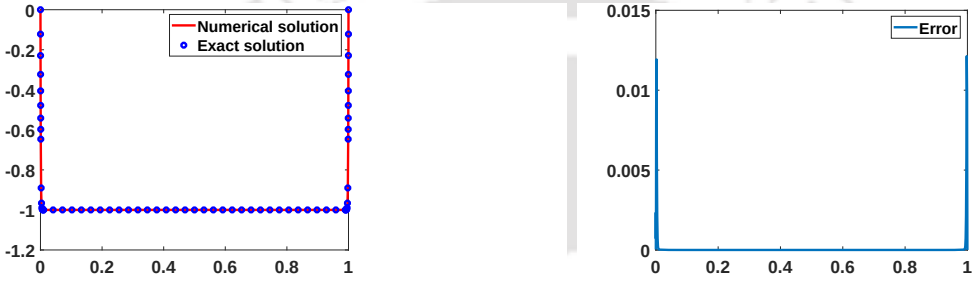

(a) Solution for $u_2(x)$. (b) Error for $u_2(x)$.

Figure 4.4: Solution $u_2(x)$ and corresponding error for Example 4.6.1 for $\varepsilon_1 = 10^{-6}$ and $\varepsilon_2 = 10^{-4}$ with $N = 64$.

4.7 Conclusion and Discussion

In this chapter, in order to obtain the numerical approximate solution of singularly perturbed system of reaction-diffusion BVP of the form (4.1.1), we have applied the NIPG method on the piecewise uniform Shishkin mesh. Theoretically, we proved that the proposed method is parameter-uniformly convergent with order k in the $\mathcal{E}-$weighted energy norm, where k is the degree of the piecewise polynomial used in the finite element space. To verify the theoretical error bound, we have implemented the proposed method to a test problem, and the results are highly convincing.

Table 4.1: *Error in $\mathcal{E}-$weighted energy norm and maximum norm for Example 4.6.1*

Norm	k	Number of mesh intervals N				
		16	32	64	128	256
$\|\|\|u-u_h\|\|\|_{\mathcal{E}}$	1	3.4893e-01	1.7965e-01	8.7736e-02	4.1533e-02	2.0297e-02
		0.95773	1.0340	1.0789	1.0330	
$\|\|\|u-u_h\|\|\|_{\mathcal{E}}$	2	6.4085e-03	1.6295e-03	4.7208e-04	2.6658e-04	2.4388e-04
		1.9756	1.7873	1.8244	1.2841	
$\|u-u_h\|_\infty$	1	8.9355e-02	3.4948e-02	1.1507e-02	3.5525e-03	1.1093e-03
		1.3544	1.6026	1.6957	1.6792	
$\|u-u_h\|_\infty$	2	7.2582e-02	1.8476e-02	3.6888e-03	8.3755e-04	2.0969e-04
		1.9739	2.3244	2.1389	1.9979	

Table 4.2: *Error in discrete energy norm for Example 4.6.1*

Norm	k	Number of mesh intervals N				
		16	32	64	128	256
$\|\|\|u-u_h\|\|\|$	1	1.4688e-03	5.5029e-04	1.9012e-04	6.2411e-05	1.9781e-05
		1.4164	1.5333	1.6070	1.6577	
$\|\|\|u-u_h\|\|\|$	2	4.5411e-06	7.8949e-07	1.2337e-07	1.7846e-08	2.4173e-09
		2.5240	2.6780	2.7893	2.8841	

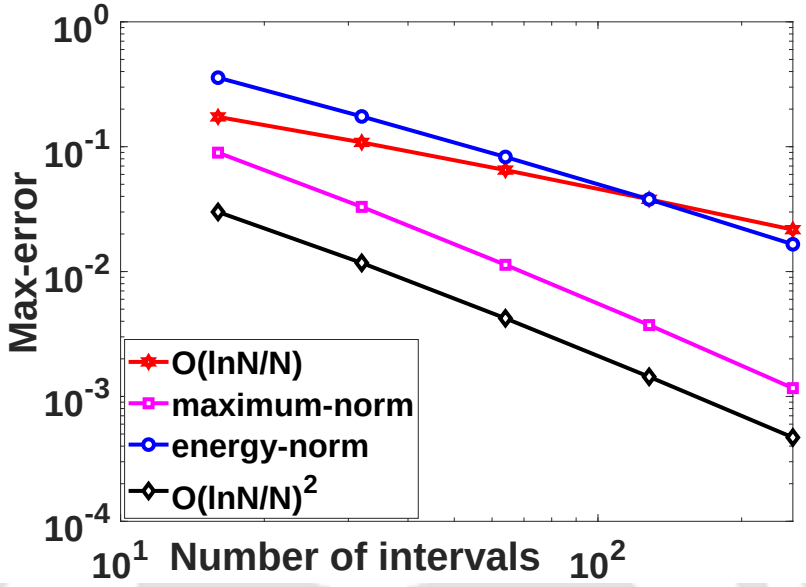

(a) For linear finite elements.

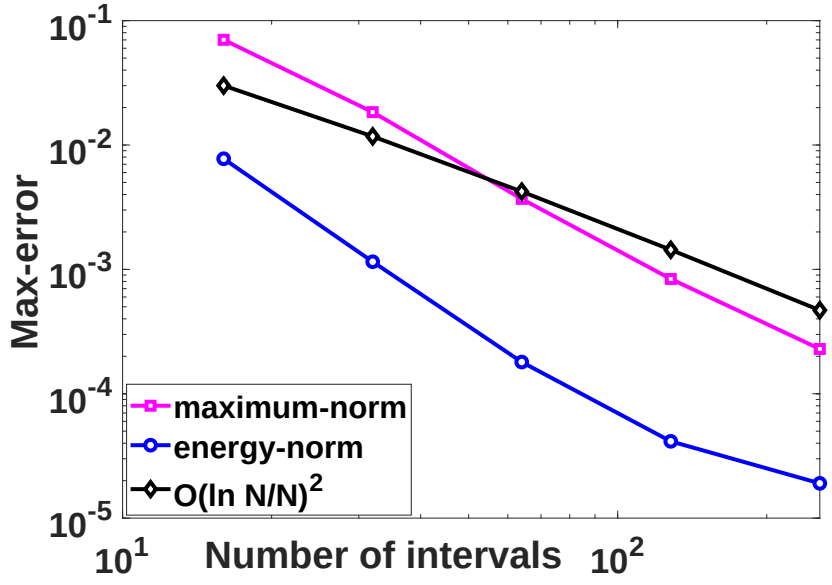

(b) For quadratic finite elements.

Figure 4.5: Order of convergence in the $\mathcal{E}-$weighted energy norm and maximum norm for Example 4.6.1.

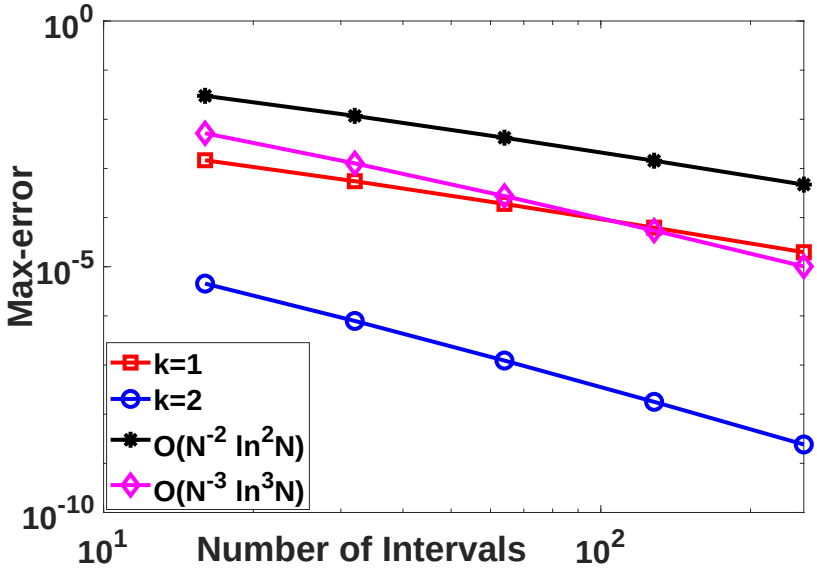

Figure 4.6: Order of convergence in the discrete energy norm through loglog plot for Example 4.6.1.

CHAPTER 5

Superconvergence Properties of Discontinuous Galerkin Method for Singularly Perturbed Parabolic IBVPs

In this chapter, a parabolic convection-diffusion-reaction problem is discretized in space by the NIPG method and in time by DG method. We have shown superconvergence properties that is $(k+1)$–order of convergence in space and $(l+1)$–order of convergence in time, where k and l are the degree of piecewise polynomial in finite element space. Numerical results are given to verify our theoretical findings.

5.1 Introduction

Superconvergence properties of DG method meaning to show faster rate of convergence for the approximate solution. In Chapter 2, we have shown superconvergence properties of the NIPG method by using the discrete energy norm and piecewise Lagrange interpolation on the Gauss points. In the present chapter, we have applied the NIPG method for the spatial variable and DG method for the temporal variable and shows superconvergence properties of DG method.

Here, we consider the following singularly perturbed parabolic convection-diffusion-reaction IBVP:

$$\begin{cases} u_t - \varepsilon u_{xx} + b(x)u_x + c(x)u = f(x,t), \quad x \in \mathcal{G} = (\Omega \times (0,\, T]), \\ u(x,\, 0) = u_0, \quad \text{for } x \in \overline{\Omega}, \\ u(0,\, t) = u(1,\, t) = 0, \quad \text{for } t \in (0,\, T], \end{cases} \tag{5.1.1}$$

here, $0 < \varepsilon \ll 1$ is a small parameter and $b(x), c(x)$ are sufficiently smooth with $b(x) > \beta > 0$. We also assume that

$$\gamma^2 = \min_{x \in \Omega} \left(c(x) - \frac{b'(x)}{2} \right) > 0, \ \ \forall x \in \Omega.$$

We decompose the exact solution $u(x,\, t)$ of the IBVP (5.1.1) into smooth and singular components as $u(x,\, t) = S(x,\, t) + E(x,\, t)$, then bounds on S, E and its derivatives are given by

$$\left|\frac{\partial^{k+l} S(x,\, t)}{\partial x^k \partial t^l}\right| \leq C, \tag{5.1.2}$$

$$\left|\frac{\partial^{k+l} E(x,\, t)}{\partial x^k \partial t^l}\right| \leq C\varepsilon^{-k} e^{-\beta(1-x)/\varepsilon}. \tag{5.1.3}$$

Proof of these bounds can be seen in [44].

The rest of the chapter is organized as follows: Domain discretization is given in Section 5.2. In Section 5.3, we have defined numerical scheme. Further, error analysis is derived in Section 5.4. Numerical results and conclusions are given in Section 5.5 and 5.6, respectively.

5.2 Domain Discretization

Here, we use uniform mesh to discretize the temporal domain and piecewise uniform Shishkin mesh for the spatial domain. On the time domain $[0,\, T]$, we introduce the equidistant meshes with uniform time step $\Delta t = (t_m - t_{m-1})$ such that

$$\mathcal{S}_t^M = \{t_m = m\Delta t,\, m = 0, 1, \cdots, M, \quad \Delta t = T/M\}.$$

Let $I_m = (t_{m-1},\, t_m]$. For the piecewise uniform Shishkin mesh, we divide $N/2$ mesh-intervals in the layer region and $N/2$ mesh-intervals in the outside layer region:

$$\overline{\Omega}_x^N = \{0 = x_0, x_1, \cdots, x_{N/2} = 1 - \tau_\varepsilon, \cdots, x_N = 1\}.$$

Here, the transition point $1-\tau_\varepsilon$, which separates the coarse and fine portion of the mesh, is obtained by taking

$$\tau_\varepsilon = \min\left\{\frac{1}{2}, \frac{2\varepsilon}{\beta}\ln N\right\}.$$

Let $\mathcal{T}_N = \{K_j = (x_{j-1}, x_j) : j = 1, \ldots, N\}$, be a partition of the domain Ω.

5.3 Numerical Scheme

By using the NIPG method for the space and DG method for the time, the finite element approximation for the parabolic convection-diffusion-reaction problem (5.1.1) is

$$\begin{cases} \text{Find } u_h \in V_{N,M}^{k,l}(\mathcal{G}) \text{ such that} \\ B(u_h,\, v_h) = l(v_h), \quad \forall v_h \in V_{N,M}^{k,l}(\mathcal{G}), \end{cases} \tag{5.3.1}$$

where $B(u,\, v)$ is defined as

$$B(u,\, v) = \sum_{m=1}^{M} \int_{t_{m-1}}^{t_m} \big((u_t,\, v) + A(u,\, v)\big)dt + \sum_{m=1}^{M-1} ([[u]]_m, v_m^+) + (u_0^+,\, v_0^+), \tag{5.3.2}$$

and $l(v)$ is defined as

$$l(v) = \int_0^{t_M} (f,\, v)dt + (u_0, v_0^+),$$

here u_t represents the derivative with respect to t and $A(u,\, v)$ is defined by

$$A(u,\, v) = A_1(u,\, v) + A_2(u,\, v) - A_2(v,\, u) + A_3(u,\, v),$$

where

$$\begin{aligned} A_1(u,\, v) &= \sum_{j=1}^{N} \varepsilon \int_{K_j} u_x v_x dx + \sum_{j=1}^{N} \int_{K_j} (b(x)u_x + c(x)u)v dx, \\ A_2(u,\, v) &= \sum_{j=1}^{N} \varepsilon \{u_x\}_j [v]_j, \\ A_3(u,\, v) &= \sum_{j=0}^{N} \sigma_j [u]_j [v]_j + \sum_{j=0}^{N} b(x_j)[u]_j v_j^-, \end{aligned}$$

here u_x denotes the derivative with respect to x.

If w_j are the weight function for the p-point Gaussian quadrature rule and x_{ij} are the Gauss points in the element $K_i = [x_{i-1},\, x_i]$, then the discrete energy norm associated with the bilinear form $A(.,\, .)$ is defined as follows:

$$|||v|||^2 = \varepsilon \sum_{i=1}^{N} h_i \sum_{j=1}^{p} w_j v_x(x_{ij},\, t)^2 + \gamma^2 \sum_{i=1}^{N} \|v\|^2_{L^2(K_i)} + \sum_{i=0}^{N} \sigma_i [v]_i^2. \tag{5.3.3}$$

We define the dG norm associated with the bilinear for $B(.,\, .)$ by

$$||v||^2_{dG} = \sum_{m=1}^{M} \int_{t_{m-1}}^{t_m} |||v|||^2 dt + \frac{1}{2}||v_0^+||^2_{L^2(\Omega)} + \frac{1}{2} \sum_{m=1}^{M-1} ||[[v]]_m||^2_{L^2(\Omega)} + \frac{1}{2}||v_M^-||^2_{L^2(\Omega)}. \tag{5.3.4}$$

Lemma 5.3.1. *(**Galerkin orthogonality**) Let u be the exact solution of the problem (5.1.1). Then the bilinear form $B(.,.)$ defined in (5.3.1) satisfies the Galerkin orthogonality property:*

$$B(u - u_h,\, v) = 0, \quad \forall v \in V_{N,M}^{k,l}(\mathcal{G}).$$

Proof. First, we claim that $B(u,\, v) = l(v)$ then combining with (5.3.1), we get the required result.

Now we prove our claim *i.e.,* $B(u,\, v) = l(v)$. As u is the exact solution of (5.1.1), hence we have $[u]_j = 0,\ 0 \le j \le N$, $[u_x]_j = 0,\ 1 \le j \le N-1$ and $[[u]]_m = 0,\ 1 \le m \le M-1$. Using these values in the bilinear form (5.3.1), we get

$$B(u,\, v) = \sum_{m=1}^{M} \int_{t_{m-1}}^{t_m} ((u_t,\, v) + A_1(u,\, v) + A_2(u,\, v))dt + (u_0,\, v_0^+). \tag{5.3.5}$$

Using integration by parts for the first term of $A_1(u,\, v)$, that is

$$\sum_{j=1}^{N} \varepsilon \int_{K_j} u_x v_x dx = -\varepsilon \sum_{j=1}^{N} \int_{K_j} u_{xx} v dx - \varepsilon \sum_{j=1}^{N} \{u_x\}_j [v]_j.$$

Using the above equation in $A_1(u,\, v)$ and adding with $A_2(u,\, v)$, we get

$$A_1(u,\, v) + A_2(u,\, v) = \sum_{j=1}^{N} \int_{K_j} ((-\varepsilon u_{xx} + b(x)u_x + c(x)u),\, v)dx. \tag{5.3.6}$$

Combining Equations (5.3.5) and (5.3.6), we get

$$B(u,\, v) = \sum_{m=1}^{M} \int_{t_{m-1}}^{t_m} (f,\, v)dt + (u_0,\, v_0^+),$$

with this we proved our claim. ∎

Lemma 5.3.2. *The bilinear form B defined in (5.3.2) satisfies the following*

$$B(v,\, v) = \sum_{m=1}^{M} \int_{t_{m-1}}^{t_m} A(v,\, v)dt + \frac{1}{2}||v_0^+||^2_{L^2(\Omega)} + \frac{1}{2}\sum_{m=1}^{M-1} ||[[v]]_m||^2_{L^2(\Omega)} + \frac{1}{2}||v_M^-||^2_{L^2(\Omega)}.$$

Proof. As we know the bilinear form defined in (5.3.2) is

$$B(u,\, v) = \sum_{m=1}^{M} \int_{t_{m-1}}^{t_m} ((u_t,\, v) + A(u,\, v))dt + \sum_{m=1}^{M-1} ([[u]]_m, v_m^+) + (u_0^+,\, v_0^+). \tag{5.3.7}$$

Using integration by parts for the first term in RHS of Equation (5.3.7), we obtained

$$\begin{aligned} B(u,\, v) \;=\; & \sum_{m=1}^{M} \int_{t_{m-1}}^{t_m} ((-u,\, v_t) + A(u,\, v))dt + \sum_{m=1}^{M} ((u_m^-,\, v_m^-) - (u_{m-1}^+,\, v_{m-1}^+)) \\ & + \sum_{m=2}^{M} (u_{m-1}^+ - u_{m-1}^-, v_{m-1}^+) + (u_0^+,\, v_0^+). \end{aligned}$$

By adding the second and third sums in RHS of the above equation, we get

$$B(u,\, v) = \sum_{m=1}^{M} \int_{t_{m-1}}^{t_m} ((-u,\, v_t) + A(u,\, v))dt - \sum_{m=1}^{M-1} (u_m^-,\, [[v]]_m) + (u_M^-,\, v_M^-). \tag{5.3.8}$$

Putting $u = v$ in Equations (5.3.7) and (5.3.8), we obtained

$$\begin{aligned} B(v,\, v) &= \sum_{m=1}^{M} \int_{t_{m-1}}^{t_m} ((v_t,\, v) + A(v,\, v))dt + \sum_{m=1}^{M-1} ([[v]]_m, v_m^+) + (v_0^+,\, v_0^+), \\ B(v,\, v) &= \sum_{m=1}^{M} \int_{t_{m-1}}^{t_m} ((-v,\, v_t) + A(v,\, v))dt - \sum_{m=1}^{M-1} (v_m^-,\, [[v]]_m) + (v_M^-,\, v_M^-). \end{aligned}$$

By adding above identities and dividing by two, we get our desired result. ∎

Lemma 5.3.3. *(**Coercivity**) The bilinear form B defined in (5.3.2) satisfies the coercive property, that is, there is a positive constant α independent of perturbation and mesh parameter such that*

$$B(v,\, v) \geq \alpha \|v\|_{dG}^2, \quad \forall v \in V_{N,M}^{k,l}(\mathcal{G}).$$

Proof. Using Lemma 5.3.2 and the coercive property of $A(u,\, v)$, we obtained

$$\begin{aligned} B(v,\, v) &\geq \alpha \left(\sum_{m=1}^{M} \int_{t_{m-1}}^{t_m} |||v|||^2 dt + \frac{1}{2}||v_0^+||_{L^2(\Omega)}^2 + \frac{1}{2} \sum_{m=1}^{M-1} ||[[v]]_m||_{L^2(\Omega)}^2 + \frac{1}{2}||v_M^-||_{L^2(\Omega)}^2 \right) \\ &\geq \alpha \|v\|_{dG}^2, \qquad \forall v \in V_{N,M}^{k,l}(\mathcal{G}). \end{aligned}$$

This completes the proof. ∎

Lemma 5.3.4. (Stability) *Let u_h be the solution of (5.3.1) then u_h is uniquely determined and satisfies the following stability estimate*

$$\|u_h\|_{dG} \leq C(\|u_{h,0}\| + \|f\|_{L^2(L^2)}),$$

where $\|f\|_{L^2(L^2)}^2 = \int_0^T \|f\|_{L^2(\Omega)}^2 dt$.

Proof. Setting $v = u_h$ in the bilinear form, we obtain that

$$B(u_h,\, u_h) = \int_0^{t_M} (f,\, u_h)dt + (u_{h,0}, u_{h,0}^+), \quad \forall u_h \in V_{N,M}^{k,l}(\mathcal{G}).$$

Using the coercivity property and the Cauchy-Schwarz inequality, we obtain the desired result. ∎

5.4 Error Analysis on Shishkin Mesh

5.4.1 Interpolation error

Let u be the solution of (5.1.1) and u_h be the solution of (5.3.1) then to get the bound on the error, we decompose the error into two parts that is interpolation error and discretization error:

$$u - u_h = (u - \pi u) + (\pi u - u_h).$$

Let the interpolation error $\eta = u - \pi u$ and discretization error $\xi = \pi u - u_h$, where $\pi u \in V_{N,M}^{k,l}(D)$ is the piecewise polynomial in t of degree l with

$$\int_{t_{m-1}}^{t_m} (\pi u(t) - u(t),\, \phi^*)dt = 0, \quad \forall \phi^* \in V_{N,M}^{k,l-1}(\mathcal{G}). \tag{5.4.1}$$

Let u_I represent piecewise Lagrange interpolation at the Gauss points, then

$$\pi u(t_m^-) = u_I(t_m^-), \quad m = 1, \cdots, M. \tag{5.4.2}$$

We split the interpolation error into two parts as

$$u - \pi u = (u - u_I) + (u_I - \pi u). \tag{5.4.3}$$

By using the methodology from Chapter 2, one can obtain that

$$|||u - u_I||| \leq C(N^{-1} \ln N)^{k+1}. \tag{5.4.4}$$

$$|||u_I - \pi u||| \leq CM^{-(l+1)}. \tag{5.4.5}$$

Theorem 5.4.1. *The interpolation error satisfies the following bound*

$$\|u - \pi u\|_{dG} \leq C\big((N^{-1} \ln N)^{k+1} + M^{-(l+1)}\big).$$

Proof. By using the decomposition (5.4.3), we can express

$$\|u - \pi u\|_{dG} = \|u - u_I\|_{dG} + \|u_I - \pi u\|_{dG}.$$

From the definition of the dG norm (5.3.4) and the fact that u_I is the interpolation of u, we have

$$\begin{aligned} \|u - u_I\|_{dG}^2 &= \sum_{m=1}^{M} \int_{t_{m-1}}^{t_m} |||u - u_I|||^2 dt \\ &\leq C(N^{-1} \ln N)^{2(k+1)}, \end{aligned}$$

here, we have used (5.4.4). Again using the definition of dG norm (5.3.4) and the fact that πu is the interpolation of u_I, we have

$$\begin{aligned} \|u_I - \pi u\|_{dG}^2 &= \sum_{m=1}^{M} \int_{t_{m-1}}^{t_m} |||u_I - \pi u|||^2 dt \\ &\leq CM^{-2(l+1)}, \text{ (from (5.4.5))}. \end{aligned}$$

By combining the above identities, we obtain the desired result. ∎

5.4.2 Discretization error

Theorem 5.4.2. *The discretization error satisfies the following bound:*

$$\|\xi\|_{dG} \leq C\big((N^{-1}\ln N)^{k+1} + M^{-(l+1)}\big).$$

Proof. By using the coercivity property, we can have

$$||\xi||_{dG}^2 \leq B(\xi, \xi) \tag{5.4.6}$$

and using the Galerkin orthogonality, we obtain

$$B(\xi, \xi) = B(\pi u - u_h, \xi) = B(u - u + \pi u - u_h, \xi) = B(u - u_h, \xi) - B(u - \pi u, \xi) = -B(\eta, \xi). \tag{5.4.7}$$

From Equation (5.3.8), we can write

$$B(\eta, \xi) = \sum_{m=1}^{M} \int_{t_{m-1}}^{t_m} -(\eta, \xi_t)dt + \sum_{m=1}^{M} \int_{t_{m-1}}^{t_m} A(\eta, \xi)dt - \sum_{m=1}^{M-1} (\eta_m^-, [[\xi]]_m) + (\eta_M^-, \xi_M^-) \tag{5.4.8}$$

Third and fourth terms in the RHS of the Equation (5.4.8) vanishes due to the interpolation error, that is,

$$\eta_m = 0, \quad \text{for } m = 1, 2, \cdots, M.$$

Therefore, we have

$$B(\eta, \xi) = \sum_{m=1}^{M} \int_{t_{m-1}}^{t_m} -(\eta, \xi_t)dt + \sum_{m=1}^{M} \int_{t_{m-1}}^{t_m} A(\eta, \xi)dt. \tag{5.4.9}$$

Using (5.4.1), first term in (5.4.9) will vanish, and hence

$$B(\eta, \xi) = \sum_{m=1}^{M} \int_{t_{m-1}}^{t_m} A(\eta, \xi)dt. \tag{5.4.10}$$

Using Equations (5.4.7) and (5.4.10) in the inequality (5.4.6), we get

$$||\xi||_{dG}^2 \leq \sum_{m=1}^{M} \int_{t_{m-1}}^{t_m} A(\eta, \xi)dt. \tag{5.4.11}$$

Now, we need the bound $A(\eta, \xi)$, using the idea from Chapter 2 one can simply show that

$$A(\eta, \xi) \leq C((N^{-1} \ln N)^{k+1} + M^{-(l+1)})|||\xi|||. \tag{5.4.12}$$

Using inequality (5.4.12) in (5.4.11), we obtained the desired result. ∎

Theorem 5.4.3. *Let u be the solution of (5.1.1) and u_h be the solution of (5.3.1), then following result hold true.*

$$\|u - u_h\|_{dG} \leq C((N^{-1} \ln N)^{k+1} + M^{-(l+1)}).$$

Proof. Combining Theorems 5.4.1 and 5.4.2, we can obtain the required result. ∎

5.5 Numerical Results

In this section, we verify experimentally the convergence result, by considering the numerical solution of singularly perturbed parabolic IBVP.

Example 5.5.1. *[22] Consider the following singularly perturbed parabolic IBVP:*

$$\begin{cases} u_t - \varepsilon u_{xx} + (1 + x(1-x))u_x = f(x,t), \quad (x,t) \in (0,1) \times (0,1), \\ u(x,0) = u_0(x), \qquad 0 < x < 1, \\ u(0,\, t) = u(1,\, t) = 0, \qquad 0 \leq t \leq 1. \end{cases}$$

We have taken initial data $u_0(x)$ and the source function $f(x,\, t)$ from the exact solution

$$u(x,\, t) = e^{-t}(C_1 + C_2 x - e^{-(1-x)/\varepsilon}),$$

where, $C_1 = e^{-1/\varepsilon}$ and $C_2 = 1 - e^{-1/\varepsilon}$.

We calculate the error in the dG norm as defined in (5.3.4). Table 5.1 provides the numerical results in the dG norm, with linear finite elements in space as well as in time using the NIPG method in space and DG method in time. Whereas Table 5.2 shows the error and the order of convergence using the standard FEM in space and implicit Euler method in time.

To visualize the order of convergence of the numerical solutions, we have given the loglog plot in Figure 5.1 for $\varepsilon = 10^{-2}, 10^{-4}, 10^{-6}$ for the NIPG method in space and DG method in time and Figure 5.2 shows loglog plot for $\varepsilon = 10^{-2}, 10^{-4}, 10^{-6}$ using the standard FEM in space and implicit Euler method in time. Further, Figure 5.3 depict the surface plots of the solution for $\varepsilon = 10^{-2}$ and $\varepsilon = 10^{-6}$ for $N = 32$.

Table 5.1: *Error and order of convergence for Example 5.5.1 using NIPG method in space and DG method in time.*

	Number of mesh-intervals N / temporal mesh-size Δt				
ε	$32/\frac{1}{32}$	$64/\frac{1}{64}$	$128/\frac{1}{128}$	$256/\frac{1}{256}$	$512/\frac{1}{512}$
10^{-1}	8.5979e-03	2.5155e-03	6.8464e-04	2.9513e-04	1.4911e-04
	1.7731	1.8774	1.2140	0.9849	
10^{-2}	1.5937e-02	6.6481e-03	2.4955e-03	8.6403e-04	2.8295e-04
	1.2613	1.4136	1.5302	1.6105	
10^{-3}	1.6079e-02	6.7349e-03	2.5167e-03	8.6901e-04	2.8416e-04
	1.2555	1.4201	1.5341	1.6127	
10^{-4}	1.6095e-02	6.7433e-03	2.5205e-03	8.7065e-04	2.8465e-04
	1.2551	1.4197	1.5336	1.6129	
10^{-5}	1.6097e-02	6.7441e-03	2.5209e-03	8.7079e-04	2.8471e-04
	1.2551	1.4197	1.5335	1.6129	
10^{-6}	1.6097e-02	6.7442e-03	2.5209e-03	8.7081e-04	2.8471e-04
	1.2551	1.4197	1.5335	1.6129	
10^{-7}	1.6097e-02	6.7442e-03	2.5209e-03	8.7078e-04	2.8471e-04
	1.2551	1.4197	1.5336	1.6128	

5.6 Conclusions

Here, in this chapter, we have applied the NIPG method in space and the DG method in time for singularly perturbed parabolic IBVPs. Theoretically, it is shown that the proposed method is almost $(k+1)$–order of convergence in space and $(l+1)$–order of convergence in time, where k and l are the degree of piecewise polynomial used in finite element space. To validate theoretical finding we have presented numerical example.

Table 5.2: *Error and order of convergence for Example 5.5.1 using standard FEM in space and implicit Euler method in time.*

	Number of mesh-intervals N / temporal mesh-size Δt				
ε	$32/\frac{1}{32}$	$64/\frac{1}{64}$	$128/\frac{1}{128}$	$256/\frac{1}{256}$	$512/\frac{1}{512}$
10^{-1}	2.0634e-02	1.0397e-02	5.2157e-03	2.6122e-03	1.3071e-03
	0.9889	0.9952	0.9975	0.9988	
10^{-2}	2.8496e-02	1.4507e-02	7.3177e-03	3.6744e-03	1.8408e-03
	0.9740	0.9872	0.9939	0.9971	
10^{-3}	2.9977e-02	1.5241e-02	7.6845e-03	3.8592e-03	1.9337e-03
	0.9759	0.9879	0.9936	0.9968	
10^{-4}	3.0183e-02	1.5362e-02	7.7436e-03	3.8868e-03	1.9472e-03
	0.9743	0.9882	0.9944	0.9972	
10^{-5}	3.0203e-02	1.5374e-02	7.7509e-03	3.8908e-03	1.9491e-03
	0.9742	0.9880	0.9943	0.9972	
10^{-6}	3.0205e-02	1.5375e-02	7.7516e-03	3.8912e-03	1.9494e-03
	0.9741	0.9880	0.9942	0.9972	
10^{-7}	3.0206e-02	1.5376e-02	7.7517e-03	3.8912e-03	1.9494e-03
	0.9741	0.9880	0.9942	0.9972	

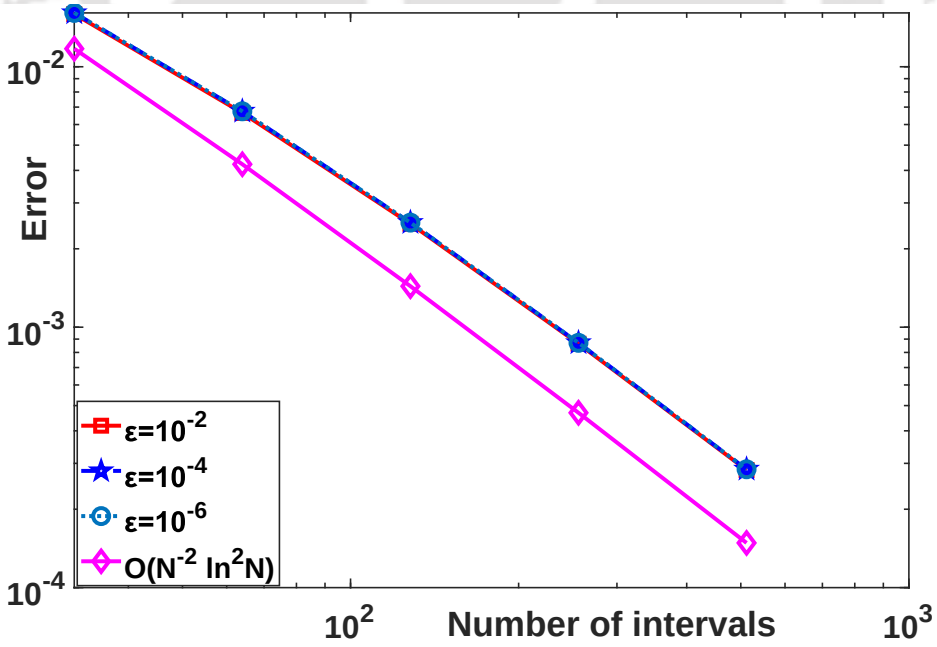

Figure 5.1: Order of convergence through loglog plot for Example 5.5.1 using the NIPG method in space and DG method in time.

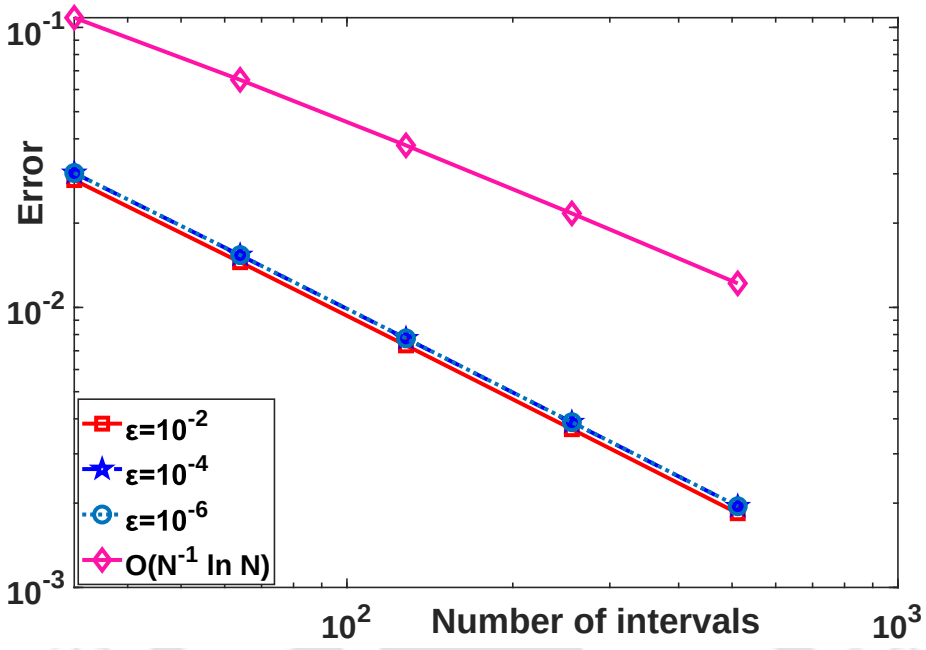

Figure 5.2: Order of convergence through loglog plot for Example 5.5.1 using standard FEM in space and implicit Euler method in time.

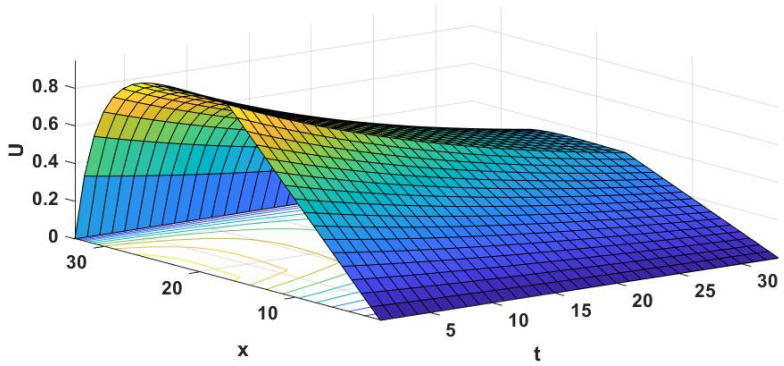

(a) For $\varepsilon = 10^{-2}$.

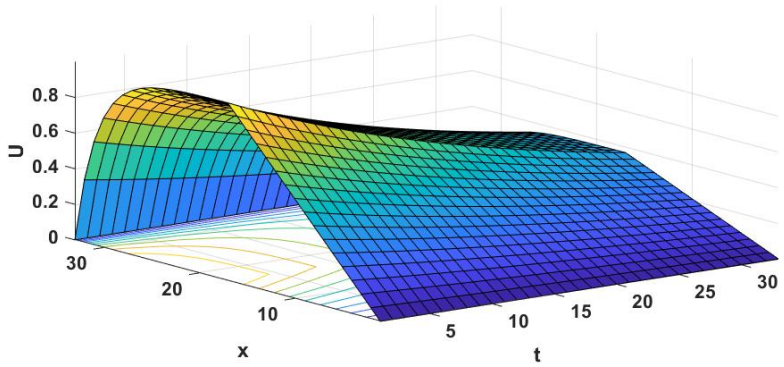

(b) For $\varepsilon = 10^{-6}$.

Figure 5.3: Surface plots of the solutions for Example 5.5.1 for $N = 32$.

CHAPTER 6

Superconvergence Error Analysis of the NIPG Method for Singularly Perturbed 2D Elliptic BVPs

This chapter focuses on numerical solution of singularly perturbed 2D elliptic BVPs. Here, we obtain the error estimates of the superconvergence of the NIPG method with interior penalties on layer-adapted meshes of Shishkin type. We have established the error bound in the discrete energy norm. Numerical tests support our theoretical estimates.

6.1 Introduction

In the present chapter, we extend the idea of the superconvergence analysis given in Chapter 2 for 1D convection-diffusion BVPs to 2D elliptic BVPs of convection-diffusion type on a square domain. Here, we apply the NIPG method on the layer-adapted piecewise uniform Shishkin mesh. In order to improve the order of convergence of the interpolation error, the piecewise Lagrange interpolation is used at the Gauss points. We use this improved order of convergence to prove the discretization error.

Here, the following singularly perturbed 2D elliptic BVP is considered:

$$\begin{cases} -\varepsilon\Delta u + \mathbf{b}\cdot\nabla u + cu = f, \quad \text{in} \quad \mathcal{D} = (0,\,1)\times(0,\,1), \\ u = 0, \quad \text{on} \quad \Gamma = \partial\mathcal{D}, \end{cases} \tag{6.1.1}$$

where ε is a small positive parameter, and $\mathbf{b}(x,\,y) = (b_1(x,\,y),\,b_2(x,\,y)) \geq (\beta_1,\,\beta_2) \geq (\beta,\,\beta) > (0,\,0)$, $c(x,\,y) \geq 0$ for all $(x,\,y) \in \overline{\mathcal{D}}$, and $\gamma^2 = \big(c(x,\,y) - \frac{1}{2}\nabla\cdot\mathbf{b}(x,\,y)\big) > 0$, where β and γ are constants.

This chapter is organized as follows: In Section 6.2, we have given the bounds for the continuous solution of the model problem (6.1.1). Piecewise uniform Shishkin mesh is described in Section 6.3. Section 6.4 contains finite element approximation for the

2D elliptic BVPs. Error analysis is carried out in Section 6.5. Numerical results and conclusions are given in Sections 6.6 and 6.7, respectively.

6.2 The Continuous Problem

For SPPs, we need to decompose the solution u into smooth and layer parts separately. For model problem (6.1.1), the solution decomposition and bounds for the smooth and layer parts and their derivatives are taken from [38]. We are providing the following lemma without the proof.

Lemma 6.2.1. *Let* $\mathbf{b}$ *and* c *be sufficiently smooth functions, and let* $f \in C^{4,1}(\overline{\mathcal{D}})$ *satisfies the compatibility conditions* $f(0,0) = f(0,1) = f(1,0) = f(1,1) = 0$. *Then the BVP (6.1.1) admits a unique solution* $u \in C^{3,1}(\overline{\mathcal{D}})$. *Further, one can decompose the solution* u *into smooth and layer components as*

$$u = S + E_1 + E_2 + E_{12},$$

where for all $(x, y) \in \overline{\mathcal{D}}$. *Then, the derivatives of the smooth and layer components satisfy the following bounds:*

$$\begin{aligned}
\left|\frac{\partial^{i+j} S}{\partial x^i \partial y^j}(x, y)\right| &\leq C, \\
\left|\frac{\partial^{i+j} E_1}{\partial x^i \partial y^j}(x, y)\right| &\leq C\varepsilon^{-i} e^{-\beta(1-x)/\varepsilon}, \\
\left|\frac{\partial^{i+j} E_2}{\partial x^i \partial y^j}(x, y)\right| &\leq C\varepsilon^{-j} e^{-\beta(1-y)/\varepsilon}, \\
\left|\frac{\partial^{i+j} E_{12}}{\partial x^i \partial y^j}(x, y)\right| &\leq C\varepsilon^{-(i+j)} e^{-\beta(1-x)/\varepsilon} e^{-\beta(1-y)/\varepsilon}.
\end{aligned}$$

Proof. One can see the detailed proof in [38]. ∎

6.3 Domain Discretization

We define the rectangular mesh $\overline{\mathcal{D}}$ using the tensor product of the 1D Shishkin meshes with N subintervals in each direction which can be seen in Figure 6.1. Mesh transition parameter is defined as

$$\tau_\varepsilon = \min\left\{\frac{1}{2}, \frac{2\varepsilon \ln N}{\beta}\right\}.$$

In the case of SPPs, we generally assume that $\tau_\varepsilon = (2\varepsilon \ln N)/\beta$. Otherwise N is exponentially large compared to $e^{(1/\varepsilon)}$.

Let the domain $\mathcal{D}$ be divided into four subdomains

$$K_{22} = (0,\, 1-\tau_\varepsilon)^2, \qquad K_{12} = (1-\tau_\varepsilon,\, 1)\times(0,\, 1-\tau_\varepsilon),$$

$$K_{21} = (0,\, 1-\tau_\varepsilon)\times(1-\tau_\varepsilon,\, 1), \qquad K_{11} = (1-\tau_\varepsilon,\, 1)^2.$$

The step-size in each of the subdomains is given by

$$h_{x,i} = \begin{cases} 4\varepsilon \ln N/N\beta, & \text{for } K_{11} \text{ and } K_{12}, \\ 2(1-\tau_\varepsilon)/N, & \text{for } K_{21} \text{ and } K_{22}, \end{cases}$$

$$h_{y,j} = \begin{cases} 4\varepsilon \ln N/N\beta, & \text{for } K_{11} \text{ and } K_{21}, \\ 2(1-\tau_\varepsilon)/N, & \text{for } K_{12} \text{ and } K_{22}, \end{cases}$$

for $i, j = 0, 1, \cdots, N$.

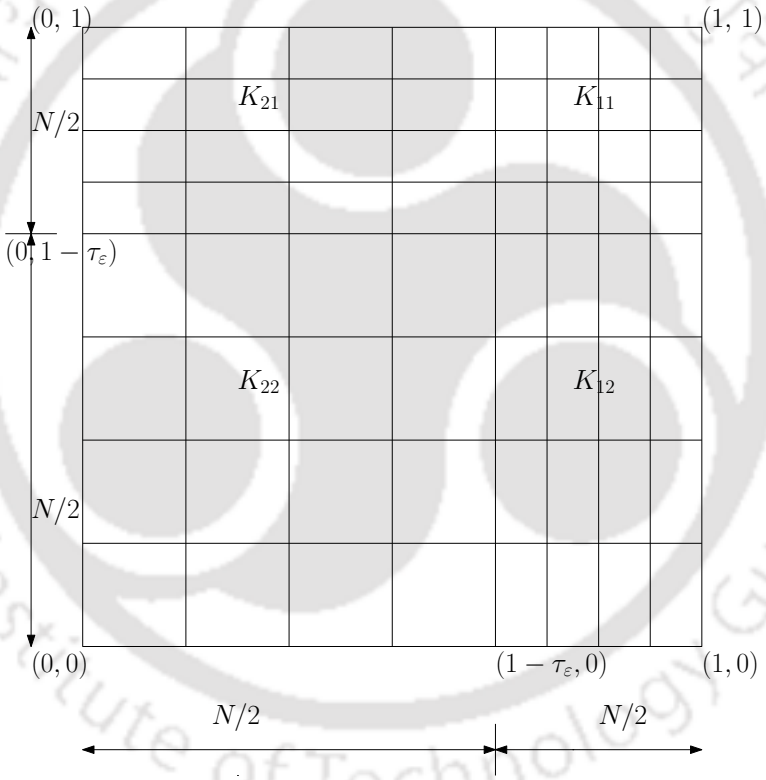

Figure 6.1: Visualization of the Shishkin mesh on the unit square $(0,1)\times(0,1)$.

6.4 Finite Element Approximation

We apply the NIPG method for the elliptic BVP given in (6.1.1) and the corresponding weak formulation is

$$\begin{cases} \text{find } u_h \in V_N(\mathcal{D}), \text{ such that} \\ B(u_h,\, v_h) = l(v_h), \quad \forall v_h \in V_N(\mathcal{D}), \end{cases} \tag{6.4.1}$$

where $B(u,\, v)$ is defined as

$$\begin{aligned} B(u,\, v) &= \sum_{K\in\mathcal{T}_N}\Big(\varepsilon\int_K \nabla u\cdot\nabla v\,dx + \int_K(\mathbf{b}\cdot\nabla u + cu)v\,dx - \int_{\partial_- K\cap\Gamma}(\mathbf{b}\cdot\mu_K)u^+v^+ds \\ &- \int_{\partial_- K\setminus\Gamma}(\mathbf{b}\cdot\mu_K)\lfloor u\rfloor v^+ds\Big) + \varepsilon\int_\Gamma(u(\nabla v\cdot\mu) - (\nabla u\cdot\mu)v)ds + \int_\Gamma \sigma uvds \\ &+ \varepsilon\int_{\Gamma_{int}}([u]\{\nabla v\cdot\nu\} - \{\nabla u\cdot\nu\}[v])ds + \int_{\Gamma_{int}}\sigma[u][v]ds, \end{aligned} \tag{6.4.2}$$

$$l(v) = \sum_{K\in\mathcal{T}_N}(f,\, v)_K$$

for $u, v \in H^1(\mathcal{D}, \mathcal{T}_N)$. Here σ denotes penalty parameter.

The discrete energy norm can be defined by

$$\begin{aligned} |||v|||^2 &= \sum_{K\in\mathcal{T}_N}\Big(\varepsilon\|\nabla v\|^2_{L^2(K)} + \gamma^2\|v\|^2_{L^2(K)}\Big) + \int_\Gamma \sigma v^2ds + \int_{\Gamma_{int}}\sigma[v]^2ds \\ &+\frac{1}{2}\sum_{K\in\mathcal{T}_N}\left(\|v^+\|^2_{\partial_- K\cap\Gamma} + \|v^+ - v^-\|^2_{\partial_- K\setminus\Gamma} + \|v^+\|^2_{\partial_+ K\cap\Gamma}\right). \end{aligned} \tag{6.4.3}$$

We define the following discrete seminorm over Gauss points

$$|v|^2_{\varepsilon,N} = \sum_{K\in\mathcal{T}_N}\varepsilon\|\nabla v\|^2_{L^2(K)} = \varepsilon\sum_{K\in\mathcal{T}_N}h_{x,i}h_{y,j}\sum_{p=0}^{k}|\nabla v(x_{ip},\, y_{jp})|^2, \tag{6.4.4}$$

where $\{x_{ip}, y_{jp}\}_{p=0}^k$ are the Gauss points on the interval $[x_{i-1},\, x_i]$ and $[y_{j-1},\, y_j]$, respectively. Using [23], we can show the the bilinear form satisfies the Galerkin orthogonality, and the existence and uniqueness of the solution of the weak formulation (6.4.1).

6.5 Error Analysis

In the theory of error analysis, we have to divide the error mainly into two parts, i.e., the interpolation and the discretization errors. Here, the piecewise Lagrange interpolation is used at the Gauss nodes. To bound the discretization error, we use bound of the interpolation error. For improving convergence order, we have to improve the convergence order of interpolation error. Let $\eta = u - u_I$ and $\xi = u_I - u_h$ be respectively, the interpolation and the discretization errors, then we have

$$u - u_h = \eta + \xi = (u - u_I) + (u_I - u_h),$$

where u_I represents the continuous piecewise bilinear interpolant of u which vanishes on the boundary Γ.

Now we will estimate $|||\eta|||$ and $|||\xi|||$, separately. Let w_I denotes the piecewise Lagrange interpolation of a continuous function w defined on $[x_{i-1},\, x_i]\times[y_{j-1},\, y_j]$ by using the Gauss points $\{x_{ip}, y_{jp}\}_{p=0}^{k}$ as nodal points in $[x_{i-1},\, x_i]$ and $[y_{j-1},\, y_j]$, respectively. Then, we have

$$\begin{aligned}
(w-w_I)(x,\,y) &= \frac{1}{2k!}\phi_{ik+1}(x)\frac{\partial^{(k+1)}w(x,\,y)}{\partial x^{(k+1)}} + \frac{1}{2k!}\phi_{ik+1}(y)\frac{\partial^{(k+1)}w(x,\,y)}{\partial y^{(k+1)}} \\
&+ \left(\frac{1}{2k!}\right)^2\phi_{ik+1}(x)\phi_{ik+1}(y)\frac{\partial^{2(k+1)}w(x,\,y)}{\partial x^{(k+1)}\partial y^{(k+1)}} - \left(\frac{1}{2k!}\right)^2\phi_{ik+1}(x)\phi_{ik+1}(y)\frac{\partial^{2(k+1)}w(x,\,y)}{\partial x^{(k+1)}\partial y^{(k+1)}} \\
&- \left(\frac{1}{2k!}\right)^2\phi_{ik+1}(x)\phi_{ik+1}(y)\frac{\partial^{2(k+1)}w(x,\,y)}{\partial x^{(k+1)}\partial y^{(k+1)}} + \mathcal{O}(h_{x,i}^{k+1})\int_{x=x_{i-1}}^{x_i}\frac{\partial^{(k+2)}w(x,\,y)}{\partial x^{(k+2)}}dx \\
&+ \mathcal{O}(h_{y,j}^{k+1})\int_{y=y_{j-1}}^{y_j}\frac{\partial^{(k+2)}w(x,\,y)}{\partial y^{(k+2)}}dy + \mathcal{O}(h_{x,i}^{k+1}h_{y,j}^{k+1})\int_{x=x_{i-1}}^{x_i}\int_{y=y_{j-1}}^{y_j}\frac{\partial^{2(k+2)}w(x,\,y)}{\partial x^{(k+2)}\partial y^{(k+2)}}dxdy,
\end{aligned}$$

where

$$\phi_{ik+1}(x) = \frac{d^{k-1}}{dx^{k-1}}\left((x-x_{i-\frac{1}{2}})^2 - \frac{h_{x,i}^2}{4}\right)^k, \text{ and } \quad \phi_{ik+1}(y) = \frac{d^{k-1}}{dy^{k-1}}\left((y-y_{j-\frac{1}{2}})^2 - \frac{h_{y,j}^2}{4}\right)^k.$$

Since, we know that $\{x_{ip}\}_{p=0}^{k}$ and $\{y_{jp}\}_{p=0}^{k}$ are the zeros of the polynomial $\phi_{ik+1}(x)$ and $\phi_{ik+1}(y)$, respectively. Hence in above equation terms containing polynomial $\phi_{ik+1}(x)$ and $\phi_{ik+1}(y)$ will be zero at the Gauss points. So above equation on the Gauss points can be written as

$$\begin{aligned}
(w-w_I)(x_{ip},\,y_{jp}) &= \mathcal{O}(h_{x,i}^{k+1})\int_{x=x_{i-1}}^{x_i}\frac{\partial^{(k+2)}w(x,\,y)}{\partial x^{(k+2)}}dx + \mathcal{O}(h_{y,j}^{k+1})\int_{y=y_{j-1}}^{y_j}\frac{\partial^{(k+2)}w(x,\,y)}{\partial y^{(k+2)}}dy \\
&+ \mathcal{O}(h_{x,i}^{k+1}h_{y,j}^{k+1})\int_{x=x_{i-1}}^{x_i}\int_{y=y_{j-1}}^{y_j}\frac{\partial^{2(k+2)}w(x,\,y)}{\partial x^{(k+2)}\partial y^{(k+2)}}dxdy. \qquad (6.5.1)
\end{aligned}$$

Derivative of the interpolation error at the Gauss points with respect to x and y can be written as

$$\begin{aligned}
\frac{\partial}{\partial x}(w-w_I)(x_{ip},\,y_{jp}) &= \mathcal{O}(h_{x,i}^{k})\int_{x_{i-1}}^{x_i}\frac{\partial^{k+2}w(x,\,y)}{\partial x^{k+2}}dx + \mathcal{O}(h_{y,j}^{k+1})\int_{y_{j-1}}^{y_j}\frac{\partial^{k+3}w(x,\,y)}{\partial x\partial y^{k+2}}dy \\
&+ \mathcal{O}(h_{x,i}^{k}h_{y,j}^{k+1})\int_{x_{i-1}}^{x_i}\int_{y_{j-1}}^{y_j}\frac{\partial^{2(k+2)}w(x,\,y)}{\partial x^{k+2}\partial y^{k+2}}dxdy. \qquad (6.5.2)
\end{aligned}$$

and

$$\begin{aligned}
\frac{\partial}{\partial y}(w-w_I)(x_{ip},\,y_{jp}) &= \mathcal{O}(h_{x,i}^{k+1})\int_{x_{i-1}}^{x_i}\frac{\partial^{k+3}w(x,\,y)}{\partial x^{k+2}\partial y}dx + \mathcal{O}(h_{y,j}^{k})\int_{y_{j-1}}^{y_j}\frac{\partial^{k+2}w(x,\,y)}{\partial y^{k+2}}dy \\
&+ \mathcal{O}(h_{x,i}^{k+1}h_{y,j}^{k})\int_{x_{i-1}}^{x_i}\int_{y_{j-1}}^{y_j}\frac{\partial^{2(k+2)}w(x,\,y)}{\partial x^{k+2}\partial y^{k+2}}dxdy. \qquad (6.5.3)
\end{aligned}$$

The solution u can be decomposed as, $u = S + E_1 + E_2 + E_{12}$, where S is the smooth part of the solution and E_1, E_2 and E_{12} are the layer parts at $x = 1$, $y = 1$ and corner

layer, respectively. Let S_I, $E_{1,I}$, $E_{2,I}$ and $E_{12,I}$ be the interpolations of S, E_1, E_2, E_{12}, respectively.

Theorem 6.5.1. *Let S and S_I represent the smooth part of the solution and its interpolant, then interpolation error for the smooth part is*

$$|||S - S_I||| \leq C(N^{-1} \ln N)^{k+1}.$$

Proof. By the definition of the discrete energy norm (6.4.3), we have

$$|||S - S_I|||^2 = \sum_{K \in \mathcal{T}_N} \left(\varepsilon \|\nabla(S - S_I)\|^2_{L^2(K)} + \gamma^2 \|(S - S_I)\|^2_{L^2(K)} \right). \tag{6.5.4}$$

Using Equation (6.4.4), Equation (6.5.4) can be written as

$$|||S - S_I|||^2 = \varepsilon \sum_{K \in \mathcal{T}_N} h_{x,i} h_{y,j} \sum_{p=0}^{k} |\nabla(S - S_I)(x_{ip}, y_{jp})|^2 + \sum_{K \in \mathcal{T}_N} \gamma^2 \|(S - S_I)\|^2_{L^2(K)}. \tag{6.5.5}$$

First term in the RHS of Equation (6.5.5) is

$$|S - S_I|^2_{\varepsilon,N} \leq C\varepsilon \sum_{K \in \mathcal{T}_N} h_{x,i} h_{y,j} \left(\sum_{p=0}^{k} \left| \frac{\partial (S - S_I)}{\partial x}(x_{ip}, y_{jp}) \right|^2 + \sum_{p=0}^{k} \left| \frac{\partial (S - S_I)}{\partial y}(x_{ip}, y_{jp}) \right|^2 \right). \tag{6.5.6}$$

Using Equations (6.5.2) and (6.5.3), we can derive the bound for (6.5.6) as

$$|S - S_I|^2_{\varepsilon,N} \leq CN^{-2(k+1)} (\ln N)^{2(k+1)}.$$

Similarly, bound for the second term in the RHS of Equation (6.5.5) can be derived using Equation (6.5.1) that is we get

$$\sum_{K \in \mathcal{T}_N} \|(S - S_I)\|^2_{L^2(K)} \leq CN^{-2(k+1)} (\ln N)^{2(k+1)}.$$

Combining both the terms, we get our required result. ∎

In the next step we estimate bound for the interpolation error for layer parts. We consider only the terms $E_1 - E_{1,I}$ because the other ones can be estimated in a similar way.

Theorem 6.5.2. *Let E_1 and $E_{1,I}$ represent the layer part of the solution at $x = 1$ and its interpolant, then the error satisfies the following bound:*

$$|||E_1 - E_{1,I}||| \leq C(N^{-1} \ln N)^{k+1}.$$

Proof. By the definition of the discrete energy norm (6.4.3), we have

$$|||E_1 - E_{1,I}|||^2 = \sum_{K\in\mathcal{T}_N}\left(\varepsilon\|\nabla(E_1 - E_{1,I})\|^2_{L^2(K)} + \gamma^2\|(E_1 - E_{1,I})\|^2_{L^2(K)}\right). \quad (6.5.7)$$

First, we will derive the bound for the first term in all subdomains, separately. On the subdomain K_{11} bound can be derived as

$$\begin{aligned}|E_1 - E_{1,I}|^2_{\varepsilon,N} \le C\varepsilon \sum_{K\in\mathcal{T}_N} h_{x,i}h_{y,j}\Bigg(& h^k_{x,i}\int_{x_{i-1}}^{x_i}\frac{\partial^{k+2}E_1(x,\,y)}{\partial x^{k+2}}dx + h^{k+1}_{y,j}\int_{y_{j-1}}^{y_j}\frac{\partial^{k+3}E_1(x,\,y)}{\partial x\partial y^{k+2}}dy\\ &+ h^k_{x,i}h^{k+1}_{y,j}\int_{x_{i-1}}^{x_i}\int_{y_{j-1}}^{y_j}\frac{\partial^{2(k+2)}E_1(x,\,y)}{\partial x^{k+2}\partial y^{k+2}}dxdy + h^{k+1}_{x,i}\int_{x_{i-1}}^{x_i}\frac{\partial^{k+3}E_1(x,\,y)}{\partial x^{k+2}\partial y}dx\\ &+ h^k_{y,j}\int_{y_{j-1}}^{y_j}\frac{\partial^{k+2}E_1(x,\,y)}{\partial y^{k+2}}dy + h^{k+1}_{x,i}h^k_{y,j}\int_{x_{i-1}}^{x_i}\int_{y_{j-1}}^{y_j}\frac{\partial^{2(k+2)}E_1(x,\,y)}{\partial x^{k+2}\partial y^{k+2}}dxdy\Bigg)^2. \quad (6.5.8)\end{aligned}$$

We will derive bound for each terms separately, first term in RHS of (6.5.8) can be bounded as

$$\begin{aligned}\varepsilon\sum_{K\in\mathcal{T}_N} h_{x,i}h_{y,j}\left(h^k_{x,i}\int_{x_{i-1}}^{x_i}\frac{\partial^{k+2}E_1(x,\,y)}{\partial x^{k+2}}dx\right)^2 &\le C\varepsilon(\varepsilon\ln N/N)^2(\varepsilon\ln N/N)^{2k}\\ &\quad\left(\int_{1-\tau_\varepsilon}^1\varepsilon^{-(k+2)}e^{-\beta(1-x)/\varepsilon}dx\right)^2\\ &\le C(\ln N/N)^{2(k+1)}.\end{aligned}$$

To derive the bound for the second term in the RHS of (6.5.8), we write

$$\begin{aligned}\varepsilon\sum_{K\in\mathcal{T}_N} h_{x,i}h_{y,j}\left(h^{k+1}_{y,j}\int_{y_{j-1}}^{y_j}\frac{\partial^{k+3}E_1(x,\,y)}{\partial x\partial y^{k+2}}dy\right)^2 &\le C\varepsilon h_{x,i}h_{y,j}h^{2(k+1)}_{y,j}\left(\int_{1-\tau_\varepsilon}^1\frac{\partial^{k+3}E_1(x,\,y)}{\partial x\partial y^{k+2}}dy\right)^2\\ &\le C\varepsilon^{2k+5}(\ln N/N)^{2k+6}.\end{aligned}$$

Bound for the third term in the RHS of (6.5.8) is

$$\varepsilon\sum_{K\in\mathcal{T}_N} h_{x,i}h_{y,j}\left(h^k_{y,j}h^{k+1}_{y,j}\int_{x_{i-1}}^{x_i}\int_{y_{j-1}}^{y_j}\frac{\partial^{2(k+2)}E_1(x,\,y)}{\partial x^{k+2}\partial y^{k+2}}dxdy\right)^2 \le C\varepsilon^{2k+2}(\ln N/N)^{4k+5}.$$

Fourth term in the RHS of (6.5.8) can be bounded by

$$\begin{aligned}\varepsilon\sum_{K\in\mathcal{T}_N} h_{x,i}h_{y,j}\left(h^{k+1}_{x,i}\int_{x_{i-1}}^{x_i}\frac{\partial^{k+3}E_1(x,\,y)}{\partial x^{k+2}\partial y}dx\right)^2 &\le \varepsilon h_{x,i}h_{y,j}h^{2(k+1)}_{x,i}\left(\int_{1-\tau_\varepsilon}^1\varepsilon^{-2(k+2)}e^{-2\beta(1-x)/\varepsilon}dx\right)\\ &\le C\varepsilon^2(\ln N/N)^{2(k+2)}.\end{aligned}$$

Now for the fifth term in the RHS of (6.5.8), we have

$$\begin{aligned}\varepsilon\sum_{K\in\mathcal{T}_N} h_{x,i}h_{y,j}\left(h^k_{y,j}\int_{y_{j-1}}^{y_j}\frac{\partial^{k+2}E_1(x,\,y)}{\partial y^{k+2}}dy\right)^2 &\le C\varepsilon h_{x,i}h_{y,j}h^{2k}_{y,j}\left(\int_{1-\tau_\varepsilon}^1 e^{-2\beta(1-x)/\varepsilon}dy\right)\\ &\le C\varepsilon^{2k+5}(N^{-1}\ln N)^{2k+4}.\end{aligned}$$

And finally bound for the sixth term in the RHS of (6.5.8) is given by

$$\varepsilon \sum_{K\in\mathcal{T}_N} h_{x,i}h_{y,j}\left(h_{x,i}^{k+1}h_{y,j}^{k}\int_{x_{i-1}}^{x_i}\int_{y_{j-1}}^{y_j}\frac{\partial^{2(k+2)}E_1(x,\,y)}{\partial x^{k+2}\partial y^{k+2}}dxdy\right)^2 \leq C\varepsilon^{2k+3}(\ln N)^{4k+5}N^{-4(k+1)}.$$

By combining all the above terms, we obtain the bound on the subdomain K_{11}

$$|E_1 - E_{1,I}|_{\varepsilon,N} \leq C(N^{-1}\ln N)^{k+1}.$$

Similarly, we can obtain the bound on the subdomain K_{12}. On the subdomains K_{21} and K_{22}, we have

$$|E_1 - E_{1,I}|_{\varepsilon,N}^2 \leq \varepsilon \sum_{K\in K_{21}\cup K_{22}} h_{x,i}h_{y,j}|\nabla E_1|^2 + \varepsilon \sum_{K\in K_{21}\cup K_{22}} h_{x,i}h_{y,j}|\nabla E_{1,I}|^2. \tag{6.5.9}$$

The first term in the RHS of (6.5.9) satisfies

$$\begin{aligned}
\varepsilon \sum_{K\in K_{21}\cup K_{22}} h_{x,i}h_{y,j}|\nabla E_1|^2 &\leq \varepsilon \sum_{K\in K_{21}\cup K_{22}} h_{x,i}h_{y,j}\left|\frac{\partial E_1}{\partial x}+\frac{\partial E_1}{\partial y}\right|^2 \\
&\leq \varepsilon \sum_{K\in K_{21}\cup K_{22}} h_{x,i}h_{y,j}(\varepsilon^{-2}+1)e^{-2\beta(1-x)/\varepsilon} \\
&\leq (\varepsilon^{-1}+\varepsilon)\int_0^{1-\tau_\varepsilon}\int_0^1 e^{-2\beta(1-x)/\varepsilon}dxdy \\
&\leq CN^{-2(k+1)}.
\end{aligned} \tag{6.5.10}$$

Now considering the second term in the RHS of the inequality (6.5.9), we obtain

$$\begin{aligned}
\varepsilon \sum_{K\in K_{21}\cup K_{22}} h_{x,i}h_{y,j}|\nabla E_{1,I}|^2 &\leq \varepsilon \sum_{K\in K_{21}\cup K_{22}} h_{x,i}h_{y,j}\left|\frac{\partial E_{1,I}}{\partial x}\right|^2 \\
&\quad + \varepsilon \sum_{K\in K_{21}\cup K_{22}} h_{x,i}h_{y,j}\left|\frac{\partial E_{1,I}}{\partial y}\right|^2.
\end{aligned} \tag{6.5.11}$$

The first term in the RHS of the inequality (6.5.11) will be bounded by

$$\begin{aligned}
\frac{\partial E_{1,I}}{\partial x}(x_i,\,y_j) &= \frac{1}{4h_{x,i}}\int_{x_i-h_{x,i}}^{x_i+h_{x,i}}\left(\frac{\partial E_1}{\partial x}(x,y_j-h_{y,j})+\frac{\partial E_1}{\partial x}(x,y_j+h_{y,j})\right)dx, \\
\left|\frac{\partial E_{1,I}}{\partial x}\right| &\leq \frac{1}{4h_{x,i}}\int_{x_i-h_{x,i}}^{x_i+h_{x,i}}\varepsilon^{-1}e^{-\beta(1-x)/\varepsilon}dx \leq C\frac{\varepsilon^{-1}}{h_{x,i}}\int_{x_i-h_{x,i}}^{x_i+h_{x,i}}e^{-\beta(1-x)/\varepsilon}dx.
\end{aligned}$$

And, hence, we have

$$\varepsilon \sum_{K\in K_{21}\cup K_{22}} h_{x,i}h_{y,j}\left|\frac{\partial E_{1,I}}{\partial x}\right|^2 \leq C\varepsilon^{-1}\frac{h_{y,j}}{h_{x,i}}\int_0^{1-\tau_\varepsilon}e^{-2\beta(1-x)/\varepsilon}dx \leq CN^{-(2k+2)}.$$

Similarly, the second term in the RHS of inequality (6.5.11) can be shown to be bounded by $N^{-(2k+2)}$. By combining the bound for the first and second term of inequality (6.5.11), we obtain

$$\varepsilon \sum_{K \in K_{21} \cup K_{22}} h_{x,i} h_{y,j} |\nabla E_{1,I}|^2 \leq C N^{-(2k+2)}. \tag{6.5.12}$$

On combining inequalities (6.5.9), (6.5.10) and (6.5.12), we obtain the following bound outside layer region:

$$|E_1 - E_{1,I}|_{\varepsilon,N} \leq C N^{-(k+1)}.$$

Hence we obtain the bound for the first term of the Equation (6.5.7) on all the domain. Now we will derive bound for the second term of the Equation (6.5.7). Using Equation (6.5.1), we obtain the following bound in L^2–norm

$$\sum_{K \in \mathcal{T}_N} \|(E_1 - E_{1,I})\|^2_{L^2(K)} \leq C N^{-2(k+1)} (\ln N)^{2(k+1)}.$$

Combining both the terms of Equation (6.5.7), we get our desired result. ∎

Theorem 6.5.3. *Let u and u_I represent the solution of the problem (6.1.1) and its piecewise Lagrange interpolation at the Gauss points, respectively. Then, bound for the interpolation error is*

$$|||u - u_I||| \leq C (N^{-1} \ln N)^{k+1}.$$

Proof. Combining the results of Theorems 6.5.1 and 6.5.2, we obtain the desired estimate. ∎

Using the coercivity property and the Galerkin orthogonality properties of bilinear form, we can obtain that

$$|||\xi|||^2 \leq B(\xi, \xi) = B(u - u_h, \xi) - B(\eta, \xi) = -B(\eta, \xi),$$

hence, to prove the discretization error $\xi = u_I - u_h$, we need to prove the following theorem.

Theorem 6.5.4. *The following estimate holds true:*

$$|B(\eta, \xi)| \leq C N^{-(k+1)} (\ln N)^{k+1} |||\xi|||.$$

Proof. From Equation (6.4.2), the bilinear form can be written in terms of η and ξ as follows

$$\begin{aligned} B(\eta,\,\xi) &= \sum_{K\in\mathcal{T}_N}\Big(\varepsilon\int_K \nabla\eta\cdot\nabla\xi\,dx+\int_K(\mathbf{b}\cdot\nabla\eta+c\eta)\xi\,dx \\ &\quad -\int_{\partial_- K\cap\Gamma}(\mathbf{b}\cdot\mu_K)\eta^+\xi^+ds-\int_{\partial_- K\setminus\Gamma}(\mathbf{b}\cdot\mu_k)\lfloor\eta\rfloor\xi^+ds\Big) \\ &\quad +\varepsilon\int_\Gamma(\eta(\nabla\xi\cdot\mu)-(\nabla\eta\cdot\mu)\xi)ds+\int_\Gamma\sigma\eta\xi ds \\ &\quad +\varepsilon\int_{\Gamma_{int}}([\eta]\{\nabla\xi\cdot\nu\}-\{\nabla\eta\cdot\nu\}[\xi])ds+\int_{\Gamma_{int}}\sigma[\eta][\xi]ds. \end{aligned} \tag{6.5.13}$$

Since u_I is the piecewise Lagrange interpolation of u and $u|_\Gamma = 0$. Hence the values of $\eta|_\Gamma$ and $[\eta]$ will be zero. Using this value in the above equation, we get

$$\begin{aligned} B(\eta,\,\xi) &= \sum_{K\in\mathcal{T}_N}\Big(\varepsilon\int_K \nabla\eta\cdot\nabla\xi\,dx+\int_K\mathbf{b}\cdot\nabla\eta\,\xi dx+\int_K c\,\eta\,\xi\,dx\Big) \\ &\quad -\varepsilon\int_\Gamma(\nabla\eta\cdot\mu)\xi ds-\varepsilon\int_{\Gamma_{int}}\{\nabla\eta\cdot\nu\}[\xi]ds. \end{aligned} \tag{6.5.14}$$

Using the Cauchy-Schwarz inequality, the first term in the RHS of Equation (6.5.14) can be bounded with

$$\begin{aligned} \Big|\sum_{K\in\mathcal{T}_N}\varepsilon\int_K\nabla\eta\cdot\nabla\xi\,dx\Big| &\le C|||\xi|||\Big(\sum_{K\in\mathcal{T}_N}\varepsilon^{1/2}||\nabla\eta||_{L^2(K)}\Big) \\ &\le C(N^{-1}\ln N)^{k+1}|||\xi|||. \end{aligned}$$

For the second term in the RHS of Equation (6.5.14), we perform integration by parts, and we get

$$\begin{aligned} \sum_{K\in\mathcal{T}_N}\int_K\mathbf{b}\cdot\nabla\eta\,\xi\,dx &= \sum_{K\in\mathcal{T}_N}\Big(-\int_K(\mathbf{b}\cdot\nabla\xi)\eta dx \\ &\quad -2\int_K c\xi\eta dx+2\gamma^2\int_K\xi\eta dx\Big). \end{aligned} \tag{6.5.15}$$

First term in the RHS of Equation (6.5.15) can be estimated as

$$\begin{aligned} \Big|\sum_{K\in\mathcal{T}_N}\int_K(\mathbf{b}\cdot\nabla\xi)\eta\,dx\Big| &\le C|||\xi|||\Big(\sum_{K\in\mathcal{T}_N}||\eta||^2_{L^2(K)}\Big)^{1/2} \\ &\le C(N^{-1}\ln N)^{k+1}|||\xi|||. \end{aligned}$$

Second and third terms in the RHS of Equation (6.5.15) can be bounded by

$$\begin{aligned} \Big|\sum_{K\in\mathcal{T}_N}\int_K c\,\eta\,\xi\,dx\Big| &\le C|||\xi|||\Big(\sum_{K\in\mathcal{T}_N}||\eta||^2_{L^2(K)}\Big)^{1/2} \\ &\le C(N^{-1}\ln N)^{k+1}|||\xi|||, \end{aligned}$$

and

$$\begin{aligned}\Big|\sum_{K\in\mathcal{T}_N}\int_K \gamma^2\,\eta\,\xi\,dx\Big| &\le C|||\xi|||\Big(\sum_{K\in\mathcal{T}_N}\gamma^2||\eta||^2_{L^2(K)}\Big)^{1/2}\\ &\le C(N^{-1}\ln N)^{k+1}|||\xi|||.\end{aligned}$$

Third term in the RHS of Equation (6.5.14) can be express as

$$\begin{aligned}\sum_{K\in\mathcal{T}_N}\int_K c\eta\xi\,dx &\le C|||\xi|||\Big(\sum_{K\in\mathcal{T}_N}||\eta||^2_{L^2(K)}\Big)^{1/2}\\ &\le C(N^{-1}\ln N)^{k+1}|||\xi|||. \qquad (6.5.16)\end{aligned}$$

Fourth term in the RHS of Equation (6.5.14) can be bounded as

$$\begin{aligned}\varepsilon\int_\Gamma(\nabla\eta\cdot\mu)\xi ds &= \sum_{e\in\mathcal{E}_N\cap\Gamma}\varepsilon\int_e(\nabla\eta\cdot\mu)\,\xi ds\\ &\le \sum_{e\in\mathcal{E}_N\cap\Gamma}\Big(\int_e\frac{\varepsilon^2}{\sigma}(\nabla\eta\cdot\mu)^2ds\Big)^{1/2}\Big(\int_e\sigma\,\xi^2ds\Big)^{1/2}\\ &\le C|||\xi|||\sum_{e\in\mathcal{E}_N\cap\Gamma}\Big(\int_e\frac{\varepsilon^2}{\sigma}(\nabla\eta\cdot\mu)^2ds\Big)^{1/2}.\end{aligned}$$

Using the trace inequality, bound for interpolation error and the value of the penalty parameter $\sigma = N/\ln N$, we obtained

$$\Big|\varepsilon\int_\Gamma(\nabla\eta\cdot\mu)\xi ds\Big| \le C(N^{-1}\ln N)^{k+1}|||\xi|||.$$

Bound for the fifth term in the RHS of Equation (6.5.14) is

$$\begin{aligned}\int_{\Gamma_{int}}\varepsilon[\xi]\{\nabla\eta\cdot\nu\}ds &= \sum_{e\in\mathcal{E}_{int}}\varepsilon\int_e\{\nabla\eta\cdot\mu\}_e\,[\xi]_e ds\\ &\le \sum_{e\in\mathcal{E}_{int}}\Big(\int_e\frac{\varepsilon^2}{\sigma}\{\nabla\eta\cdot\mu\}^2_e ds\Big)^{1/2}\Big(\int_e\sigma\,[\xi]^2_e ds\Big)^{1/2}\\ &\le C\sum_{e\in\mathcal{E}_{int}}\Big(\int_e\frac{\varepsilon^2}{\sigma}(\nabla\eta\cdot\mu)^2|_{\partial K\cap e}\,ds+\int_e\frac{\varepsilon^2}{\sigma}(\nabla\eta\cdot\mu)^2|_{\partial K'\cap e}\,ds\Big)^{1/2}|||\xi|||,\end{aligned}$$

where we have used the definition of average $\{.\}$ and $e\in\mathcal{E}_{int}$ is an interior edge shared by the elements K and K'. Again using the trace inequality, bound for the interpolation error and value of the penalty parameter, we get

$$\Big|\int_{\Gamma_{int}}\varepsilon[\xi]\{\nabla\eta\cdot\nu\}ds\Big| \le C(N^{-1}\ln N)^{k+1}|||\xi|||.$$

Combining all the above estimates, we get the required bounds. ∎

Theorem 6.5.5. *Let u be the solution of the problem (6.1.1) and u_h be the solution of the problem (6.4.1), then, we have*

$$|||u - u_h||| \leq C(N^{-1} \ln N)^{k+1}.$$

Proof. Using Theorems 6.5.3 and 6.5.4, we get the required estimate. ∎

6.6 Numerical Results

In this section, we present numerical results for the following two examples, first one with constant coefficients and second one with variable coefficients. The results are given in the form of tables and figures, which reveal the superconvergence of the NIPG method, as discussed in Theorem 6.5.5.

Example 6.6.1. *Consider the following 2D elliptic BVP:*

$$\begin{cases} -\varepsilon\Delta u - u_x - u_y + u = f, & in \quad \mathcal{D}, \\ u = 0, & on \quad \Gamma = \partial\mathcal{D}, \end{cases} \tag{6.6.1}$$

where f is chosen such that

$$u(x, y) = \sin(1 - x)\sin(1 - y)(1 - e^{-x/\varepsilon})(1 - e^{-y/\varepsilon})$$

is the exact solution of (6.6.1).

Table 6.1: *L^2–error and order of convergence for Example 6.6.1*

	Number of mesh intervals N				
	32	64	128	256	512
$k = 1$	6.1710e-03	1.7771e-03	4.7017e-04	1.2061e-04	3.0530e-05
	1.7960	1.9183	1.9628	1.9821	
$k = 2$	6.8710e-04	8.2726e-05	1.0134e-05	1.2447e-06	1.7266e-07
	3.0541	3.0292	3.0253	2.8498	

Example 6.6.2. *Consider the following elliptic BVP:*

$$-\varepsilon\Delta u - (2 - x)u_x - u_y + \frac{3}{2}u = f, \quad in \quad \mathcal{D}, \tag{6.6.2}$$

where f is chosen such that

$$u(x, y) = \left(\cos(\frac{\pi x}{2}) - \frac{e^{-x/\varepsilon} - e^{-1/\varepsilon}}{1 - e^{-1/\varepsilon}}\right)\frac{1 - e^{-y/\varepsilon}}{1 - e^{-1/\varepsilon}}$$

is the exact solution of (6.6.2) and dirichlet boundary condition are taken from the exact solution.

Table 6.2: *Discrete energy norm error and order of convergence for Example 6.6.1*

	Number of mesh intervals N				
	32	64	128	256	512
$k=1$	2.2794e-03	1.3808e-03	6.4311e-04	2.3955e-04	7.5455e-05
	0.72313	1.1024	1.4247	1.6666	
$k=2$	8.0241e-04	1.4679e-04	2.2228e-05	2.9990e-06	3.8541e-07
	2.4506	2.7233	2.8898	2.9601	

Table 6.3: *L^2–error and order of convergence for Example 6.6.2*

	Number of mesh intervals N				
	32	64	128	256	512
$k=1$	1.5269e-02	3.6068e-03	8.7499e-04	2.1528e-04	5.3385e-05
	2.0818	2.0434	2.0230	2.0117	
$k=2$	5.8618e-03	8.7566e-04	1.1235e-04	1.4131e-05	1.7776e-06
	2.7429	2.9624	2.9910	2.9909	

Table 6.1 and Table 6.2 show the error and order of convergence in L^2–norm and discrete energy norm, respectively for Example 6.6.1. From the order of convergence results given in these tables, we can observe that when we are using the linear elements in the finite element space, we are getting second-order convergence in the L^2–norm and almost second-order in discrete energy norm and when we are using the quadratic elements in the finite element space, we are getting third-order convergence in L^2–norm and almost third-order in discrete energy norm.

Similarly, Table 6.3 and Table 6.4 show the error and order of convergence in L^2–norm and discrete energy norm, respectively, for Example 6.6.2.

Figure 6.2 and Figure 6.3 represent the log-log plot of the error in L^2–norm and discrete energy norm for Example 6.6.1 for linear finite elements and quadratic finite elements, respectively. Similarly, Figure 6.4 and Figure 6.5 depict the log-log plot of error in L^2–norm and discrete energy norm for Example 6.6.2 for linear finite elements

Table 6.4: *Discrete energy norm error and order of convergence for Example 6.6.2*

	Number of mesh intervals N				
	32	64	128	256	512
$k=1$	1.9485e-03	8.1781e-04	3.3446e-04	1.1917e-04	3.7017e-05
	1.2525	1.2900	1.4889	1.6867	
$k=2$	3.6115e-03	1.1203e-03	2.4235e-04	4.0314e-05	5.7208e-06
	1.6887	2.2087	2.5878	2.8170	

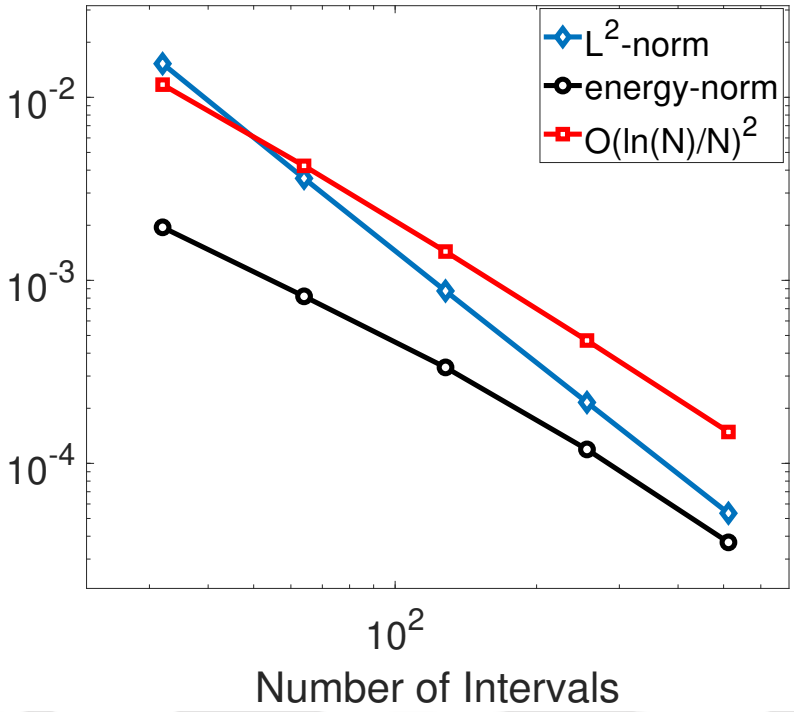

Figure 6.2: Order of convergence in L^2–norm and discrete energy norm for Example 6.6.1 for linear finite elements.

and quadratic finite elements, respectively.

Further, Figure 6.6 and Figure 6.7 provide the surface plots of the exact and numerical solution for $\varepsilon = 10^{-4}$ and $N = 32$ for Example 6.6.1 and Example 6.6.2, respectively.

6.7 Conclusions

In this chapter, we have applied the NIPG method for singularly perturbed 2D elliptic convection-diffusion BVPs. We have showed the superconvergence of the NIPG method that is, we have proved $\mathcal{O}(N^{-1} \ln N)^{k+1}$ order of convergence in the discrete energy norm. Finally, the theoretical error estimates are supported by the numerical results.

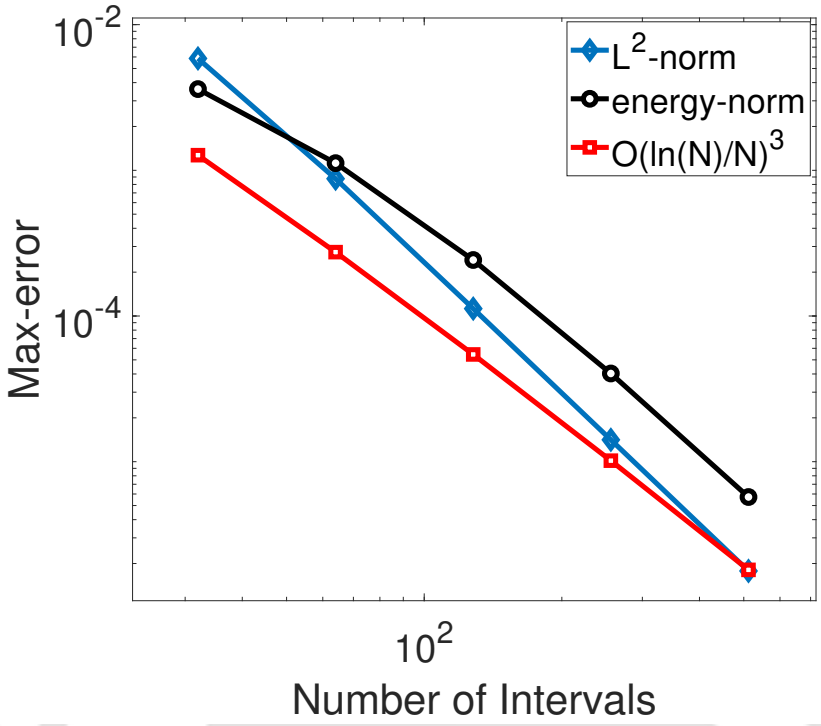

Figure 6.3: Order of convergence in L^2–norm and discrete energy norm for Example 6.6.1 for quadratic finite elements.

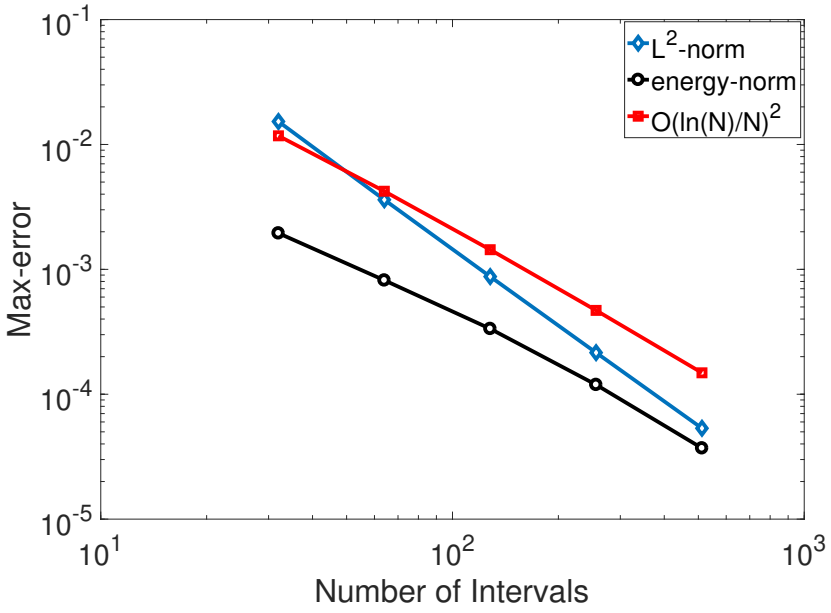

Figure 6.4: Order of convergence in L^2–norm and discrete energy norm for Example 6.6.2 for linear finite elements.

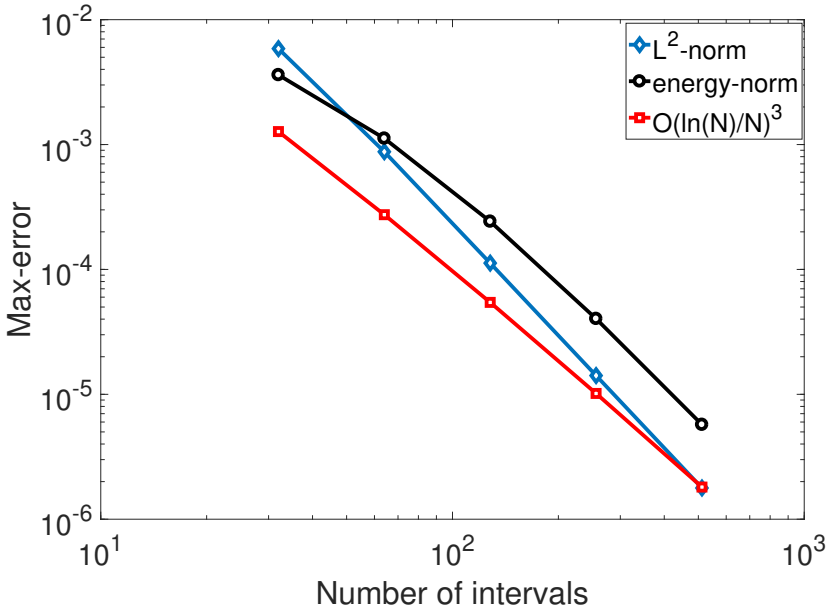

Figure 6.5: Order of convergence in L^2–norm and discrete energy norm for Example 6.6.2 for quadratic finite elements.

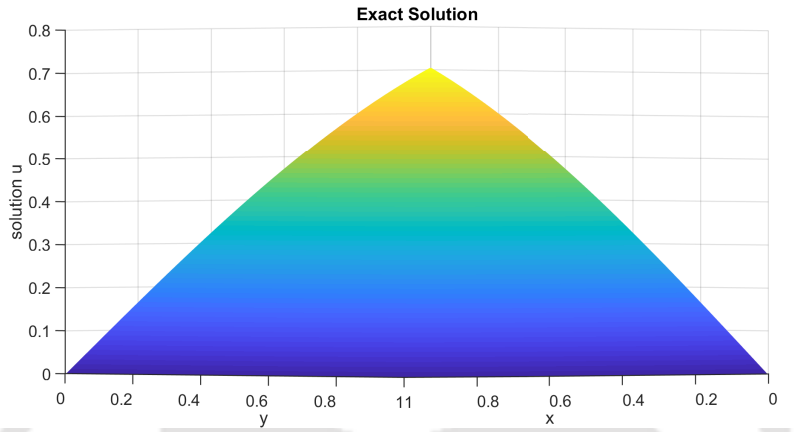

(a) Exact solution.

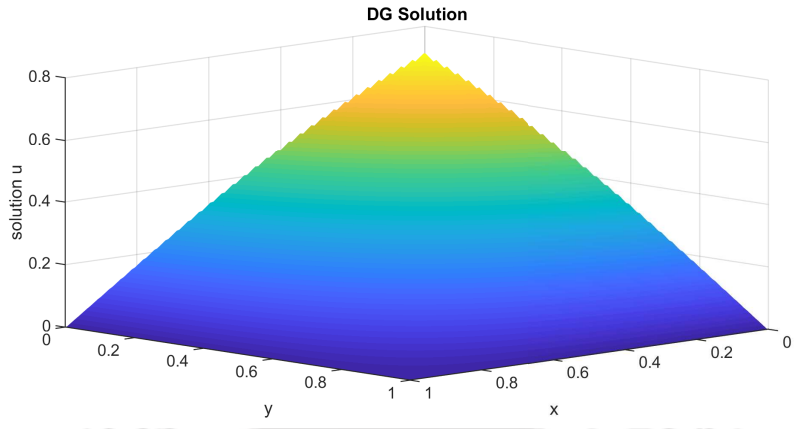

(b) DG solution.

Figure 6.6: Surface plot of the exact and numerical solutions for Example 6.6.1 for $\varepsilon = 10^{-4}$ and $N = 32$.

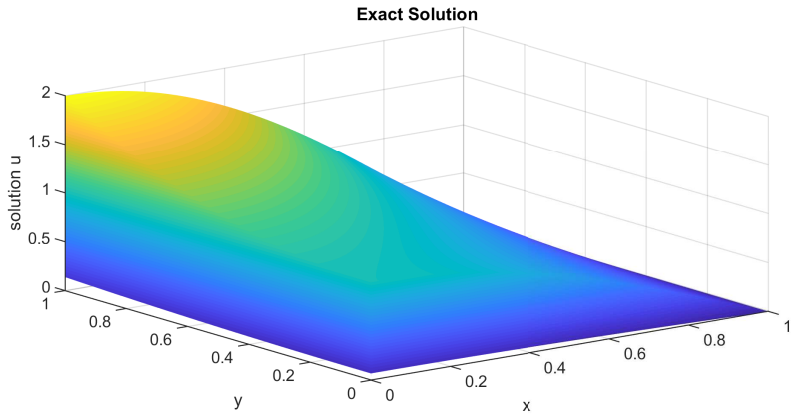

(a) Exact solution.

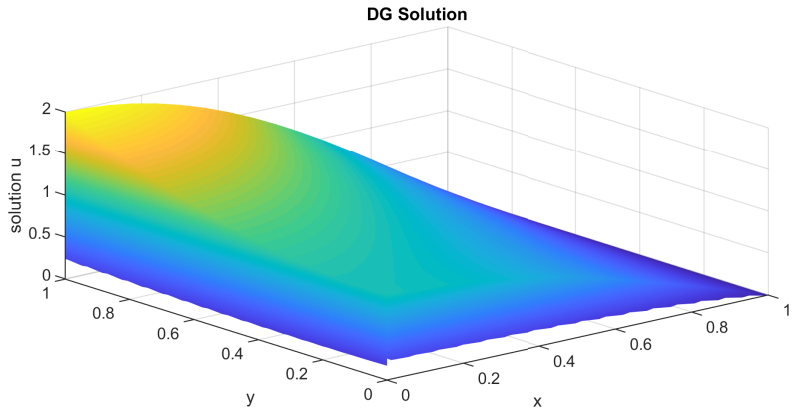

(b) DG solution.

Figure 6.7: Surface plot of the exact and numerical solutions for Example 6.6.2 for $\varepsilon = 10^{-4}$ and $N = 32$.

CHAPTER 7

Summary and Future Scopes

A brief overview of main result of this thesis is given in this chapter. Further, possible extensions of the present works are given.

7.1 Summary of the Results

The main aim of this thesis is to study superconvergence properties of the NIPG method for solving singularly perturbed problems. Some important results of this thesis are highlighted below:

- Superconvergence properties of the NIPG method for singularly perturbed two-point BVPs of reaction-diffusion and convection-diffusion types are studied. We consider singularly perturbed 1D reaction-diffusion and convection-diffusion problems, and we use the NIPG method to discretize the problems on the Shishkin mesh. We study the convergence of the scheme in the discrete energy norm, which shows the method converges uniformly with order of convergence $(N^{-1}\ln N)^{k+1}$, where k and N are the degree of the piecewise polynomials and number of elements, respectively. To validate the theoretical findings, numerical experiments are carried out.

- Next, we applied the NIPG method to obtain the numerical solution of two-parameter singularly perturbed convection-diffusion-reaction BVPs. First, we discretize the domain using the piecewise uniform Shishkin mesh and establish a superconvergence result of the NIPG method, that is, the proposed method is parameter-uniformly convergent with the order almost $(k+1)$, where k is the order of the polynomials. Then to improve the order of convergence, we discretize the domain using the Bakhvalov mesh and the exponentially-graded mesh and show

the proposed method is parameter-uniformly convergent with the order $(k+1)$. Numerical results comparing the three different types of meshes are presented.

- Then, we studied the numerical solution of singularly perturbed system of two-point BVPs of reaction-diffusion type. The solutions of these problems exhibit twin overlapping exponential boundary layers. Here, we applied the NIPG method on layer-adapted piecewise uniform Shishkin mesh to obtain the numerical solutions of these problems and we have proved that the proposed method is uniformly convergent with order k in the $\mathcal{E}$-weighted discrete energy norm, where k is the degree of the piecewise polynomial in the finite element space. Further, to improve the order of convergence, we use piecewise Lagrange interpolation on Gauss points. Then we derived error bound in discrete energy norm. Numerical results are presented to support the theoretical results.

- Further, singularly perturbed 1D parabolic convection-diffusion-reaction IBVP is discretized in space by the NIPG method and in time by the DG method. We have shown the superconvergence properties, that is, $(k+1)$–order of convergence in space and $(l+1)$–order of convergence in time, where k and l are the degree of piecewise polynomial in finite element space. Numerical results are given to verify our theoretical findings.

- Finally, we propose a parameter-uniform NIPG method to solve singularly perturbed 2D elliptic BVPs. Here, we obtain the error estimates of the superconvergence of the NIPG method on layer-adapted meshes of Shishkin type. We have established the error bound in the discrete energy norm. Numerical tests support our theoretical estimates.

7.2 Scope for Future Work

A brief outline, describing the possible extensions of the current work to be carried out in the future with suitable model problems, are presented below:

In Chapter 2 we have applied the NIPG method for singularly perturbed two-point BVPs of reaction-diffusion and convection-diffusion types. In the NIPG method, we integrate by parts on each mesh element, and then sum over all the elements. Two stabilization terms are then added: symmetrizing term and penalty term. Another related DG method is the SIPG method, this method differ from the NIPG method by only one sign: symmetrizing term are subtracted instead of being added. In the SIPG method, we get symmetric linear systems that can be easily solved by standard solvers

for symmetric matrices (such as conjugate gradient). It will be interesting to solve this type of the problems using the SIPG method.

The numerical scheme discussed in Chapter 3 can be applied to solve the following singularly perturbed 2D elliptic BVPs with two parameters:

$$\begin{cases} -\varepsilon_d \Delta u + \varepsilon_c \mathbf{b} \cdot \nabla u + c(x,\, y)u = f(x,\, y), \quad \text{in} \quad \mathcal{D}, \\ u = 0, \quad \text{on} \quad \Gamma = \partial\mathcal{D}, \end{cases} \tag{7.2.1}$$

where $0 < \varepsilon_d, \varepsilon_c \ll 1$ is a small positive parameter, and $\mathbf{b}(x,\, y) = (b_1(x,\, y),\, b_2(x,\, y)) \geq (\beta_1,\, \beta_2) \geq (\beta,\, \beta) > (0,\, 0)$, $c(x,\, y) \geq 0$ for all $(x,\, y) \in \overline{\mathcal{D}}$, and $\gamma^2 = \left(c(x,\, y) - \varepsilon_c \frac{\nabla \cdot \mathbf{b}(x,\, y)}{2}\right) > 0$, where β and γ are constants.

The computational technique developed in Chapter 4 can be applied to solve the following singularly perturbed system of 2D reaction-diffusion BVPs:

$$\begin{cases} -\mathcal{E}\Delta\vec{u} + A\vec{u} = f \quad \text{in} \quad \mathcal{D}, \\ \vec{u} = 0 \qquad\qquad \text{on} \quad \Gamma = \partial\mathcal{D}, \end{cases} \tag{7.2.2}$$

where $\vec{u}(x) = (u_1(x), u_2(x), \cdots, u_M(x))$ and $\mathcal{E} = diag(\varepsilon_1, \cdots, \varepsilon_M)$ is an diagonal matrix of order M with parameters $0 < \varepsilon_i \leq 1$. We assume that $A(x) = (a_{ij}(x))$ and $f(x) = (f_1(x), \cdots, f_M(x))$ are sufficiently smooth.

In Chapter 5, we considered singularly perturbed 1D parabolic convection-diffusion IBVPs. It will be interesting to extend this method to singularly perturbed 2D parabolic IBVPs of the form:

$$\begin{cases} u_t - \varepsilon\Delta u + bu = f(x, y, t), \quad \forall (x,\, y,\, t) \in (\mathcal{D} \times (0,\, T]), \\ u(x, y, 0) = 0, \quad \forall (x,\, y) \in \mathcal{D}, \\ u(x, y, t) = 0, \quad \forall (x, y, t) \in \partial\mathcal{D} \times (0,\, T]. \end{cases}$$

Finally, in Chapter 6, we applied the NIPG method to solve singularly perturbed 2D elliptic BVP. It is well-known that in the continuous and discontinuous Galerkin finite element method, one needs to choose approximating function in such a way that the gradient operator ∇ can be successfully applied to them in the classical sense. Recently in 2013, Wang and Ye [62] introduced a weak gradient operator defined on a space of generalized functions. Now by using the weak gradient operator, we can discretize the standard weak formulation of the problem. The corresponding finite element method is called the weak Galerkin finite element method. In future, we are planning to solve singularly perturbed 2D elliptic BVP using weak Galerkin finite element method.
colorblue

7.3 Possible Limitations

In this thesis, we have applied the NIPG method to solve singular perturbation problems of different types. But because of the NIPG method we get non-symmetric matrices, solving non-symmetric matrices are more difficult and costly. In future, we are planning to solve these problems using SIPG method. In the SIPG method, we get symmetric linear systems that can be easily solved by standard solvers for symmetric matrices (such as conjugate gradient).

As we know in the discontinuous Galerkin method, one needs to choose approximating function in such a way that the gradient operator ∇ can be successfully applied to them in the classical sense. In future, we are planning to solve these problems using weak Galerkin finite element method (WGFEM). In WGFEM, we use weak gradient operator defined on a space of generalized functions.

[1] N. Ahmed, G. Matthies, L. Tobiska, and H. Xie. Discontinuous Galerkin time stepping with local projection stabilization for transient convection-diffusion-reaction problems. *Comput. Methods Appl. Mech. Engrg.*, 200(21-22):1747–1756, 2011.

[2] D. N. Arnold. An interior penalty finite element method with discontinuous elements. *SIAM J. Numer. Anal.*, 19(4):742–760, 1982.

[3] D. N. Arnold, F. Brezzi, B. Cockburn, and L. D. Marini. Unified analysis of discontinuous Galerkin methods for elliptic problems. *SIAM J. Numer. Anal.*, 39(5):1749–1779, 2001/02.

[4] N. S. Bakhvalov. The optimization of methods of solving boundary value problems with a boundary layer. *Comput. Math. Math. Phys.*, 9(4):139–166, 1969.

[5] S. Bellew and E. O'Riordan. A parameter robust numerical method for a system of two singularly perturbed convection-diffusion equations. *Appl. Numer. Math.*, 51(2-3):171–186, 2004.

[6] M. Brdar, S. Franz, and H.-G. Roos. Numerical treatment of singularly perturbed fourth-order two-parameter problems. *Electron. Trans. Numer. Anal.*, 51:50–62, 2019.

[7] M. Brdar and H. Zarin. A singularly perturbed problem with two parameters on a Bakhvalov-type mesh. *J. Comput. Appl. Math.*, 292:307–319, 2016.

[8] W. Cao, C.-W. Shu, Y. Yang, and Z. Zhang. Superconvergence of discontinuous Galerkin methods for two-dimensional hyperbolic equations. *SIAM J. Numer. Anal.*, 53(4):1651–1671, 2015.

[9] Z. Cen. Parameter-uniform finite difference scheme for a system of coupled singularly perturbed convection-diffusion equations. *Int. J. Comput. Math.*, 82(2):177–192, 2005.

[10] H. Chen. Superconvergence properties of discontinuous Galerkin methods for two-point boundary value problems. *Int. J. Numer. Anal. Model.*, 3(2):163–185, 2006.

[11] A. Das and S. Natesan. Uniformly convergent hybrid numerical scheme for singularly perturbed delay parabolic convection-diffusion problems on shishkin mesh. *Appl. Math. Comput.*, 271:168–186, 2015.

[12] P. Das and S. Natesan. Optimal error estimate using mesh equidistribution technique for singularly perturbed system of reaction-diffusion boundary-value problems. *Appl. Math. Comput.*, 249:265–277, 2014.

[13] D. N. de G. Allen and R. V. Southwell. Relaxation methods applied to determine the motion in two dimensions of a viscous fluid past a fixed cylinder. *The Quarterly Journal of Mechanics and Applied Mathematics*, 8(2):129–145, 1955.

[14] M. Ding, X. Cai, W. Guo, and J.-M. Qiu. A semi-lagrangian discontinuous galerkin (dg) - local dg method for solving convection-diffusion equations. *J. Comput. Phys.*, 409(1):109295, 2020.

[15] E. P. Doolan, J. J. H. Miller, and W. H. A. Schilders. *Uniform Numerical Methods for Problems with Initial and Boundary Layers*. Boole Press, Dublin, 1980.

[16] P. A. Farrell, A. F. Hegarty, J. J. H. Miller, E. O'Riordan, and G. I. Shishkin. *Robust computational techniques for boundary layers*. Chapman & Hall/CRC, Boca Raton, FL, 2000.

[17] M. Feistauer, J. Hájek, and K. Svadlenka. Space-time discontinuous Galerkin method for solving nonstationary convection-diffusion-reaction problems. *Appl. Math.*, 52(3):197–233, 2007.

[18] M. Feistauer and K. Švadlenka. Discontinuous Galerkin method of lines for solving nonstationary singularly perturbed linear problems. *J. Numer. Math.*, 12(2):97–117, 2004.

[19] S. Franz. Continuous interior penalty method on a Shishkin mesh for convection-diffusion problems with characteristic boundary layers. *Comput. Methods Appl. Mech. Engrg.*, 197(45-48):3679–3686, 2008.

[20] K. O. Friedrichs and W. R. Wasow. Singular perturbations of nonlinear oscillations. *Duke Math. J.*, 13:367–381, 1946.

[21] S. Gowrisankar and S. Natesan. The parameter uniform numerical method for singularly perturbed parabolic reaction-diffusion problems on equidistributed grids. *Appl. Math. Lett.*, 26(11):1053–1060, 2013.

[22] S. Gowrisankar and S. Natesan. Uniformly convergent numerical method for singularly perturbed parabolic initial-boundary-value problems with equidistributed grids. *Int. J. Comput. Math.*, 91(3):553–577, 2014.

[23] P. Houston, C. Schwab, and E. Süli. Discontinuous *hp*-finite element methods for advection-diffusion-reaction problems. *SIAM J. Numer. Anal.*, 39(6):2133–2163, 2002.

[24] M. K. Kadalbajoo and K. C. Patidar. A survey of numerical techniques for solving singularly perturbed ordinary differential equations. *Appl. Math. Comput.*, 130(2-3):457–510, 2002.

[25] M. K. Kadalbajoo and K. C. Patidar. Singularly perturbed problems in partial differential equations: a survey. *Appl. Math. Comput.*, 134(2-3):371–429, 2003.

[26] M. K. Kadalbajoo and Y. N. Reddy. Asymptotic and numerical analysis of singular perturbation problems: a survey. *Appl. Math. Comput.*, 30(3):223–259, 1989.

[27] M. K. Kadalbajoo and A. S. Yadaw. Parameter-uniform Ritz-Galerkin finite element method for two parameter singularly perturbed boundary value problems. *Int. J. Pure Appl. Math.*, 55(2):287–300, 2009.

[28] L. Kaland and H.-G. Roos. Parabolic singularly perturbed problems with exponential layers: robust discretizations using finite elements in space on Shishkin meshes. *Int. J. Numer. Anal. Model.*, 7(3):593–606, 2010.

[29] R. Lin and M. Stynes. A balanced finite element method for a system of singularly perturbed reaction-diffusion two-point boundary value problems. *Numer. Algorithms*, 70(4):691–707, 2015.

[30] R. Lin, X. Ye, S. Zhang, and P. Zhu. Analysis of a dg method for singularly perturbed convection-diffusion problems. *J. appl. anal. comput.*, 10(3):830–841, 2020.

[31] T. Linß. The necessity of Shishkin decompositions. *Appl. Math. Lett.*, 14(7):891–896, 2001.

[32] T. Linß. Sufficient conditions for uniform convergence on layer-adapted grids. *Appl. Numer. Math.*, 37(1-2):241–255, 2001.

[33] T. Linß. *Layer-adapted meshes for reaction-convection-diffusion problems*, volume 1985 of *Lecture Notes in Mathematics*. Springer-Verlag, Berlin, 2010.

[34] T. Linß and N. Madden. Accurate solution of a system of coupled singularly perturbed reaction-diffusion equations. *Computing*, 73(2):121–133, 2004.

[35] T. Linß and N. Madden. A finite element analysis of a coupled system of singularly perturbed reaction-diffusion equations. *Appl. Math. Comput.*, 148(3):869–880, 2004.

[36] T. Linß and N. Madden. Layer-adapted meshes for a linear system of coupled singularly perturbed reaction-diffusion problems. *IMA J. Numer. Anal.*, 29(1):109–125, 2009.

[37] T. Linß and H.-G. Roos. Analysis of a finite-difference scheme for a singularly perturbed problem with two small parameters. *J. Math. Anal. Appl.*, 289(2):355–366, 2004.

[38] T. Linß and M. Stynes. Asymptotic analysis and Shishkin-type decomposition for an elliptic convection-diffusion problem. *J. Math. Anal. Appl.*, 261(2):604–632, 2001.

[39] N. Madden and M. Stynes. A uniformly convergent numerical method for a coupled system of two singularly perturbed linear reaction-diffusion problems. *IMA J. Numer. Anal.*, 23(4):627–644, 2003.

[40] A. Majumdar and S. Natesan. An ε uniform hybrid numerical scheme for a singularly perturbed degenerate parabolic convection-diffusion problem. *Int. J. Comput. Math.*, 96:1–23, 2018.

[41] S. Matthews, E. O'Riordan, and G. I. Shishkin. A numerical method for a system of singularly perturbed reaction-diffusion equations. *J. Comput. Appl. Math.*, 145(1):151–166, 2002.

[42] J. J. H. Miller, E. O'Riordan, and G. I. Shishkin. *Fitted numerical methods for singular perturbation problems*. World Scientific Publishing Co., Inc., River Edge, NJ, 1996.

[43] J. Mohapatra and S. Natesan. The parameter-robust numerical method based on defect-correction technique for singularly perturbed delay differential equations with layer behavior. *Int. J. Comput. Math.*, 7(4):573–594, 2010.

[44] K. Mukherjee and S. Natesan. Richardson extrapolation technique for singularly perturbed parabolic convection-diffusion problems. *Computing*, 92(1):1–32, 2011.

[45] K. Mukherjee and S. Natesan. ε-uniform error estimate of hybrid numerical scheme for singularly perturbed parabolic problems with interior layers. *Numer. Algorithms*, 58(1):103–141, 2011.

[46] S. Natesan and B. Sundar Deb. A robust computational method for singularly perturbed coupled system of reaction-diffusion boundary-value problems. *Appl. Math. Comput.*, 188(1):353–364, 2007.

[47] E. O'Riordan and M. Stynes. An analysis of some exponentially fitted finite element methods for singularly perturbed elliptic problems. In *Computational methods for boundary and interior layers in several dimensions*, volume 1 of *Adv. Comput. Methods Bound. Inter. Layers*, pages 138–153. Boole, Dublin, 1991.

[48] E. O'Riordan and M. Stynes. Numerical analysis of a strongly coupled system of two singularly perturbed convection-diffusion problems. *Adv. Comput. Math.*, 30(2):101–121, 2009.

[49] L. Prandtl. Uber flussigkeits-bewegung bei kleiner reibung. In *Verhandlungen, III Inter. Math. Kongresses, Tuebner, Leipzig*, pages 484–491, 1905.

[50] W. Reed and T. Hill. Triangular mesh methods for the neutron transport equation. *Technical Report Tech*, 1973.

[51] B. Rivière. *Discontinuous Galerkin methods for solving elliptic and parabolic equations*. Society for Industrial and Applied Mathematics (SIAM), Philadelphia, PA, 2008.

[52] H.-G. Roos. Layer-adapted grids for singular perturbation problems. *ZAMM Z. Angew. Math. Mech.*, 78(5):291–309, 1998.

[53] H.-G. Roos and C. Reibiger. Numerical analysis of a system of singularly perturbed convection-diffusion equations related to optimal control. *Numer. Math. Theory Methods Appl.*, 4(4):562–575, 2011.

[54] H.-G. Roos and M. Schopf. Layer structure and the Galerkin finite element method for a system of weakly coupled singularly perturbed convection-diffusion equations with multiple scales. *ESAIM Math. Model. Numer. Anal.*, 49(5):1525–1547, 2015.

[55] H.-G. Roos and T. Skalický. A comparison of the finite element method on Shishkin and Gartland-type meshes for convection-diffusion problems. *CWI Quarterly*, 10(3-4):277–300, 1997.

[56] H.-G. Roos, M. Stynes, and L. Tobiska. *Robust numerical methods for singularly perturbed differential equations*. Springer-Verlag, Berlin, 2008.

[57] H.-G. Roos and H. Zarin. A supercloseness result for the discontinuous Galerkin stabilization of convection-diffusion problems on Shishkin meshes. *Numer. Methods Partial Differential Equations*, 23(6):1560–1576, 2007.

[58] M. K. Singh and S. Natesan. An ε uniform hybrid numerical scheme for a singularly perturbed degenerate parabolic convection-diffusion problem. *Appl. Math. Comput.*, 333:254–275, 2018.

[59] M. Stynes and E. O'Riordan. A uniformly convergent Galerkin method on a Shishkin mesh for a convection-diffusion problem. *J. Math. Anal. Appl.*, 214(1):36–54, 1997.

[60] L. Tobiska. Analysis of a new stabilized higher order finite element method for advection-diffusion equations. *Comput. Methods Appl. Mech. Engrg.*, 196(1-3):538–550, 2006.

[61] G. I. Šiškin and V. A. Titov. A difference scheme for a differential equation with two small parameters at the derivatives. *Čisl. Metody Meh. Splošn. Sredy*, 7(2):145–155, 1976.

[62] J. Wang and X. Ye. A weak Galerkin finite element method for second-order elliptic problems. *J. Comput. Appl. Math.,*, 241:103–115, 2013.

[63] Z. Xie and Z. Zhang. Superconvergence of DG method for one-dimensional singularly perturbed problems. *J. Comput. Math.*, 25(2):185–200, 2007.

[64] Y. Yang and P. Zhu. Discontinuous Galerkin methods with interior penalties on graded meshes for 2D singularly perturbed convection-diffusion problems. *Appl. Numer. Math.*, 111:36–48, 2017.

[65] H. Zarin. Exponentially graded mesh for a singularly perturbed problem with two small parameters. *Appl. Numer. Math.*, 120:233–242, 2017.

[66] H. Zarin and H.-G. Roos. Interior penalty discontinuous approximations of convection-diffusion problems with parabolic layers. *Numer. Math.*, 100(4):735–759, 2005.

[67] Z. Zhang. Finite element superconvergence approximation for one-dimensional singularly perturbed problems. *Numer. Methods Partial Differential Equations*, 18(3):374–395, 2002.

[68] Z. Zhang. Finite element superconvergence on Shishkin mesh for 2-D convection-diffusion problems. *Math. Comp.*, 72(243):1147–1177, 2003.

[69] P. Zhu, Z. Xie, and S. Zhou. A coupled continuous-discontinuous FEM approach for convection diffusion equations. *Acta Math. Sci. Ser. B Engl. Ed.*, 31(2):601–612, 2011.

[70] P. Zhu, Y. Yang, and Y. Yin. Higher order uniformly convergent NIPG methods for 1-d singularly perturbed problems of convection-diffusion type. *Appl. Math. Model.*, 39(22):6806–6816, 2015.

List of published and communicated papers

Based on the work in this thesis, the following research articles are published or communicated.

1. G. Singh and S. Natesan. Superconvergence of discontinuous Galerkin method with interior penalties for singularly perturbed two-point boundary-value problems. *Calcolo.*, 55:54, 2018.
2. G. Singh and S. Natesan. Study of the NIPG method for two-parameter SPPs on several layer adapted grids. *J. Appl. Math. Comput.* , 63(1–2):683–705, 2020.
3. G. Singh and S. Natesan. A uniformly convergent numerical scheme for a coupled system of singularly perturbed reaction-diffusion equation. *Numer. Fun. Anal. Opt.*, 41(10), 1172–1189, 2020.
4. G. Singh and S. Natesan. Superconvergence properties of discontinuous Galerkin time stepping for singularly perturbed parabolic problems. (communicated).
5. G. Singh and S. Natesan. Superconvergence error analysis of discontinuous Galerkin method with interior penalties for singularly perturbed 2D elliptic BVPs. (communicated).